مقدمة الفيزياء النووية

محاضرات في مقدمة الفيزياء النووية

الفرقة : الثالثة انجليزي كلية التربية

الشعبة : الفيزياء

السنة : ٢٠٢٣/٢٠٢٢

أ . د نور خليفة احمد

المحتوى

Chapter (1) : The nuclear atom.

3–1 The Thomson atom. The discovery of radioactivity, together with Thomson's proof of the independent existence of the electron, provided a starting point for theories of atomic structure. The fact that atoms of a radioactive element are transformed into atoms of another element by emitting positively or negatively charged particles led to the view that atoms are made up of positive and negative charges. If this view is correct, the total negative charge in an atom must be an integral multiple of the electronic charge and, since the atom is electrically neutral under normal conditions, the positive and negative charges must be numerically equal. The emission of electrons by atoms under widely different conditions was convincing evidence that electrons exist as such inside atoms. The first modern theories of atomic structure were, therefore, based on the hypothesis that atoms are made up of electrons and positive charges. No particular assumptions could be made about the nature of the positive charges because the properties of the positive particles from radioactive substances and from gas discharge tubes did not have the uniformity shown by the properties of the negative particles.

Two important questions then arose: (1) how many electrons are there in an atom, and (2) how are the electrons and the positive charges arranged in an atom? Information about the first question was obtained experimentally by studying the way in which x-rays interact with atoms, and this problem will be treated in some detail in the next chapter. It will suffice, for the present, to state that early experiments of this kind indicated that the number of electrons per atom is of the order of the atomic weight. It was known that the mass of an electron is about one two-thousandth of the mass of a hydrogen atom, which has an atomic weight very close to unity. Hence, the total mass of the electrons in an atom is only a very small part of the mass of the atom, and it was logical to assume that practically the entire mass of an atom is associated with the positive charge.

In the absence of information about the way in which the positive and negative charges are distributed in an atom, Thomson proposed a simple model. He assumed that an atom consisted of a sphere of positive electricity of uniform density, throughout which was distributed an equal and opposite charge in the form of electrons. It was remarked that the atom, under this assumption, was like a plum pudding, with the negative

electricity dispersed like currants in a dough of positive electricity. The diameter of the sphere was supposed to be of the order of 10^{-8} cm, the magnitude found for the size of an atom. With this model, Thomson was able to calculate theoretically how atoms should behave under certain conditions, and the theoretical predictions could be compared with the results of experiments. It became clear when this comparison was made that Thomson's theory was inadequate; but the failure of the Thomson model in the particular case of the scattering of α-particles proved to be most profitable because it led to the concept of the nuclear atom. This concept is fundamental to atomic and nuclear physics, and the scattering of α-particles will therefore be discussed in some detail.

When a parallel beam of rays from a radioactive substance or from a discharge tube passes through matter, some of the rays are deflected, or scattered, from their original direction. The scattering process is a result of the interaction between the rays of the beam and the atoms of the material, and a careful study of the process can yield information about the rays, the atoms, or both. The scattering of α-particles was first demonstrated by Rutherford, who found that when a beam of α-particles passed through a narrow slit and fell on a photographic plate, the image of the slit had sharply defined edges if the experiment was performed in an evacuated vessel. When the apparatus contained air, the image of the slit on the photographic plate was broadened, showing that some of the rays had been deflected from their original path by the molecules in the air. Alpha-particles are also scattered by a very thin film of matter such as gold or silver foil. When a beam of particles passes through a small circular hole and falls on a zinc sulfide screen, scintillations are seen over a well-defined circular area equal to the cross section of the beam. If a very thin foil is placed in the path of the beam, the area over which the scintillations occur becomes larger, and its boundary is much less definite than in the absence of the foil, showing again that some of the particles have been deflected from their original direction.

The scattering of charged particles such as α-particles can be described qualitatively in terms of the electrostatic forces between the particles and the charges which make up atoms. Since atoms contain both positive and negative charges, an α-particle is subjected to both repulsive and attractive electrostatic forces in passing through matter. The magnitude and direction of these forces depend on how near the particle happens to approach to the centers of the atoms past which or through which it moves. When a particular atomic model is postulated, the extent of the scattering of the α-particles can be calculated quantitatively and compared with experiment. In the case of the Thomson atom, it was shown that the average deflection caused by a single atom should be very small. The

mean deflection of a particle in passing through a thin foil of thickness t should be, according to Thomson's theory,[1]

$$\phi_m = \theta(\pi n a^2 t)^{1/2}, \tag{3-1}$$

where θ is the average deflection caused by a single atom, n is the number of atoms per cubic centimeter, a is the radius of the atom in centimeters, and t is the thickness of the foil in centimeters. If the scatterer is a gold foil 4×10^{-5} cm thick, and if a is assumed to be 10^{-8} cm, then ϕ_m turns out to be about 30θ. The scattering of α-particles by a thin foil, according to the Thomson theory, is the result of a relatively large number of small deflections caused by the action of a large number of atoms of the scattering material on a single α-particle. This process is called *compound*, or *multiple*, scattering.

In an experiment, it is convenient to count the number of α-particles scattered through a certain angle. Rutherford showed that the number of α-particles N_ϕ scattered through an angle equal to, or greater than, ϕ should be given by

$$N_\phi = N_0 e^{-(\phi/\phi_m)^2}, \tag{3-2}$$

where N_0 is the number of particles corresponding to $\phi = 0$, and ϕ_m is the average deflection after passing through the foil. It was found experimentally by Geiger[2] that when a gold foil 4×10^{-5} cm thick was used, the most probable angle of deflection of a beam of α-particles was about 1°. If this value is used for ϕ_m in Eq. (3-2), it can be seen that the probability that an α-particle is scattered through a large angle becomes vanishingly small. For example, the number of α-particles which should be scattered through an angle of 10° or more is

$$N_{10^\circ} = N_0 e^{-100} \approx 10^{-43} N_0.$$

Geiger found that the scattering agreed with that predicted by Eq. (3-2) for very small angles, that is, for very small values of ϕ, but the number of particles scattered through large angles was much greater[3] than that predicted by the Thomson theory. In fact, one out of about every 8000 α-particles was scattered through an angle greater than 90°, which means that a significant number of α-particles in a beam incident on a foil had their directions changed to such an extent that they emerged again on the side of incidence. The experimental scattering of α-particles at large angles could not possibly be reconciled with the theoretical predictions based on multiple scattering by a Thomson atom, and it was necessary to look for a better model for the atom.

3-2 Rutherford's theory of the scattering of alpha-particles. Rutherford[4] (1911) proposed a new theory of the scattering of α-particles by

matter; this theory was based on a new atomic model and was successful in describing the experimental results. Rutherford suggested that the deflection of an α-particle through a large angle could be caused by a single encounter with an atom rather than by multiple scattering. Photographs of the tracks of α-particles in a cloud chamber showed that α-particles often traveled in a straight line for a considerable distance and then were deflected suddenly through a large angle. Rutherford's suggestion was in agreement with this kind of experimental evidence. For large angle scattering to be possible, it was necessary to suppose that there is an intense electric field near an atom. Rutherford proposed a simple model of the atom which could provide such a field. He assumed that the positive charge of the atom, instead of being distributed uniformly throughout a region of the size of the atom, is concentrated in a minute center or nucleus, and that the negative charge is distributed over a sphere of radius comparable with the atomic radius. On this model, an α-particle can penetrate very close to the nucleus before the repulsive force on it becomes large enough to turn it back, but the repulsive force can then be very large, and can result in a large deflection. At the same time, when the α-particle is near the nucleus, it is relatively far from the negative charges, which are spread over a much larger volume, so that the attractive forces exerted on the α-particle by the electrons can be neglected. For purposes of calculation, Rutherford assumed that the nuclear and α-particle charges act as point charges and that the scattering is caused by the repulsive electrostatic force between the nucleus and the α-particle. If the magnitude of the α-particle charge is $2e$ and that of the nucleus is Ze, where Z is an integer, and if r is the distance between the two charges, the magnitude of this force is

$$F = \frac{2Ze^2}{r^2}. \tag{3-3}$$

In his first calculation, Rutherford treated the case of an atom sufficiently heavy so that the nucleus could be considered to remain at rest during the scattering process. With the above assumptions, the calculation of the orbit of the α-particle is reduced to a familiar problem of classical mechanics, that of the motion of a highly energetic particle under a repulsive inverse square law of force.[5] The orbit is one branch of a hyperbola with the nucleus of the atom as the external focus,* as shown in Fig. 3–1, and the formula for the deflection can be derived from geometrical and physical relationships.

The first step in the derivation of the Rutherford scattering formula is to write down some useful geometrical relationships. In Fig. 3–1, the

* This statement is proved in Appendix IV, where a second derivation of the Rutherford scattering formula is given which contains certain points of special interest.

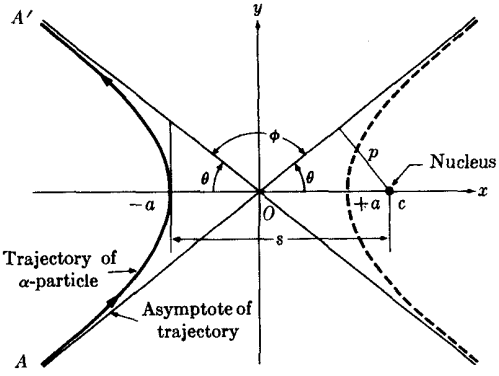

FIG. 3-1. The scattering of an α-particle by the Rutherford nuclear atom.

origin of the coordinate system is taken at the center of the hyperbola, one of whose branches is the path of the α-particle. The initial path of a particle, when the latter is far from the nucleus, is along AO, one of the asymptotes of the hyperbola; the perpendicular distance from the nucleus, situated at the external focus $x = c$, to the line OA is called the *impact parameter* and is denoted by p. The α-particle, on nearing the nucleus, is deflected through the angle ϕ and approaches the asymptote OA'. The vertex of the orbit is at $x = -a$, while that of the second branch of the hyperbola is at $x = a$. The equation of the hyperbola is, from analytic geometry,

$$\frac{x^2}{a^2} - \frac{y^2}{c^2 - a^2} = 1, \tag{3-4}$$

where a is the major semiaxis of the hyperbola. It can also be seen from the figure that $p^2 = c^2 - a^2$, so that p is the minor semiaxis. The eccentricity ϵ is defined as the ratio $\epsilon = c/a$, and the angle between the x-axis and the initial direction of the α-particle is denoted by θ. The angle of deviation ϕ is then equal to $\pi - 2\theta$ radians. Now, let s denote the distance of the nucleus from the vertex of the orbit of the α-particle; the magnitude of s is

$$s = c + a = c\left(1 + \frac{a}{c}\right) = c(1 + \cos\theta).$$

Also, $c = p/\sin\theta$, so that

$$s = \frac{p(1 + \cos\theta)}{\sin\theta} = p\cot\frac{\theta}{2}. \tag{3-5}$$

The next step is to find a relationship between the impact parameter p and the scattering angle ϕ, which can be done by applying the laws of

conservation of energy and angular momentum. According to the former, the sum of the kinetic energy and the potential energy is constant. When the α-particle is at a great distance from the nucleus, its potential energy, which is inversely proportional to this distance, is practically zero. If the velocity of the α-particle is V at this large separation, which is assumed to be infinite, its total energy is equal to its initial kinetic energy, $MV^2/2$, where M is the mass. This energy must also be equal to the total energy of the α-particle when it is just at the vertex of the hyperbola. If the velocity at this point is V_0, then

$$\tfrac{1}{2}MV^2 = \tfrac{1}{2}MV_0^2 + \frac{2Ze^2}{s}. \tag{3-6}$$

The second term on the right represents the potential energy of the α-particle, at the vertex of its orbit, in the electric field of the nucleus. If the last equation is divided through by $\frac{1}{2}MV^2$ and if a new quantity b is introduced, $b = 4Ze^2/MV^2$, the result is

$$\frac{V_0^2}{V^2} = 1 - \frac{b}{s}. \tag{3-7a}$$

When the expression for s from Eq. (3-5) is inserted into the last equation,

$$\frac{V_0^2}{V^2} = 1 - \frac{b}{p}\frac{\sin\theta}{(1+\cos\theta)}. \tag{3-7b}$$

It follows from the law of conservation of angular momentum that

$$MVp = MV_0 s, \tag{3-8}$$

or

$$\frac{V_0}{V} = \frac{p}{s} = \frac{\sin\theta}{1+\cos\theta},$$

and

$$\frac{V_0^2}{V^2} = \frac{\sin^2\theta}{(1+\cos\theta)^2} = \frac{1-\cos\theta}{1+\cos\theta}. \tag{3-9}$$

When this value for $(V_0/V)^2$ is put into Eq. (3-7), it is found that

$$p = \frac{b\tan\theta}{2}, \tag{3-10}$$

and, since $\phi = \pi - 2\theta$,

$$p = \frac{b}{2}\cot\frac{\phi}{2}. \tag{3-11}$$

Equation (3-11) is the desired relation between the impact parameter and the scattering angle.

It is now possible to calculate the fraction of the α-particles scattered through a given angle ϕ. Suppose that the beam of α-particles is incident perpendicularly on a thin foil of material of thickness t, containing n atoms per unit volume. It is assumed that the foil is so thin that the particles pass through without any significant change in velocity and that, with the exception of a few particles which are scattered through a large angle, the beam passes perpendicularly through the foil. Then the chance that a particle passes within a distance p of a nucleus is

$$q = \pi p^2 nt. \tag{3-12}$$

A particle which moves so as to pass within a distance p of the nucleus is scattered through an angle greater than ϕ, where ϕ is given by Eq. (3-11). Hence the fraction of the total number of α-particles deflected through an angle greater than ϕ is obtained by inserting for p, from Eq. (3-11), and

$$q = \tfrac{1}{4}\pi nt b^2 \cot^2 \frac{\phi}{2}. \tag{3-13}$$

Similarly, the probability of deflection through an angle between ϕ and $\phi + d\phi$ is equal to the probability of striking between the radii p and $p + dp$, and is given by

$$dq = 2\pi pnt\, dp.$$

Then,

$$\begin{aligned} dq &= \tfrac{1}{4}\pi nt b^2 \cot \frac{\phi}{2} \operatorname{cosec}^2 \frac{\phi}{2}\, d\phi \\ &= \tfrac{1}{4}\pi nt b^2 \cos \frac{\phi}{2} \operatorname{cosec}^3 \frac{\phi}{2}\, d\phi \\ &= \tfrac{1}{8}\pi nt b^2 \sin \phi \operatorname{cosec}^4 \frac{\phi}{2}\, d\phi. \end{aligned} \tag{3-14}$$

In the experiments made to test the theory, the scattering was determined by counting the number of α-particles incident perpendicularly on a constant area of a zinc sulfide screen placed at a distance R from the foil. The fraction of the scattered α-particles falling on an element of area of the screen at a distance R is given by

$$\frac{dq}{2\pi R^2 \sin \phi\, d\phi} = \frac{nt b^2 \operatorname{cosec}^4(\phi/2)}{16 R^2}. \tag{3-15}$$

If now, Q is the total number of α-particles incident on the foil, and if Y is the number of α-particles scattered to unit area of the zinc sulfide

screen placed at a distance R from the foil and at an angle ϕ with the original direction of the particles, then

$$Y = \frac{Qntb^2 \operatorname{cosec}^4(\phi/2)}{16R^2}. \tag{3-16}$$

According to Rutherford's theory, the number of α-particles falling on a unit area of the zinc sulfide screen at a distance R from the point of scattering should be proportional to

1. $\operatorname{cosec}^4(\phi/2)$, where ϕ is the scattering angle,
2. t, the thickness of the scattering material,
3. $1/(MV^2)^2$, or to the reciprocal of the square of the initial energy of the α-particle,
4. $(Ze)^2$, the square of the nuclear positive charge.

3–3 The experimental test of the Rutherford scattering theory. Rutherford's nuclear theory of the scattering of α-particles was tested point by point in 1913 by Geiger and Marsden.[6] The dependence of the scattering on the four quantities listed at the end of the last section will be considered in order.

1. *The dependence of the scattering on the angle of deflection.* The effect of varying the angle of deflection ϕ was studied in the apparatus shown schematically in Fig. 3–2. In the diagram, R represents a radioactive substance which is the source of the α-particles, F is a very thin foil of scattering material, and S is a zinc sulfide screen rigidly attached to a microscope M. The source and foil were held fixed, while the screen and microscope could be rotated in an airtight joint, varying the angle of deflection. The entire apparatus was enclosed in a metal box which could be evacuated. The number of α-particles reaching unit area of the screen in a chosen time interval was obtained by counting the scintillations. In the experiment, the angle ϕ was varied while all of the other variables in Eq. (3–16) were held constant. The number of scintillations counted, N, is proportional to Y, or to $\operatorname{cosec}^4(\phi/2)$; hence, the ratio $N/\operatorname{cosec}^4(\phi/2)$ should be constant for a given foil under the conditions of the experiment.

The results of two sets of experiments, one with a silver scattering foil, the other with a gold foil, are given in Table 3–1. The first column gives the values of the angle ϕ between the direction of the incident beam of α-particles and the direction in which the scattered particles were counted; the second column gives the corresponding values of $\operatorname{cosec}^4(\phi/2)$. Columns III and V give the observed numbers N of scintillations for silver and gold respectively; columns IV and VI show the value of the ratio $N/\operatorname{cosec}^4(\phi/2)$. The variation in the value of the ratio is very small

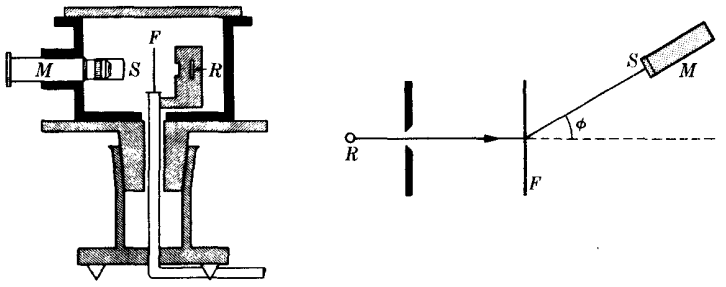

FIG. 3-2. Apparatus of Geiger and Marsden for testing the angular dependence of α-particle scattering.[6]

TABLE 3-1*

THE DEPENDENCE OF THE SCATTERING OF ALPHA-PARTICLES ON THE ANGLE OF DEFLECTION

I	II	III	IV	V	VI
		Silver		Gold	
Angle of deflection ϕ	$\text{cosec}^4(\phi/2)$	Number of scintillations N	$N/\text{cosec}^4(\phi/2)$	Number of scintillations N	$N/\text{cosec}^4(\phi/2)$
150°	1.15	22.2	19.3	33.1	28.8
135	1.38	27.4	19.8	43.0	31.2
120	1.79	33.0	18.4	51.9	29.0
105	2.53	47.3	18.7	69.5	27.5
75	7.25	136	18.8	211	29.1
60	16.0	320	20.0	477	29.8
45	46.6	989	21.2	1435	30.8
37.5	93.7	1760	18.8	3300	35.3
30	223	5260	23.6	7800	35.0
22.5	690	20,300	29.4	27,300	39.6
15	3445	105,400	30.6	132,000	38.4
30	223	5.3	0.024	3.1	0.014
22.5	690	16.6	0.024	8.4	0.012
15	3445	93.0	0.027	48.2	0.014
10	17,330	508	0.029	200	0.012
7.5	54,650	1710	0.031	607	0.011
5	276,300	.....	.....	3320	0.012

* From Geiger and Marsden.[6]

compared with that of $\text{cosec}^4(\phi/2)$, for angles between $\phi = 15°$ and $\phi = 150°$. For smaller angles, it was found desirable to reduce the number of scintillations counted; the value of the ratio was practically constant between $\phi = 5°$ and $\phi = 30°$. The results for the smaller angles can be compared with those of the larger angles by noting that in the case of the gold foil, the number of scintillations was reduced by about 2500. When the results are fitted to those for the larger angles, it is clear that the value of the ratio changes little over the entire range of values of ϕ, while the value of $\text{cosec}^4(\phi/2)$ varies by a factor of 250,000. The deviations of the ratio from constancy were thought to be within the experimental error and it was concluded that the theory predicts the correct dependence of the scattering on the angle of deviation.

2. *The dependence of the scattering on the thickness of the scattering material.* The dependence of the scattering on the thickness of the scattering material was tested by fixing the angle of deflection and using foils of different thicknesses and also of different materials. The results of several experiments are shown in Fig. 3–3, in which the number of particles per minute scattered through an angle of 25° is plotted as ordinate and the thickness t of the scattering foil is plotted as abscissa. The thickness of the foil is expressed in terms of the equivalent length of path in air, that is, the thickness of air which produces the same loss in energy of the α-particles traversing it as that produced by the material being studied. The equivalent path length in air often serves as a useful standard for comparison

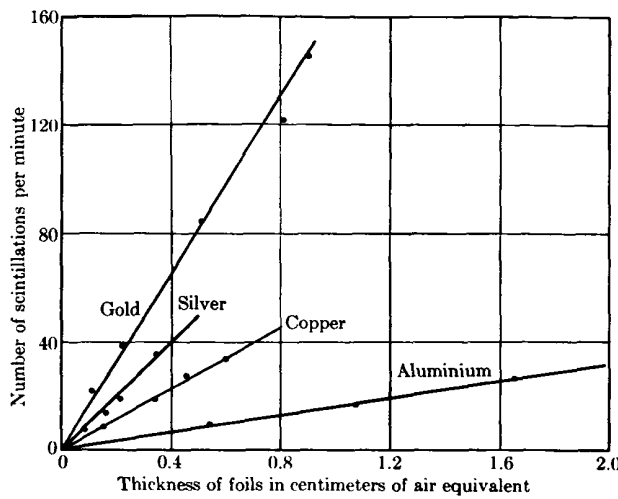

FIG. 3–3. The variation of the scattering of α-particles with the thickness of the scattering material.[6]

in work with α-particles. The straight lines show that for any one element, the number of particles scattered through a given angle per unit time is directly proportional to the thickness of the foil, in agreement with the theory.

3. *The dependence of the scattering on the energy or the velocity of the α-particles.* According to the Rutherford scattering formula, the number of α-particles scattered through an angle ϕ should be inversely proportional to the square of the energy of the particles, or to the fourth power of the velocity. In a series of experiments, Geiger and Marsden varied the velocity of the α-particles from a given source by placing screens of mica between the source and the scattering foil; the thicker the screen, the slower were the particles which reached the scattering foil. The velocities of the particles were determined by finding how far they traveled in air. This distance, called the *range* of the α-particles, could be determined in several ways, which will be discussed in Chapter 13. The range R was known to be related to the velocity by the empirical formula,

$$R = aV^3, \tag{3-17}$$

where a is a known constant. When the velocity of the α-particles which passed through a given thickness of mica screen had been obtained in this way, the scattering through a known angle was measured by counting the number N of scintillations. The product NV^4 should be constant when V is varied. The results of a typical experiment are shown in Table 3-2. The fourth column gives the number N of scintillations per minute under fixed conditions, when α-particles of the ranges given in the second column were used. The relative values of $1/V^4$ are given in the

TABLE 3-2*

THE VARIATION OF ALPHA-PARTICLE SCATTERING WITH VELOCITY

Number of sheets of mica	Range of α-particles (cm)	Relative values of $1/V^4$	Number N of scintillations per minute	NV^4
0	5.5	1.0	24.7	25
1	4.76	1.21	29.0	24
2	4.05	1.50	33.4	22
3	3.32	1.91	44	23
4	2.51	2.84	81	28
5	1.84	4.32	101	23
6	1.04	9.22	255	28

* From Geiger and Marsden.[6]

third column. The product NV^4 given in the last column is very nearly constant over the range of values of V studied, showing that the scattering varies inversely as the fourth power of the velocity, as predicted by Rutherford's theory.

4. *The dependence of the scattering on the nuclear charge.* The scattering angle, the thickness of the scatterer, and the velocity of the incident α-particles are quantities which could be measured directly and their effect on the scattering determined. The nuclear charge, unlike the other parameters, could not be measured directly, and a direct comparison between theory and experiment could not be made in this case. It is evident from Eq. (3–16), however, that the value of Z can be found by counting the number of α-particles in the beam incident on the scattering foil and the number in the scattered beam under fixed geometric conditions. Some information about Z could also be obtained from experiments on the scattering by different foil materials. From these two types of experiments it was found that for elements heavier than aluminum, the positive charge Ze on the nucleus was approximately $\frac{1}{2}Ae$, that is, $Z \approx A/2$, where A is the atomic weight and e is the electronic charge. These experiments were not accurate enough to provide a reliable determination of the nuclear charge Z. It was not until 1920 that Chadwick,[7] using improved scattering techniques, succeeded in measuring the nuclear charge with good precision. For platinum, silver, and copper foils, he obtained

$$\begin{aligned} \text{copper:} \quad & Z = 29.3 \pm 0.5, \\ \text{silver:} \quad & Z = 46.3 \pm 0.7, \\ \text{platinum:} \quad & Z = 77.4 \pm 1. \end{aligned}$$

These results are not precise enough to determine unique, integral values of Z, but, as will be seen in the next chapter, they agree well with the values 29, 47, and 78 for the three elements, obtained by an entirely independent method. Thus, all four tests of the Rutherford scattering theory were met successfully and constitute the earliest if not the greatest single piece of experimental evidence for the nuclear model of the atom.

3–4 Some characteristics of the atomic nucleus. The remarkably good agreement between the predictions of Rutherford's theory and the experimental results was interpreted as establishing the correctness of the concept of the nuclear atom. Since 1913 the atom has therefore been considered to consist of a minute, positively charged nucleus around which is distributed, in some way, an equal and opposite negative charge in the form of electrons.

So far, the atomic nucleus itself is a vague concept. It has been described as "minute" or "very small" and has been treated mathematically as a

point; at the same time, it is supposed to contain practically all of the mass of the atom. It is clear that quantitative information is now needed about the size of the nucleus. The first information of this kind was obtained from the experiments on the scattering of α-particles; it came from the consideration of the distance of closest approach of an α-particle to a nucleus, and of the range of validity of the Coulomb force law.

For any hyperbolic orbit, the distance of closest approach is s, the distance from the vertex of the hyperbola to the nucleus as given by Eq. (3–5). The smallest value that s can have is that for a head-on collision, when the α-particle is deflected through an angle of 180°. In such a collision, the velocity of the α-particle at the turning point is just zero. It follows from Eq. (3–7a), that for V_0 to vanish, s must be equal to b; furthermore, since V_0 can never be negative, this is the smallest value which s may have. Hence, the quantity b, defined by

$$b = \frac{4Ze^2}{MV^2}, \tag{3–18}$$

gives the closest distance which an α-particle of velocity V can approach to a nucleus of charge Z. The magnitude of this distance can be estimated by calculating a typical value of b. Consider the case of a copper nucleus bombarded by α-particles from radon. Copper has an atomic weight of 63.5; if the results of Geiger and Marsden for Z as given by scattering experiments are used, then Z for copper is approximately half of 63.5, or 32. An α-particle has a mass four times that of the hydrogen atom, or $4 \times 1.67 \times 10^{-24}$ gm; the velocity of an α-particle from radon is close to 1.6×10^9 cm/sec. With $e = 4.8 \times 10^{-10}$ esu, the result for b is

$$b = \frac{4(32)(4.8)^2 10^{-20}}{(1.67)4(10^{-24})(1.6)^2(10^{18})} \approx 1.7 \times 10^{-12} \text{ cm}.$$

The above calculation depends on the assumption that the Coulomb force law between the α-particle and the nucleus is still valid at such small distances from the nucleus. The validity of this assumption was borne out by the agreement between the Rutherford scattering theory and the results of the experiments of Geiger and Marsden. By using faster α-particles, Rutherford and others extended the experiments to see how close to the nucleus the $1/r^2$ force law holds. The results showed that for silver the Coulomb law held down to 2×10^{-12} cm, for copper down to 1.2×10^{-12} cm, and for gold down to 3.2×10^{-12} cm. It might be expected that if an α-particle approaches more closely to a nucleus, the inverse square law would eventually break down. If this happens, the forces between the α-particle and the nucleus should begin to change very rapidly with the distance, and the scattering of α-particles should depart widely

from the predictions of the theory. If the nucleus is *defined* as the region of deviation from the Coulomb force law, then for the elements mentioned, the radii of the respective nuclei are smaller than the distances listed. Thus, the nuclei of these elements are about 10^{-12} cm in radius, and are indeed very small compared with an atom, with its radius of 10^{-8} cm. It will be seen in later chapters that other methods of estimating values of nuclear radii give results in good agreement with that just obtained.

It is seen from Eq. (3–18) that for α-particles of a given energy the distance of closest approach is proportional to the nuclear charge Z. On the basis of the finding that Z was approximately proportional to the atomic weight, it was expected that α-particles might come closer than 10^{-12} cm to light nuclei, and that it might be possible to find departures from the Coulomb force law. Theoretical and experimental studies showed that such departures from the inverse square law do indeed exist.[8] In the case of aluminum, the inverse square law was found to break down at about 6 to 8×10^{-13} cm, with similar results for other light elements. The deviations from the inverse square law scattering showed that very close to the nucleus, the repulsion was smaller than that calculated from the Coulomb force alone. These results provided the first evidence of the existence of a nonelectrical, specifically nuclear force.

The study of the scattering of α-particles has continued to be an important source of information concerning the atomic nucleus.[9,10,11] By 1935, data had been collected on the elastic scattering of α-particles from most of the light elements through aluminum. In each case departures from Coulomb scattering were observed. With the aid of newer theoretical methods, these data could be used to make quantitative estimates of nuclear radii. It was shown[9] that the data could be interpreted in a consistent way if the radius of the nucleus is assumed to be approximately proportional to the cube root of the atomic weight, that is, if

$$r = r_0 A^{1/3},$$

where A is the atomic weight, and $r_0 = 1.4$ to 1.5×10^{-13} cm. This property will be discussed further in Chapter 13.

Chapter (2) : The constitution of the nucleus .

THE CONSTITUTION OF THE NUCLEUS

In the last chapter, it was shown that the application of quantum theory to the nuclear model of the atom led to the development of a satisfactory theory for those properties of atoms that depend on the extranuclear electrons. The development of a theory of the nucleus is a more difficult problem. The density of matter in the nucleus offers a clue to the source of the difficulty. The work of Rutherford and his colleagues on the scattering of α-particles showed that the atomic nucleus has a radius of 10^{-12} to 10^{-13} cm, so that the volume of the nucleus is of the order of 10^{-36} cm^3 or less. Now, the mass of one of the lighter atoms is about 10^{-24} gm, and it is almost all concentrated in the nucleus, with the result that the density of the nucleus is at least 10^{12} gm/cm^3. A density of this magnitude is inconceivably large, and it is clear that in the atomic nucleus, matter is put together in a way which may not be amenable to ordinary experimental and theoretical methods of analysis. Consequently, the interpretation of the nuclear properties of atoms in terms of a theory of nuclear structure presents great problems.

There is now available a large amount of experimental information about nuclei, derived from work in several fields: (1) the precise measurement of the masses of atoms; (2) radioactivity, natural and artificial; (3) the artificial transmutation of nuclei by bombardment with particles from radioactive substances or with high-speed particles produced by laboratory methods; (4) optical spectroscopy in the visible and ultraviolet regions; (5) the direct measurement of certain nuclear properties, such as spin and magnetic moment. The main problems of nuclear physics are the collection and correlation of the experimental facts and their interpretation in terms of a theory or model of the nucleus. In this chapter, the problem of the constitution of the nucleus will be discussed, and some ideas will be developed which will be useful in the interpretation of experimental data in the following chapters. In addition, some new and unfamiliar properties of the nucleus will be considered.

8–1 The proton-electron hypothesis of the constitution of the nucleus. The fact that certain radioactive atoms emit α- and β-rays, both of which are corpuscular in nature, led to the idea that atoms are built up of elementary constituents. As early as 1816, on the basis of the small number of atomic weights then known, Prout suggested that all atomic weights are whole numbers, that they might be integral multiples of the atomic

weight of hydrogen, and that all elements might be built up of hydrogen. Prout's hypothesis was discarded when it was found that the atomic weights of some elements are fractional, as for example, those of chlorine (35.46) and copper (63.54). Nevertheless, so many elements have atomic weights which are very close to whole numbers that there seemed to be some basis for Prout's hypothesis. The idea that all elements are built up from one basic substance received new support during the early years of the 20th century when the study of the radioactive elements led to the discovery of isotopes. It was found that there are atomic species which have different masses in spite of the fact that they belong to the same element and have the same atomic number and chemical properties; the different species belonging to the same element are called *isotopes*. For example, four radioactive isotopes of lead were discovered with atomic weights of 214, 212, 211, and 210, as well as three nonradioactive isotopes with atomic weights of 206, 207, and 208. The nuclei of these isotopes, varying in mass from 206 to 214, show a wide range of stability as measured by the extent of their radioactivity, although all have the same charge.

The proof of the existence of isotopes in the radioactive elements led to experiments to test whether some of the ordinary elements also consist of a mixture of isotopes. It was found that this is indeed the case. Most elements are mixtures of isotopes, and the atomic masses of the isotopes are very close to whole numbers. Chlorine, as found in nature, has two isotopes with atomic weights of 34.98 and 36.98, respectively; 75.4% of the chlorine atoms have the smaller mass, while 24.6% have the greater mass, and this distribution explains the atomic weight 35.46 of chlorine. Analogous results were obtained for copper. The different isotopes of an element have the same number and arrangement of extranuclear electrons, and consequently their spectra have the same general structure; they are distinguished from one another by their different atomic masses.

The fact that the atomic masses of the isotopes of an element are close to whole numbers led Aston to formulate his *whole number rule*. According to this rule, which is really a modified form of Prout's hypothesis, all atomic weights are very close to integers, and the fractional atomic weights determined by chemical methods are caused by the presence of two or more isotopes each of which has a nearly integral atomic weight. Much of the experimental work on isotopes involved the analysis of the positive rays from different substances; and in all the work of this kind the lightest positively charged particle that was ever found had the same mass as the hydrogen atom, and carried one positive charge equal in magnitude to the electronic charge, but of opposite sign. This particle is evidently the nucleus of a hydrogen atom and, as shown in Chapter 1, has a mass very close to *one* atomic mass unit. The combination of the whole number rule and the special properties of the hydrogen nucleus led to the assump-

tion that atomic nuclei are built up of hydrogen nuclei, and the hydrogen nucleus was given the name *proton* to indicate its importance as a fundamental constituent of all atoms.

The whole number rule is actually an approximation, holding to an accuracy of about 1 part in 1000. The most precise experiments show that there are small but systematic departures from this rule over the whole range of elements. It will be shown in the next chapter that these variations are of great importance in adding to our knowledge of the structure of nuclei.

To account for the mass of a nucleus whose atomic weight is very close to the integer A, it was necessary to assume that the nucleus contained A protons. But if this were the case, the charge on the nucleus would be equal to A, nearly the same as the atomic weight and not equal to the atomic number Z, which is half, or less, of the atomic weight. To get around this difficulty, it was assumed that in addition to the protons, atomic nuclei contained $A - Z$ electrons; these would contribute a negligible amount to the mass of the nucleus, but would make the charge equal to $+Z$, as required. It was thus possible to consider the atom as consisting of a nucleus of A protons and $A - Z$ electrons surrounded by Z extranuclear electrons. The number A is called the *mass number* and is the integer closest to the atomic weight.

The proton-electron hypothesis of the nucleus seemed to be consistent with the emission of α- and β-particles by the atoms of radioactive elements. The interpretation of certain generalizations about radioactivity in terms of the nuclear atom showed that both the α- and β-particles were ejected from the nuclei of the atoms undergoing transformation; and the presence of electrons in the nucleus made it seem reasonable that under the appropriate conditions one of them might be ejected. It was also reasonable to assume that α-particles could be formed in the nucleus by the combination of four protons and two electrons. The α-particles could exist as such, or they might be formed at the instant of emission.

8–2 The angular momentum of the nucleus; failure of the proton-electron hypothesis. Although the hypothesis that nuclei are built up of protons and electrons had some satisfactory aspects, it eventually led to contradictions and had to be abandoned. One of the failures of the hypothesis was associated with a hitherto unknown property of the nucleus, the angular momentum. The discovery that the atomic nucleus has an angular momentum, or *spin*, with which is associated a magnetic moment, was the result of the detailed study of spectral lines. When individual components of multiplet lines were examined with spectral apparatus of the highest possible resolution, it was found that each of these components is split into a number of lines lying extremely close together; this further

splitting is called *hyperfine structure*. The total splitting, in units of wave number, is only about 2 cm^{-1} or less. The hyperfine structure could not be accounted for in terms of the extranuclear electrons, and it was necessary to assume, as Pauli did in 1924, that it is related to properties of the atomic nucleus. The properties associated with the hyperfine structure are the mass and angular momentum of the nucleus.

It was shown in Chapter 7 that because of the simultaneous motion of nucleus and electron around the common center of gravity, the Rydberg constant of an element depends on the mass of the atomic nucleus. Hence, if an element has more than one isotope, each isotope has a slightly different value of the Rydberg constant, and corresponding spectral lines of different isotopes have slightly different wave numbers. This effect has been found experimentally, and the theoretical predictions have been confirmed. In many cases, however, the isotope effect is not enough to explain the hyperfine structure because the number of components is greater than the number of isotopes. Elements which have only one isotope, such as bismuth, also show hyperfine structure. In these cases, the hyperfine structures can be accounted for quantitatively if it is assumed, as for the extranuclear electrons, that the nucleus has an angular momentum.

A magnetic moment is associated with the angular momentum of the nucleus just as one is associated with the angular momentum of an electron. The two magnetic moments interact, and the interaction energy perturbs the total energy of the electrons; there is, therefore, a splitting of the atomic levels, which gives rise to the hyperfine structure of the lines of the atomic spectrum. The multiplicity and the relative spacings of the lines can be derived theoretically and depend on the magnitudes of the nuclear angular momentum and magnetic moment. The nuclear angular momentum can then be deduced from the experimentally determined multiplicity and relative spacings. Newer methods, which involve radiofrequency spectroscopy, microwave spectroscopy, or the deflection of molecular beams in magnetic fields, have been developed for measuring the nuclear magnetic moment, and a large body of experimental information has been built up concerning these nuclear properties.

The nuclear angular momentum has quantum mechanical properties analogous to those of the angular momentum of the electron. It is a vector, **I**, of magnitude $\sqrt{I(I+1)}\,h/2\pi$, where I is the quantum number which defines the greatest possible component of **I** along a specified axis, according to the rule

$$I_z = I\,\frac{h}{2\pi}. \tag{8-1}$$

The value of I has been found experimentally to depend on the mass

number A of the nucleus; if A is even, I is an integer or zero; if A is odd, I has an odd half-integral value (half of an odd integer). In other words, if the mass number of the nucleus is even, I may have one of the values: 0, 1, 2, 3, . . .; if A is odd, I may have one of the values $\frac{1}{2}$, $\frac{3}{2}$, $\frac{5}{2}$, ...

The rules just cited lead to one of the failures of the proton-electron hypothesis for the constitution of the nucleus. Nitrogen has an atomic number of 7 and a mass number of 14, and its nucleus would have 14 protons and 7 electrons under this hypothesis. The contribution of the protons to the angular momentum should be an integral multiple of $h/2\pi$, whether the angular momentum of a proton is an integral or odd half-integral multiple of $h/2\pi$. An electron has spin $\frac{1}{2}(h/2\pi)$ so that its total angular momentum is always an odd half-integral multiple of $h/2\pi$ (see Section 7–9). The contribution of 7 electrons is, therefore, an odd half-integral multiple of $h/2\pi$, and the total angular momentum of the nitrogen nucleus should be an odd half-integral multiple of $h/2\pi$. But the angular momentum of the nitrogen nucleus has been found experimentally to be $I = 1$, an integer, in contradiction to the value predicted by the hypothesis. Experiments show that the proton, like the electron, has an intrinsic spin of $\frac{1}{2}(h/2\pi)$, and it is possible with this additional information to predict the angular momenta of many other nuclei on the basis of the proton-electron hypothesis. Thus, the isotopes of cadmium ($Z = 48$), mercury ($Z = 80$), and lead ($Z = 82$) with odd mass numbers should each have an odd number of electrons and an even number of particles all together. The angular momenta of these nuclei should, therefore, be zero or integral; they have been found experimentally to be odd half-integers, and the hypothesis again predicts values which disagree with the experimental results.

The proton-electron hypothesis also fails to account for the order of magnitude of nuclear magnetic moments. Measurements of the magnetic moments of many nuclei have given values which are only about 1/1000 of the value of the magnetic moment of the electron. The magnitude of the latter is

$$\mu_B = \frac{eh}{4\pi mc}, \tag{8–2}$$

where m is the mass of the electron; this quantity is called the *Bohr magneton* and has the value 0.92×10^{-20} erg/gauss. All measured nuclear magnetic moments are of the order 10^{-23} erg/gauss, and their values can be expressed appropriately in terms of the quantity

$$\mu_N = \frac{eh}{4\pi M_H c} = 0.505 \times 10^{-23} \text{ erg/gauss}, \tag{8–3}$$

in which the electron mass has been replaced by the proton mass; the

quantity μ_N is called the *nuclear magneton*. Measured values of the nuclear magnetic moment vary from zero to about 5 nuclear magnetons, and the proton has a magnetic moment of 2.7926 ± 0.0001 nuclear magnetons. If electrons were present in the nucleus, we should expect to find nuclear magnetic moments of the order of magnitude of the Bohr magneton, at least in those nuclei for which $A - Z$ is odd (and which would, on the proton-electron hypothesis, contain an odd number of electrons). The fact that nuclear magnetic moments are only of the order of magnitude of the nuclear magneton is, therefore, another strong argument against the existence of electrons inside the nucleus.

There is also a wave-mechanical argument against the existence of free electrons in the nucleus. According to the uncertainty principle (cf. Section 7–8),

$$\Delta x \Delta p \sim h, \tag{8–4}$$

where Δx is the uncertainty in the position of a particle and Δp is the uncertainty in its momentum. Suppose that the principle is applied to an electron in the nucleus. The uncertainty Δx in the position of an electron is roughly the same as the diameter of the nucleus, which is assumed here to be 2×10^{-12} cm. Then

$$\Delta p \sim \frac{h}{\Delta x} = \frac{6.6 \times 10^{-27}}{2 \times 10^{-12}} = 3.3 \times 10^{-15} \text{ erg-sec/cm}.$$

From the uncertainty in the momentum, it is possible to get a rough estimate of the energy of an electron in the nucleus. Relativistic formulas must be used because the electron moves very rapidly in the nucleus, as will be seen. From Eqs. (6–36) and (6–38), the total energy of a particle can be expressed in terms of the momentum,

$$E^2 = p^2c^2 + m_0^2c^4, \tag{8–5}$$

where m_0 is the rest mass of the electron, and c is the velocity of light. If it is now assumed that the momentum p of the electron is no larger than the values just found for the uncertainty Δp, then $p \simeq 3.3 \times 10^{-15}$, and $p^2c^2 = (3.3 \times 10^{-15})^2(3 \times 10^{10})^2 = 10^{-8}$ erg. This value is much greater than the term $m_0^2c^4 = (9 \times 10^{-28})^2(3 \times 10^{10})^3 \simeq 10^{-12}$, which can consequently be neglected. Then $E^2 \simeq 10^{-8}$ and

$$E \simeq 10^{-4} \text{ erg} = \frac{10^{-4}}{1.6 \times 10^{-12}} \simeq 6 \times 10^7 \text{ ev} = 60 \text{ Mev}.$$

According to this result, a free electron confined within a space as small as the nucleus would have to have a kinetic energy of the order of 60 Mev, and a velocity greater than $0.999c$. Experimentally, however, the electrons

emitted by radioactive nuclei have never been found to have kinetic energies greater than about 4 Mev, or at least an order of magnitude smaller than that calculated from the uncertainty principle. Although the calculation is a rough one, similar results are obtained from more rigorous calculations, and in view of the large discrepancy it seems improbable that nuclei can contain free electrons.

The above argument does not apply to a proton in the nucleus because the proton mass (1.67×10^{-24} gm) is nearly 2000 times as great as the electron rest mass. For the proton in the nucleus, Δx is also about 2×10^{-12} cm, and $\Delta p \simeq 3.3 \times 10^{-15}$ erg-sec/cm. If it is assumed, as in the case of the electron, that the momentum is of the order of the uncertainty in the momentum, then from Eq. (8–5),

$$E^2 \simeq 10^{-8} + (1.67 \times 10^{-24})^2(3 \times 10^{10})^4$$
$$= 10^{-8} + 2.3 \times 10^{-6},$$

and now the first term may be neglected in comparison with the second. Then

$$E \simeq 1.5 \times 10^{-3} \text{ erg} = \frac{1.5 \times 10^{-3}}{1.6 \times 10^{-12}} = 9.4 \times 10^{8} \text{ ev} = 940 \text{ Mev}.$$

This value is only slightly greater than the rest energy of the proton, which is $1.008 \times 931 = 938$ Mev. Hence, the kinetic energy of a proton in the nucleus is of the order of a few Mev, and it should be possible for a free proton to be contained in the nucleus.

8–3 Nuclear transmutation and the discovery of the neutron. The failure of the proton-electron hypothesis of the nucleus was related to the properties of the free electron. It was proposed, therefore, that the electrons are bound to the positively charged particles and have no independent existence in the nucleus. One possibility, which had been suggested by Rutherford as early as 1920, was that an electron and a proton might be so closely combined as to form a neutral particle, and this hypothetical particle was given the name *neutron*. Now, all of the methods that have been discussed so far for detecting particles of nuclear size depend on effects of the particle's electric charge, as deflection in magnetic or electric fields and ionization. The presence of a neutron, which has no charge, would be very hard to detect, and many unsuccessful attempts were made to find neutrons. Finally, in 1932, as one of the results of research on the disintegration or transmutation of nuclei by α-particles, Chadwick demonstrated the existence of neutrons. This discovery opened up a vast field for further experimental work and led to the presently accepted idea of the constitution of the nucleus: that it is built of protons and neutrons.

It has been mentioned that the fact that the masses of the atoms of all elements, or their isotopes, are very close to whole numbers led to the hypothesis that the atomic nucleus is a composite structure made up of an integral number of elementary particles with masses close to unity. If so, it should be possible by suitable means to break down the nucleus and to change one element into another. Radioactivity is a naturally occurring process of this kind. Rutherford and his colleagues used energetic α-particles from radioactive substances as projectiles with which to bombard atomic nuclei in the attempt to produce artificial nuclear disintegrations. They found that when nitrogen was bombarded with α-particles, energetic protons were obtained. The protons were identified by magnetic deflection measurements, and their energies were considerably greater than those of the bombarding α-particles. They must have been shot out from the struck nucleus in such a way that part, at least, of their energy was derived from the internal energy of the nucleus. Cloud-chamber studies of the process showed that the α-particle was captured by the nitrogen nucleus, and then the proton was ejected. This explanation corresponds to the formation from nitrogen (atomic number 7, atomic weight 14) of an atom of atomic number 8 and atomic weight 17, i.e., the oxygen isotope of mass 17. The bombardment with α-particles was found by Rutherford to cause emission of protons from all the elements of atomic number up to 19 with the exception of hydrogen, helium, lithium, carbon, and beryllium. The most marked transmutation effects occurred with boron, nitrogen, and aluminum.

Closer investigation of the bombardment of boron and beryllium by α-particles gave some additional and unexpected results. Bothe and Becker (1930) discovered that these elements emitted a highly penetrating radiation when so bombarded. It was thought that this radiation might be a form of γ-ray of very high energy. Curie and Joliot (1932) found that when the radiation was allowed to fall on substances containing hydrogen, it caused the production of highly energetic protons. Chadwick (1931) was also able to show that the rays emitted from bombarded beryllium gave rise to rapidly moving atoms when allowed to fall on other substances, for example, He, Li, Be, C, O, and N. These results could not be explained under the assumption that the new radiation consisted of high-energy γ-rays. Chadwick finally (1932) proved that the energies of the protons ejected from hydrogenous materials, and of the other rapidly moving atoms, could only be explained on the view that the "rays" from bombarded beryllium actually consisted of particles with a mass close to that of the proton. These particles, unlike protons, produce no tracks in the cloud chamber and no ionization in the ionization chamber. These facts, together with the extremely high penetrating power of the particles, show that the charge of the latter must be zero. Since the new

particle was found to be neutral and to have a mass close to unity, it was identified with Rutherford's neutron. Later measurements have shown that the mass of the neutron is 1.00898 amu, so that it is slightly heavier than the proton, with a mass of 1.00758 amu.

8–4 The proton-neutron hypothesis. The discovery of a particle, the neutron, with an atomic weight very close to unity and without electric charge, led to the assumption that every atomic nucleus consists of protons and neutrons. This hypothesis was used for the first time as the basis of a detailed theory of the nucleus by Heisenberg in 1932. Under the proton-neutron hypothesis, the total number of elementary particles in the nucleus, protons and neutrons together, is equal to the mass number A of the nucleus; the atomic weight is therefore very close to a whole number. The number of protons is given by the nuclear charge Z, and the number of neutrons is $A - Z$.

The new nuclear model avoids the failures of the proton-electron hypothesis. The empirical rule connecting mass number and nuclear angular momentum can be interpreted as showing that the neutron, as well as the proton, has a half-integral spin; the evidence is now convincing that the spin of the neutron is indeed $\frac{1}{2}h/2\pi$. If both proton and neutron have spin $\frac{1}{2}$ then, according to quantum theory, the resultant of the spins of A elementary particles, neutrons and protons, will be an integral or half-integral multiple of $h/2\pi$ according to whether A is even or odd. This conclusion is in accord with all the existing observations of nuclear angular momenta. The value of the magnetic moment of the neutron is close to -2 nuclear magnetons; it is opposite in sign to that of the proton, but not very different in magnitude. The values for both the proton and neutron are consistent with those measured for many different nuclei. Finally, since the mass of the neutron is very close to that of the proton, the argument showing that protons can be contained within the nucleus is also valid for neutrons.

The neutron-proton hypothesis is consistent with the phenomena of radioactivity. Since there are several reasons why electrons cannot be present in the nucleus, it must be concluded that in β-radioactivity, the electron is created in the act of emission. This event is regarded as the result of the change of a neutron within the nucleus into a proton, an electron, and a new particle called a *neutrino*, and both experimental and theoretical evidence offer strong support for this view. In β-radioactivity, then, the nucleus is transformed into a different one with one proton more and one neutron less, and an electron is emitted. An α-particle can be formed by the combination of two protons and two neutrons. It may exist as such in the nucleus, or it may be formed at the instant of emission; the latter possibility is now regarded as more likely.

It must be emphasized, however, that in considering the nuclei of different elements as being built of protons and neutrons, the neutron is not regarded as a composite system formed by a proton and an electron. The neutron is a fundamental particle in the same sense that the proton is. The two are sometimes called *nucleons* in order to indicate their function as the building blocks of nuclei.

One of the main problems of nuclear physics is that of understanding the nature of the forces holding the protons and neutrons together. Much of the research in nuclear physics is aimed at the clarification of the laws of interaction between nuclear particles. This problem will not be treated in a detailed, quantitative way in this book because of its complexity, but it will be discussed in a later chapter. The emphasis in the following chapters will be rather on the facts about nuclei, and on the transformation of one nuclear species into another by the rearrangement of its constituent nucleons. The information accumulated will be considered and interpreted in terms of the proton-neutron hypothesis. This aspect of nuclear physics is analogous to the application of atomic physics to the chemical properties of the elements, and is sometimes referred to among physicists as *nuclear chemistry*.

For the present, it will suffice to point out some of the qualitative properties of the forces between the protons and neutrons in the nucleus. Because of the positive charge of the proton, there must be repulsive, electrostatic forces between the protons tending to push the nucleus apart. It is apparent from the small size and great density of the nucleus that these forces must be very large in comparison with the forces between the nucleus and the extranuclear electrons. Hence, if stable complex nuclei are to exist, there must be attractive forces in the nucleus strong enough to overcome the repulsive forces. These attractive forces are the specifically *nuclear* forces between a proton and a neutron, between two neutrons, or between two protons. They seem to be more complex than the gravitational or electromagnetic forces of classical physics. The nuclear attractive forces must be very strong at distances of the order of the nuclear radius, i.e., they are *short-range* forces. Outside the nucleus, they decrease very rapidly, and the Coulomb repulsive forces responsible for the scattering of α-particles predominate. The magnitude of the nuclear forces is such that the work required to divide a nucleus into its constituent particles (the binding energy of the nucleus) is very much greater than the work needed to separate an extranuclear electron from an atom. Whereas the latter is of the order of electron volts, energy changes in the nucleus are of the order of millions of electron volts. It is the magnitude of the energies associated with nuclear transformations that is responsible for the large-scale applications of nuclear physics, and for the rise of the new field of nuclear engineering.

8-5 Magnetic and electric properties of the nucleus. It will be convenient to include in this chapter a few more remarks about the angular momentum of the nucleus, as well as a brief discussion of some magnetic and electric properties of the nucleus. These properties are important in the interpretation of many nuclear phenomena and in the theory of the nucleus, and they occupy a prominent place in nuclear physics. They are, however, among the less elementary aspects of the subject and will not be treated in detail in this book. Nevertheless, some familiarity with the ideas and terminology of these matters will be helpful to the reader.

Each proton and each neutron in the nucleus has an angular momentum which may be pictured as being caused by the particle's spinning motion about an axis through its center of mass. The magnitude of this spin angular momentum is $\frac{1}{2}h/2\pi$. The wave-mechanical properties of an angular momentum of this kind are such that its orientation in space can be described by only two states: the spin axis is either "parallel" or "antiparallel" to any given direction. The component of the spin along a given direction, say the z-axis, is either $\frac{1}{2}h/2\pi$ or $-\frac{1}{2}h/2\pi$. In addition, each nucleon may be pictured as having an angular momentum associated with orbital motion within the nucleus. According to quantum theory, the orbital angular momentum is a vector whose greatest possible component in any given direction is an integral multiple of $h/2\pi$. Each nucleon has a total angular momentum i about a given direction, with

$$i = l \pm s, \tag{8-6}$$

where l is the orbital angular momentum and s is the spin angular momentum. The spin of any single nucleon can add or subtract $\frac{1}{2}h/2\pi$ depending on its orientation with respect to the axis of reference, and i is therefore half-integral. For nuclei containing more than one particle, it is customary to write corresponding relationships between the momenta in capitals; the resultant total angular momentum of the nucleus is then

$$I = L \pm S, \tag{8-7}$$

where L is the total orbital angular momentum, and S is the total spin angular momentum. The total angular momentum is actually a vector, denoted by $\mathbf{I}$, and the scalar quantity I is defined as the maximum possible component of $\mathbf{I}$ in any given direction. The orbital angular momentum L is an integral multiple of $h/2\pi$; S is an even half-integral multiple of $h/2\pi$ if the number of nuclear particles is even, and an odd half-integral multiple if the number of particles is odd. Hence, I is an integral multiple of $h/2\pi$ when A is even, and an odd half-integral multiple when A is odd, in agreement with experimental results.

There are two possible sources of confusion which arise from careless usage. The term "spin" is often used for the total angular momentum of a nucleus rather than for the spin S alone. This incorrect usage was introduced before the problem of the internal structure of nuclei had attained its present importance and has been continued. In addition, the total orbital angular momentum of a nucleus is often denoted by l rather than by L. The meaning of the term "spin" and the symbol l can usually be inferred without difficulty from the context in which they appear.

The magnetic moment of a nucleus can be represented as

$$\boldsymbol{\mu}_I = \gamma_I \frac{h}{2\pi} \mathbf{I} = g_I \mu_N \mathbf{I}, \tag{8-8}$$

where γ_I and g_I are defined by Eqs. (8-3) and (8-8) and are called the *nuclear gyromagnetic ratio* and *nuclear g-factor*, respectively; μ_N is the nuclear magneton defined by Eq. (8-3), and has the numerical value 5.04929×10^{-24} erg/gauss. The quantity which measures the magnitude of $\boldsymbol{\mu}_I$, and is called the nuclear magnetic moment μ_I, is

$$\mu_I = \gamma_I \frac{h}{2\pi} I. \tag{8-9}$$

The details of the methods for measuring nuclear spins and magnetic moments will not be discussed in this book. The interested reader is referred to the works by Ramsey and Kopfermann listed at the end of the chapter, for a treatment of the methods and results. The spins and magnetic moments of many nuclei have been measured, particularly for the ground state of the nucleus, and certain patterns have been observed in the experimental results. Significant conclusions as to the structure of the nucleus may be obtained from data on nuclear spin and magnetic moment, just as knowledge of the arrangement of the extranuclear electrons was obtained from information about their angular momenta. It has been found, for example, that $I = 0$ for nuclei containing even numbers of protons and neutrons. It follows from Eq. (8-9) that a so-called even-even nucleus should have no magnetic moment, and this has been found experimentally to be the case. This generalization, and others, have proved very useful in the study of nuclear structure and other properties.

Another property which is highly important in connection with the *shape* of the nucleus is the *electric quadrupole moment*. This quantity, which cannot be discussed in a simple way, is a measure of the deviation of a nucleus from spherical symmetry. If a nucleus is imagined to be an ellipsoid of revolution whose diameter is $2b$ along the symmetry axis and $2a$ at right angles to this axis, and if the electric charge density is assumed

uniform throughout the ellipsoid, the quadrupole moment Q is given by

$$Q = \tfrac{2}{5} Z(b^2 - a^2). \tag{8–10}$$

Its magnitude depends on the size of the nucleus, the extent of the deviation from spherical symmetry, and the magnitude of the charge; the sign may be positive or negative. Many nuclei have been found to have quadrupole moments; thus, deuterium, a nucleus with one proton and one neutron, has a Q-value of $+0.00274 \times 10^{-24}$ cm^2, while an isotope of lutecium containing 176 nucleons has a Q-value of 7×10^{-24} cm^2. The investigation of quadrupole moments along with spins and magnetic moments has led to important developments in the theory of nuclear structure, as will be shown in Chapter 17.

8–6 Additional properties of atomic nuclei. In addition to their electric and magnetic properties, nuclei have certain properties which are not obviously physical in nature. Although these properties will not be treated in detail, the reader should at least know of the existence and usefulness of the concepts involved. The properties which will be discussed very briefly are the *statistics* to which nuclei are subject, and the *parity*.

The concept of statistics in physics is related to the behavior of large numbers of particles. Thus, the distribution of energies or velocities among the molecules of a gas can be described by the classical Maxwell-Boltzmann statistics, as can many other macroscopic properties of gases. The properties of assemblies of photons, electrons, protons, neutrons, and atomic nuclei cannot, in general, be described on the basis of classical statistics, and two new forms of statistics have been devised, based on quantum mechanics rather than on classical mechanics. These are the Bose-Einstein statistics, and the Fermi-Dirac statistics. The question of which form of quantum statistics applies to a system of particles of a given kind is related to a particular property of the wave function which describes the system. This property has to do with the effect on the wave function of interchanging all of the coordinates of two identical particles, say of two protons in a nucleus. A nucleon is described by a function of its three space coordinates and the value of its spin, whether it is $\frac{1}{2}h/2\pi$ or $-\frac{1}{2}h/2\pi$. The Fermi-Dirac statistics apply to systems of particles for which the wave function of the system is *antisymmetrical*, i.e., it changes sign when *all* of the coordinates (three spatial and one spin) of two identical particles are interchanged. It follows from this property of the wave function that each completely specified quantum state can be occupied by only one particle; that is, the Pauli exclusion principle applies to particles obeying the Fermi-Dirac statistics. It has been deduced from experiments that electrons, protons, and neutrons obey

the Fermi-Dirac statistics, as do all nuclei of odd mass number A. In the Bose-Einstein statistics, the wave function is symmetrical, i.e., it does not change sign when all the coordinates of any pair of identical particles are interchanged. Two or more particles may be in the same quantum state. All nuclei having even mass number A obey the Bose-Einstein statistics. There is a direct correlation between the total angular momentum of a nucleus and its statistics: Fermi-Dirac particles (odd A) have total nuclear angular momenta which are odd half-integral multiples of $h/2\pi$, while Bose-Einstein particles (even A) have momenta which are integral multiples of $h/2\pi$.

The last property that will be mentioned is the *parity*. To a good approximation, the wave function of a nucleus may be expressed as the product of a function of the space coordinates and a function depending only on the spin orientation. The motion of a nucleus is said to have *even parity* if the spatial part of its wave function is unchanged when the space coordinates (x,y,z) are replaced by $(-x, -y, -z)$. This transformation of coordinates is equivalent to a reflection of the nucleus' position about the origin of the x, y, z system of axes. When reflection changes the sign of the spatial part of the wave function, the motion of the nucleus is said to have *odd parity*. It has been shown that the parity of a nucleus in a given state is related to the value of the orbital angular momentum L; if L is even, the parity is even; if L is odd, the parity is odd. A system of particles will have even parity when the sum of the numerical values for L for all its particles is even, and odd parity when the sum is odd. Although the parity seems to be an abstract sort of property, the selection rules for many nuclear transitions involve conditions on the parity, as well as on the total angular momentum.

Chapter (3) : isotopes.

9–3 Isotopic masses and abundances: the mass spectrograph and mass spectrometer. The Thomson parabola method of analyzing positive rays was adequate for a general survey of masses and velocities, but it could not yield precise values of isotopic masses and abundances. The further quantitative study of the constitution of the elements required the determination of isotopic masses with a precision of at least one part in a thousand. To meet this need, Aston[3] (1919) designed the mass spectrograph. Aston's method of analysis was an improvement on that of Thomson in that greater dispersion was achieved (i.e., greater separation of ions of different masses) and all ions with a given value of q/M were brought to a focus instead of being spread out in a parabola. By these means, greater sensitivity and precision were attained.

A schematic diagram of Aston's first mass spectrograph is shown in Fig. 9–3. The positive rays from a discharge tube pass through two very narrow parallel slits S_1 and S_2 and enter the space between the metal plates P_1 and P_2. An electric field between these plates causes a deflection of the ions toward P_2, the amount of the deflection being greater the smaller the velocity of the ions. The narrow beam contains particles with a wide range of velocities, with the result that it is broadened as it passes through the field. A group of these particles is selected by means of the relatively wide diaphragm D. After passing through D, this diverging stream of ions enters a magnetic field, indicated by the circle at O, perpendicular to the plane of the paper. The magnetic field causes deflections, as shown in the diagram, the more slowly moving ions being deflected more than the faster ones. The paths of the slow-moving ions, therefore, intersect those of the faster-moving ions at some point F. If the instrument is properly designed, ions having the same value of q/M but slightly different energies can be brought to a single focus on a photographic plate. Other ions with the same range of energies but a different value of q/M are brought to a focus at a different point on the photographic plate. The

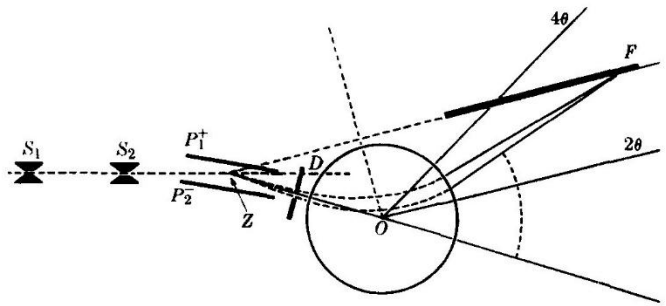

FIG. 9–3. Diagram of Aston's first mass spectrograph (1920).

focus for a particular value of q/M is actually a line, and the result of an analysis is a series of lines reminiscent of an optical line spectrum. Because of this similarity, the series of lines is called a *mass spectrum* and the apparatus a *mass spectrograph*. Some typical mass spectra are shown in Fig. 9–4.

The isotopic masses can be determined quantitatively in several different ways. In one method, for example, the positions of the lines caused by the masses in question are compared with the positions of the lines caused by standard substances whose masses are accurately known. With this new instrument, Aston was able to prove beyond a doubt that neon has two isotopes with masses very close to the integers 20 and 22, respectively.[4] He also showed that in the mass spectrum of chlorine there was no line corresponding to the chemical atomic weight (35.46) of chlorine. Instead, *two* lines were seen, corresponding very closely to the masses 35.0 and 37.0, the former being the more intense line. This result showed that chlorine has two isotopes of nearly integral atomic mass, and ordinary chlorine is a mixture of these two kinds of atoms in such proportions that the chemical atomic weight is 35.46.

Aston improved the design of the mass spectrograph, and in his second instrument[5] isotopic masses could be determined with an accuracy of 1 part in 10,000. With this instrument, Aston determined the masses of the isotopes of a large number of elements, as well as their abundances, and showed that the masses of atoms are very nearly, *but not quite*, integers, when the mass of oxygen is taken as 16. For example, the isotopes of chlorine were found to have the masses 34.983 and 36.980 rather than 35.0 and 37.0, respectively. Later instruments designed and built by Aston, Dempster, Bainbridge, Jordon, Mattauch, and others have yielded isotopic masses with accuracies approaching 1 part in 100,000.

Modern mass spectroscopic measurements are based on the *mass-doublet* technique in which the quantity actually determined is the difference in mass between two ions of the same mass number but having slightly different masses. The newer spectrometers yield high dispersion,

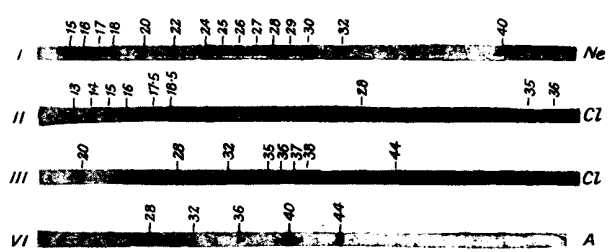

FIG. 9–4. Mass spectra obtained by Aston with his first spectrograph (1920).

that is, the distance between the two lines of a doublet are relatively large, and differences in mass can be measured with high precision. The mass of one of the members of the doublet must be known accurately. Hydrocarbon compounds (which give molecular ions) are used as sources of reference masses because of the relative ease with which fragments of almost any mass number can be obtained for comparison with other ions of the same mass number. The masses of C^{12}, the carbon isotope of mass number 12, and H^1, the hydrogen isotope of mass number 1, are used as secondary standards, with 0^{16} the primary standard.

The masses of C^{12} and H^1 relative to that of 0^{16} can be determined in a number of different ways. One method is to measure the following mass-doublet differences:

$$(0^{16})_2 - S^{32} = a,$$
$$(C^{12})_4 - S^{32}O^{16} = b,$$
$$C^{12}(H^1)_4 - O^{16} = c.$$

The three equations are solved simultaneously, with $O^{16} = 16$ atomic mass units (exactly), and the result is

$$S^{32} = 32 - a,$$
$$C^{12} = 12 + \frac{b - a}{4},$$
$$H^1 = 1 + \frac{a - b + c}{16}.$$

More complicated cycles involving a larger number of atoms can also be used, and highly precise results can be obtained; values of mass-doublet differences have been compiled,[6,7] and values of atomic masses determined by this method.[8–17]

It will be seen in Chapter 11 that information from nuclear reactions can also be used to determine atomic masses with precision comparable to that obtained with mass spectroscopic methods. Authoritative compilations of atomic masses usually combine results obtained with both methods.[18–21]

Other techniques have also been developed[22] which will only be mentioned here. The *chronotron* of Goudsmit[23–25] measures the time needed for ions to describe a number of revolutions in a uniform magnetic field. This time is proportional to the mass of the ion, with the result that the precision is practically constant for all masses, whereas the precision which can be obtained with the mass spectrograph decreases with increasing mass. Another device which depends on the angular

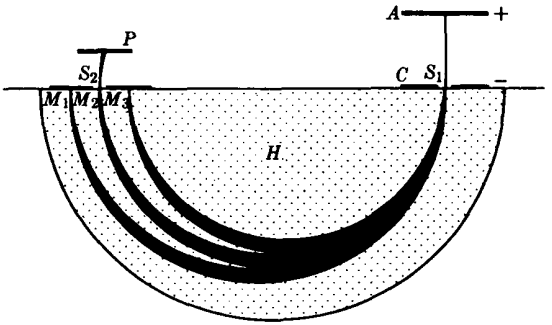

FIG. 9–5. Diagram of Dempster's mass spectrometer.

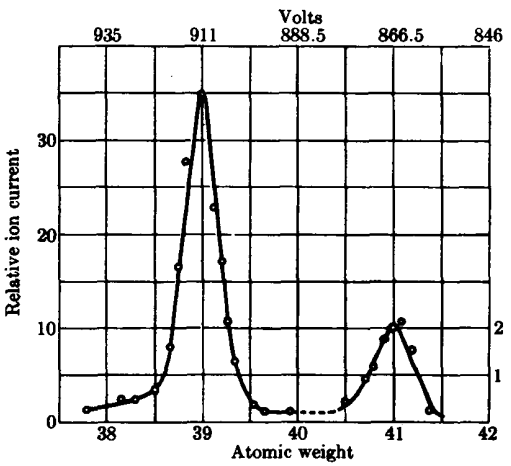

FIG. 9–6. Mass spectrum of potassium (Dempster, 1922).

motion of ions in a known magnetic induction is the *mass synchrometer*,[26] which has given good results. Microwave spectroscopy[27] has also been used successfully for the measurement of atomic masses.

In the systematic study of isotopes, it is essential to know not only the isotopic masses, but also the relative numbers of atoms of each isotope of an element. The mass spectrograph can be used for making abundance measurements, and indeed many of the isotopes now known were first discovered and their abundances measured by Aston by means of this instrument. When used for abundance measurements, however, a mass spectrograph is inconvenient because a photographic plate is used to record the different isotopic ions, and the procedure of determining abun-

dances from the plate traces is both more tedious and less reliable than the direct measurements made with a somewhat simpler instrument, the *mass spectrometer*.

About the time of the development of the mass spectrograph by Aston, Dempster[28] built an instrument which was basically simpler and which was well suited for making abundance measurements, although it could not be used for making accurate mass measurements. It was called a mass spectrometer because the ion current was measured electrically rather than recorded on a photographic plate. A schematic diagram of one of Dempster's spectrometer models is shown in Fig. 9–5. Ions of the element to be analyzed are formed by heating a salt of the element, or by bombarding it with electrons. Upon emerging from the source A, the ions are accelerated through a potential difference V of about 1000 volts by an electric field maintained in the region between A and C. A slit S_1 in the plate C allows a narrow bundle of ions to pass into the region of the magnetic field H. In passing from A to C, the positive ions carrying a charge q acquire energy equal to qV. This energy may also be represented by $\frac{1}{2}Mv^2$, where M is the mass of the positive ion and v its velocity on emerging from the slit in C; consequently,

$$qV = \tfrac{1}{2}Mv^2. \tag{9–4}$$

If the magnetic field is perpendicular to the plane of the paper, the ions

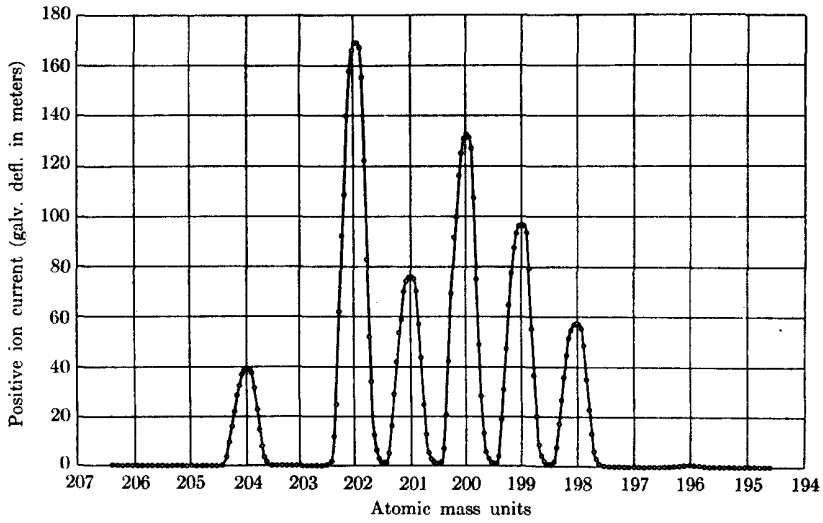

FIG. 9–7. Mass spectrum of mercury (Nier, 1937).

will be forced to move along a circular path defined by the relationship

$$Hqv = \frac{Mv^2}{R}, \tag{9–5}$$

where R is the radius of the circle. Since the radius of the circle must have a certain definite value in order that the ions enter the slit S_2 and be detected by an electrometer at P, it is clear that ions with only one particular value of q/M, say q/M', will be received for a given combination of accelerating potential and magnetic field. By varying the potential difference V, ions with different values of q/M are, in turn, made to pass through the second slit S_2 to the collector plate P. The current recorded by the electrometer is proportional to the number of positive ions reaching it per unit time and, since each accelerating potential corresponds to a definite mass of particle reaching the electrometer, the current can be plotted against the atomic weight. A typical curve obtained by Dempster

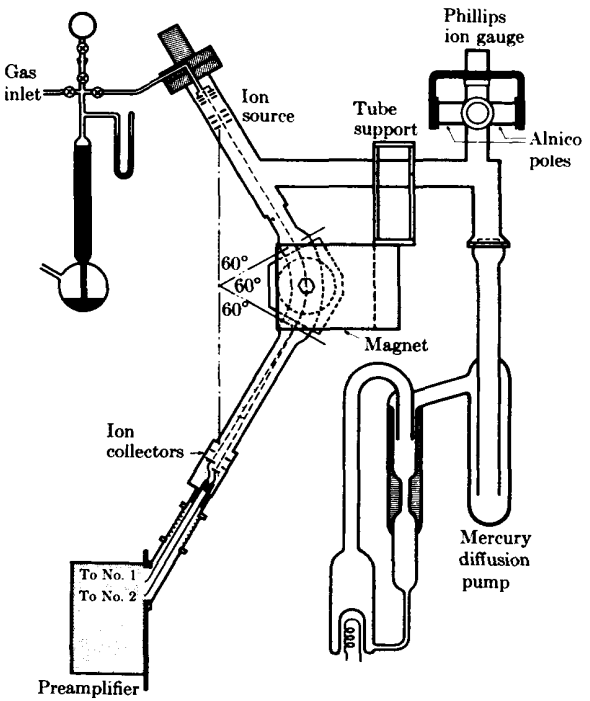

FIG. 9–8. Schematic diagram of a Nier mass spectrometer (Nier[30]).

for potassium with a slightly modified apparatus is shown in Fig. 9–6. There are two isotopes with atomic weights 39 and 41 units, the former being much more abundant; for the ratio of the abundances, Dempster obtained 18:1.

During recent years, owing largely to improved vacuum techniques and the development of new methods of electrical measurement, mass spectrometry has advanced rapidly. One of the most useful instruments was that of Nier,[29] which had extremely high resolving power and sensitivity and was especially designed for searching for rare isotopes and measuring relative abundances. It was a modification of the Dempster apparatus and gave results like those shown in Fig. 9–7. The figure shows a "mass spectrogram" of mercury, and the isotope abundances are closely proportional to the magnitude of the peaks of the positive ion current. A more recent form of spectrometer designed by Nier[30] is shown in Fig. 9–8. Ions are produced by the electron bombardment of the gas under investigation, and are accelerated by a potential drop of about 1000 volts. The beam of ions passes into a wedge-shaped magnetic field in which they suffer a deflection of 60°, rather than 180° as in the Dempster spectrometer. This deflection makes it possible to obtain high resolution with a simple magnet. In the diagram the ion beam is shown broken into two parts which fall on separate collectors and are measured by separate amplifiers. This instrument has been used to get highly precise isotopic abundances.

9–4 The stable isotopes of the elements and their percentage abundances. The mass spectra of the elements have been investigated in detail and the isotopic composition of the elements has been determined.[31,32,33] The results obtained for the isotopes of 83 elements are collected in Table 9–1. Before discussing these results, some remarks about terminology are in order. In recent years, the term *nuclide* has been widely accepted for a species of atom characterized by the constitution of its nucleus, i.e., by the numbers of protons and neutrons it contains. Thus, the atomic species listed in Table 9–1 may be referred to as the naturally occurring stable nuclides. Similarly, every radioactive species is a radioactive nuclide or radionuclide. An isotope is then one of a group of two or more nuclides having the same number of protons or, in other words, having the same atomic number. An element like beryllium or aluminum, of which only one species exists in nature, is said to form a single stable nuclide, rather than a single stable isotope, since the word isotope implies more than one species occupying the same place in the periodic system. A nuclide is usually indicated by the chemical symbol with a subscript at the lower left giving the atomic number, and a superscript at the upper right giving the mass number; in the symbol ${}_Z\mathrm{S}^A$, Z is the atomic number,

TABLE 9–1

THE STABLE NUCLIDES AND THEIR PERCENTAGE ABUNDANCE

Symbol	Atomic number, Z	Mass number, A	Relative abundance, %	Symbol	Atomic number, Z	Mass number, A	Relative abundance, %
H	1	1	99.9849–99.9861	Al	13	27	100
				Si	14	28	92.21
D	1	2	0.0139–0.0151			29	4.70
						30	3.09
He	2	3	$\sim 10^{-5}$–10^{-4}	P	15	31	100
		4	~100				
				S	16	32	95.0
Li	3	6	7.52			33	0.760
		7	92.48			34	4.22
						36	0.014
Be	4	9	100				
				Cl	17	35	75.529
B	5	10	18.45–19.64			37	24.471
		11	80.36–81.55	A	18	36	0.337
						38	0.063
						40	99.600
C	6	12	98.892				
		13	1.108	K	19	39	93.10
						40	0.012
N	7	14	99.634			41	6.88
		15	0.366				
				Ca	20	40	96.97
O	8	16	99.759			42	0.64
		17	0.037			43	0.145
		18	0.204			44	2.06
						46	0.003
						48	0.185
F	9	19	100				
				Sc	21	45	100
Ne	10	20	90.92				
		21	0.257	Ti	22	46	7.93
		22	8.82			47	7.28
						48	73.94
Na	11	23	100			49	5.38
						50	5.34
Mg	12	24	78.70				
		25	10.13	V	23	50	0.24
		26	11.17			51	99.76

TABLE 9–1 (*Continued*)

Symbol	Atomic number, Z	Mass number, A	Relative abundance, %	Symbol	Atomic number, Z	Mass number, A	Relative abundance, %
Cr	24	50	4.31	Br	35	79	50.54
		52	83.76			81	49.46
		53	9.55				
		54	2.38	Kr	36	78	0.354
						80	2.27
Mn	25	55	100			82	11.56
						83	11.55
Fe	26	54	5.82			84	56.90
		56	91.66			86	17.37
		57	2.19				
		58	0.33	Rb	37	85	72.15
						87	27.85
Co	27	59	100				
Ni	28	58	67.88	Sr	38	84	0.56
		60	26.23			86	9.86
		61	1.19			87	7.02
		62	3.66			88	82.56
		64	1.08				
				Y	39	89	100
Cu	29	63	69.1				
		65	30.9	Zr	40	90	51.46
						91	11.23
Zn	30	64	48.89			92	17.11
		66	27.81			94	17.40
		67	4.11			96	2.80
		68	18.56				
		70	0.62	Nb	41	93	100
Ga	31	69	60.4				
		71	39.6	Mo	42	92	15.84
						94	9.04
Ge	32	70	20.52			95	15.72
		72	27.43			96	16.53
		73	7.76			97	9.46
		74	36.54			98	23.78
		76	7.76			100	9.63
As	33	75	100	Ru	44	96	5.51
Se	34	74	0.87			98	1.87
		76	9.02			99	12.72
		77	7.58			100	12.62
		78	23.52			101	17.07
		80	49.82			102	31.61
		82	9.19			104	18.58

(*Continued*)

TABLE 9–1 (*Continued*)

Symbol	Atomic number, Z	Mass number, A	Relative abundance, %	Symbol	Atomic number, Z	Mass number, A	Relative abundance, %
Rh	45	103	100	Te	52	126	18.71
						128	31.79
Pd	46	102	0.96			130	34.49
		104	10.97				
		105	22.23	I	53	127	100
		106	27.33				
		108	26.71	Xe	54	124	0.096
		110	11.81			126	0.090
						128	1.919
Ag	47	107	51.35			129	26.44
		109	48.65			130	4.08
						131	21.18
Cd	48	106	1.215			132	26.89
		108	0.875			134	10.44
		110	12.39			136	8.87
		111	12.75				
		112	24.07				
		113	12.26	Cs	55	133	100
		114	28.86				
		116	7.58	Ba	56	130	0.101
						132	0.097
In	49	113	4.28			134	2.42
		115	95.72			135	6.59
						136	7.81
Sn	50	112	0.96			137	11.32
		114	0.66			138	71.66
		115	0.35				
		116	14.30	La	57	138	0.089
		117	7.61			139	99.911
		118	24.03				
		119	8.58	Ce	58	136	0.193
		120	32.85			138	0.250
		122	4.72			140	88.48
		124	5.94			142	11.07
Sb	51	121	57.25				
		123	42.75	Pr	59	141	100
Te	52	120	0.089	Nd	60	142	27.11
		122	2.46			143	12.17
		123	0.87			144	23.85
		124	4.61			145	8.30
		125	6.99			146	17.22

TABLE 9–1 (*Continued*)

Symbol	Atomic number, Z	Mass number, A	Relative abundance, %	Symbol	Atomic number, Z	Mass number, A	Relative abundance, %
Sm	62	144	3.09	Yb	70	172	21.82
		147	14.97			173	16.13
		148	11.24			174	31.84
		149	13.83			176	12.73
		150	7.44				
		152	26.72	Lu	71	175	97.40
		154	22.71			176	2.60
Eu	63	151	47.82	Hf	72	174	0.18
		153	52.18			176	5.20
						177	18.50
Gd	64	152	0.20			178	27.14
		154	2.15			179	13.75
		155	14.73			180	35.24
		156	20.47				
		157	15.68	Ta	73	181	100
		158	24.87				
		160	21.90	W	74	180	0.135
						182	26.41
Tb	65	159	100			183	14.40
						184	30.64
Dy	66	156	0.0524			186	28.41
		158	0.0902				
		160	2.294	Re	75	185	37.07
		161	18.88			187	62.93
		162	25.53				
		163	24.97	Os	76	184	0.018
		164	28.18			186	1.59
						187	1.64
Ho	67	165	100			188	13.3
						189	16.1
Er	68	162	0.136			190	26.4
		164	1.56			192	41.0
		166	33.41				
		167	22.94	Ir	77	191	37.3
		168	27.07			193	62.7
		170	14.88				
				Pt	78	190	0.0127
Tm	69	169	100			192	0.78
						194	32.9
Yb	70	168	0.135			195	33.8
		170	3.03			196	25.3
		171	14.31			198	7.21

(*Continued*)

TABLE 9–1 (*Concluded*)

Symbol	Atomic number, Z	Mass number, A	Relative abundance, %	Symbol	Atomic number, Z	Mass number, A	Relative abundance, %
Au	79	197	100	Pb	82	204	1.48
						206	23.6
Hg	80	196	0.146			207	22.6
		198	10.02			208	52.3
		199	16.84				
		200	23.13	Bi	83	209	100
		201	13.22				
		202	29.80	Th	90	232	100
		204	6.85				
				U	92	234	0.0056
Tl	81	203	29.50			235	0.7205
		205	70.50			238	99.2739

A is the mass number, and S is the chemical symbol. Thus, the symbol ${}_{50}Sn^{120}$ represents the nuclide with 50 protons and a mass number of 120; it is one of the ten isotopes of tin. The number of neutrons is, of course, equal to $A - Z$. Sometimes it is not necessary to show the number of protons explicitly, and the symbol for a nuclide is then shortened to S^A.

Not all of the nuclides listed in Table 9–1 are actually stable. Thorium and uranium are radioactive, but they occur in sufficient amounts and with sufficiently weak activity so that they can be handled in the same way as the stable elements. At least nine naturally occurring isotopes of "stable" elements show feeble radioactivity: K^{40}, Rb^{87}, In^{115}, La^{138}, Nd^{144}, Sm^{147}, Lu^{176}, Re^{187} and Pt^{190}. These nuclides are distinct from the families or chains of the heavy naturally occurring radionuclides and are much feebler in activity. It is therefore more convenient to include them with the stable elements than with the radioactive ones.

With the exceptions noted, Table 9–1 contains 284 stable nuclides divided among 83 elements. Twenty elements, about one-fourth in all, are single species; all the others consist of two or more isotopes. Hydrogen has two isotopes, the one with mass number 2 having a relative abundance of only about 0.015%. This rare isotope, however, has a mass about double that of the common isotope, so that the difference in mass is as great as the mass of the ordinary hydrogen atom itself. This relationship between the masses is an exceptional one and, as a result, the differences between the properties of the two isotopes are more marked than in any other pair of isotopes. The hydrogen isotope of mass 2 has therefore been given its own name, *deuterium*, with the occasionally used symbol D.

TABLE 9–2

SOME ISOTOPE STATISTICS

	Number of elements	Odd A	Even A	Total	Average number of isotopes
Odd Z	40	53	8	61	1.5
Even Z	43	57	166	223	5.2
Total	83	110	174	284	3.4

Carbon and nitrogen also have two isotopes, while oxygen has three, two of which are rare. Tin has the greatest number of isotopes, ten, while xenon has nine, cadmium and tellurium have eight each, and several elements have seven.

There are some striking regularities in Table 9–1. Nuclides of even Z are much more numerous than those of odd Z, and nuclides of even A are much more numerous than those of odd A. Nearly all nuclides with even A have even Z, the only common exceptions being ${}_1H^2$, ${}_3Li^6$, ${}_5B^{10}$, and ${}_7N^{14}$. The nuclides ${}_{19}K^{40}$ and ${}_{71}Lu^{176}$ have odd Z and even A but are weakly radioactive, while ${}_{23}V^{50}$ and ${}_{57}La^{138}$ are very rare. The numbers of nuclides with the various combinations of even and odd atomic and mass numbers are listed in Table 9–2. Of the 20 elements which have only a single nuclide, only beryllium has an even value of Z, while the other 19 have odd Z. Nineteen elements with odd Z have two isotopes apiece, and each of these nuclides has odd A. One element with odd Z, potassium, has three isotopes; two of these have odd mass numbers, and the only isotope with an even mass number is the weakly radioactive K^{40}. The four common elements which have odd values of Z and A, hydrogen lithium, boron, and nitrogen, have equal numbers of protons and neutrons. The elements which have more than two isotopes (apart from potassium) all have even values of Z.

An examination of the values of Z and A in Table 9–1 shows that in the stable nuclei, with the exception of H^1 and He^3, the number of neutrons is always greater than or equal to the number of protons. There is always at least one neutron for each proton. This property of the stable nuclides is shown in Fig. 9–9, in which the number of neutrons $A - Z$ is plotted against the number of protons. The number of neutrons which can be included in a stable nucleus with a given number of protons is limited. For example, tin with an atomic number of 50 has neutron numbers from 62 to 74, and the mass numbers of the tin isotopes lie between 112 and 124. Apparently the tin nucleus cannot contain less than 62 neutrons nor more than 74 neutrons and still remain stable. For the other elements (except

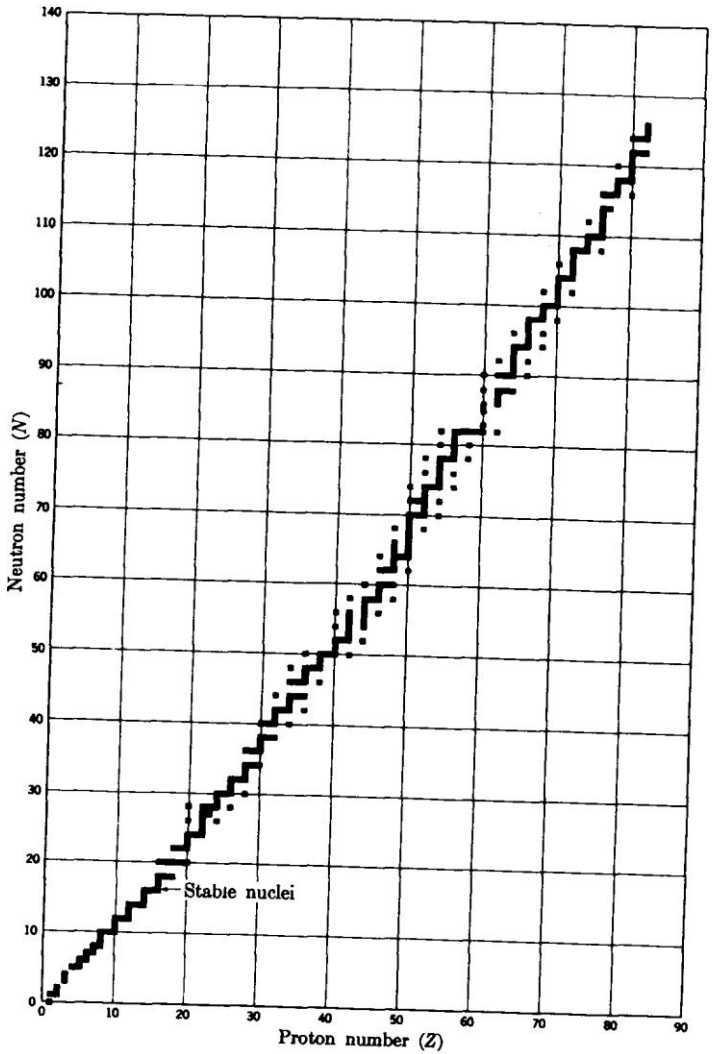

FIG. 9–9. Neutron-proton plot of the stable nuclides.

xenon) this range is smaller and the limits for the existence of stable nuclei are narrower.

The regularities that have just been noted are closely connected with the problem of nuclear stability and must eventually be accounted for in terms of the proton-neutron theory of the nucleus, in particular, in terms of the forces between nucleons. From this standpoint, the hydrogen isotope of mass two (deuterium) is especially important because its nucleus consists of one proton and one neutron. The properties of this nucleus yield information about the force between a proton and a neutron, and deuterium has a prominent place in theoretical nuclear physics.

In the preceding discussion it was assumed that the relative abundance of an isotope is constant in nature, that is, independent of the source of the sample that is measured. This assumption is true, in general. There are, however, some exceptions which, although interesting, do not affect any of the conclusions previously drawn from the consideration of abundances. The relative abundances of H^1 and H^2 depend somewhat on the source, and the spread in the values listed in Table 9–1 shows that the variation is small. The ratio of hydrogen to deuterium abundance has been determined as 6700 ± 50 for samples of tap water from London, Osaka, and various cities in the United States; this corresponds to a value of 0.0149% for the relative abundance of H^2 in tap water. The range 0.0139 to 0.0151% includes the variation over a wide range of substances such as water, snow, ice, organic compounds, and animal and mineral materials from many sources. There are wide variations in the ratio of He^3 and He^4 abundances; for example, the abundance of He^3 is approximately ten times as great in atmospheric helium as in well helium. Helium is formed in radioactive minerals because of alpha-decay, and such helium is all He^4. In nonradioactive ores, the He^3 content varies widely, and it has been suggested that He^3 can be formed as a result of the transformation of various nuclides in the air and on the ground by cosmic-ray bombardment. Cosmic rays are highly penetrating radiations which originate outside the earth and consist of protons, electrons, neutrons, photons, and other particles. The range of abundances of the boron isotopes shown in the table is equivalent to a variation in the B^{11}/B^{10} ratio from 4.27 to 4.42 or about 3%. Although this variation seems small, it affects the use of certain boron standards in nuclear physics; it is necessary, therefore, to cite the abundance ratios when measurements involving this standard are reported. The abundance of the carbon isotopes cited in Table 9–1 are those found in limestone and correspond to a C^{12}/C^{13} ratio of 89.2; in coal the ratio is 91.8. In general, the relative content of C^{12} seems to be somewhat greater in plant material than in limestone.

The relative abundances of the oxygen isotopes also vary, and the value of the O^{16}/O^{18} ratio in nature has a spread of about 4%. The values of

the abundances quoted in the table are those for atmospheric oxygen and correspond to a value of the O^{16}/O^{18} ratio of 489.2 ± 0.7. This value is also correct for the oxygen from limestone, but for oxygen from water or iron ores the ratio may be 4% higher. The values used for the abundances of the oxygen isotopes affect the value of the factor for converting atomic weights from the physical scale to the chemical scale (see Section 9–5). The variation in the value of the conversion factor may be large enough to affect the precision of atomic weight determinations and, if the latter are to be made to more than five significant figures, the isotopic composition of the oxygen used as a reference must be specified.

Wide variations in the abundances of the lead isotopes are also found, and these are usually associated with the radioactive sources from which the different lead samples are derived. Even for common lead, it is not possible to give exact isotopic abundances without specifying the source of the material; the values in the table are for Great Bear Lake galena.

The abundance variations which have been discussed are the most important ones known and, for the remaining elements, either there are no significant variations, or else they do not seriously affect further work in nuclear physics.

9–5 Atomic masses: packing fractions and binding energies. Some atomic masses[18,19,36] are given in Table 9–3. The standard of mass used here is slightly different from that used for the chemical atomic weights. It is seen from Table 9–1 that oxygen actually has three isotopes, the most abundant of which has the mass number 16. The other two isotopes together constitute only about 0.2% of the oxygen atoms. In the determination of isotopic weights by the mass spectrograph it is the practice to take as the standard the value of 16.00000 for the weight of the common isotope of oxygen. The weights so obtained differ slightly from those based on the ordinary chemical atomic weight scale. In the latter case, the number 16.00000 is associated with ordinary atmospheric oxygen, which is a mixture of isotopes, whereas on the mass spectrographic, or physical, atomic weight scale, this is taken as the isotopic weight of the single, most abundant isotope. The relationship between the chemical and physical atomic weight scales may be determined in the following way. Atmospheric oxygen consists of 99.759% of the isotope of mass 16.00000, together with 0.037% of the isotope of mass 17.004529, and 0.204% of the isotope of mass 18.004840. The weighted mean of these values is 16.004462, and this is the atomic weight of atmospheric oxygen on the physical scale, as compared with the postulated value of 16.00000 on the chemical scale. Then

$$\frac{\text{Physical atomic weight}}{\text{Chemical atomic weight}} = \frac{16.004462}{16.000000} = 1.000279.$$

TABLE 9–3

ATOMIC MASSES, PACKING FRACTIONS, AND BINDING ENERGIES OF SOME OF THE STABLE NUCLIDES

Nuclide	Number of protons, Z	Number of neutrons, $A - Z$	Mass, amu	Packing fraction, $\times 10^4$	Binding energy	
					total, Mev	per nucleon, Mev
n^1	0	1	1.0089830 (±1.7)	89.8		
H^1	1	0	1.0081437 (±1.8)	81.4		
H^2	1	1	2.0147361 (±2.9)	73.7	2.225	1.113
He^4	2	2	4.0038727 (±2.1)	9.7	28.29	7.07
Li^7	3	4	7.018222 (±6)	26.0	39.24	5.61
Be^9	4	5	9.015041 (±5)	16.7	58.15	6.46
B^{11}	5	6	11.012795 (±5)	11.6	76.19	6.93
C^{12}	6	6	12.0038065 (±3.9)	3.2	92.14	7.68
C^{13}	6	7	13.0074754 (±4.1)	5.8	97.09	7.47
N^{14}	7	7	14.0075179 (±3.0)	5.4	104.63	7.47
O^{16}	8	8	16.0000000	0	127.58	7.97
O^{17}	8	9	17.0045293 (±3.9)	2.7	131.73	7.75
O^{18}	8	10	18.004840 (±9)	2.7	139.80	7.77
F^{19}	9	10	19.004447 (±7)	2.3	147.75	7.78
Ne^{20}	10	10	19.998765 (±10)	−0.6	160.62	8.03
Al^{27}	13	14	26.990080 (±14)	−3.7	224.92	8.33
Si^{28}	14	14	27.985777 (±16)	−5.1	236.51	8.45
P^{31}	15	16	30.983563 (±18)	−5.3	262.88	8.48
S^{32}	16	16	31.982190 (±20)	−5.6	271.74	8.49
Cl^{35}	17	18	34.979906 (±80)	−5.7	298.13	8.52
Cl^{37}	17	20	36.9776573 (±16)	−6.0	317.00	8.57
A^{40}	18	22	39.975088 (±4)	−6.2	343.71	8.59
Ca^{40}	20	20	39.975330 (±30)	−6.2	341.92	8.55
Fe^{56}	26	30	55.952722 (±6)	−8.4	492.11	8.79
Cu^{63}	29	34	62.949607 (±11)	−8.0	551.22	8.75
As^{75}	33	42	74.945510 (±100)	−7.3	652.23	8.70
Sr^{88}	38	50	87.933680 (±300)	−7.5	768.13	8.73
Mo^{98}	42	56	97.937240 (±350)	−6.3	845.73	8.63
Sn^{116}	50	66	115.938850 (±300)	−5.3	988.14	8.52
Sn^{120}	50	70	119.940330 (±140)	−5.0	1020.2	8.50
Xe^{130}	54	76	129.944810 (±30)	−4.3	1096.6	8.44
Xe^{136}	54	82	135.950420 (±25)	−3.7	1141.5	8.39
Nd^{150}	60	90	149.968490 (±70)	−2.1	1237.1	8.25
Hf^{178}	72	104	175.99650 (±800)	−0.2	1419.1	8.06
W^{184}	74	110	184.008300 (±600)	0.4	1473.5	8.01
Au^{197}	79	118	197.028000 (±1000)	1.4	1560.0	7.92
Pb^{206}	82	124	206.037900 (±500)	1.8	1623.7	7.88
Th^{232}	90	142	232.109800 (±500)	4.7	1768.0	7.62
U^{238}	92	146	238.124300 (±500)	5.2	1803.1	7.58

Hence, isotopic weights obtained by means of the mass spectrograph must be divided by 1.000279 in order to convert the results to the chemical atomic weight scale. The conversion factor is used only when it is necessary to compare mass spectrographic results with weights obtained by chemical methods; in nuclear work the atomic masses on the physical scale are used.

Estimates of the errors of the mass spectrographic measurements have been included in order to indicate the high precision with which atomic masses can now be determined. The error, given in parentheses, is expressed in units of 10^{-6} amu. This precision is essential in the study of nuclear reactions and transformations, as will be seen in later chapters. It is also important in the precise calculation of packing fractions and binding energies, as will now be shown.

It is seen from Table 9–3 that the isotopic masses are indeed very close to whole numbers. It seemed clear to the early workers in this field that the systematic study of the divergences of the masses of nuclides from whole numbers was an important problem. Aston expressed these divergences in the form of a quantity called the *packing fraction* defined by

$$\text{Packing fraction} = \frac{\text{Atomic mass} - \text{Mass number}}{\text{Mass number}}$$

$$= \frac{M_{Z,A} - A}{A}, \tag{9–6}$$

where $M_{Z,A}$ is the actual weight of a nuclide on the physical atomic weight scale, and A is the mass number. If the packing fraction is denoted by f, then

$$M_{Z,A} = A(1 + f). \tag{9–7}$$

Sample values of the packing fraction are listed in Table 9–3, and the variation of the packing fraction with mass number for a larger number of nuclides is shown graphically in Fig. 9–10. The packing fractions, with the exception of those for He^4, C^{12}, and O^{16}, fall on or near the solid curve. The values are high for elements of low mass number, apart from the nuclides mentioned. For O^{16}, the value is zero, by definition. As A increases, the packing fraction becomes negative, passes through a rather flat minimum and then rises gradually, becoming positive again at values of A of about 180. The packing fraction was very useful in the study of isotopic masses, but it does not have a precise physical meaning. The explanation for its usefulness will appear from the discussion of the binding energies of nuclei.

The atomic mass of a nuclide can be understood in terms of the masses of its constituent particles and a quantity called the *binding energy*. It

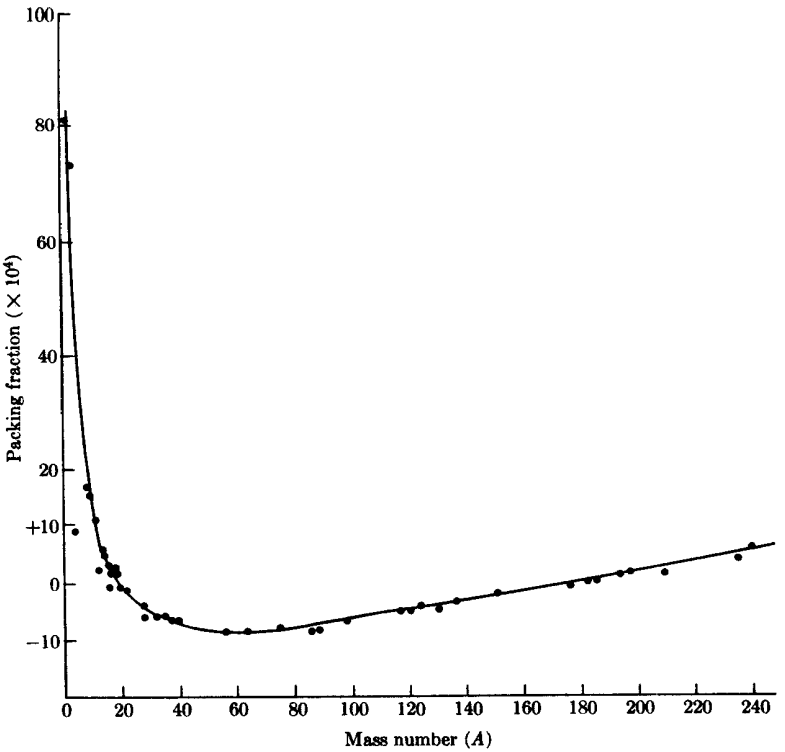

FIG. 9–10. Packing fraction as a function of mass number.

might at first be supposed that the mass of an atom should be the sum of the masses of its constituent particles. A survey of the atomic masses shows, however, that the atomic mass is less than the sum of its constituent particles in the free state. To account for this difference in mass, the principle of the equivalence of mass and energy, derived from the special theory of relativity, is used. If ΔM is the decrease in mass when a number of protons, neutrons, and electrons combine to form an atom, then the above principle states that an amount of energy equal to

$$\Delta E = c^2 \Delta M \tag{9–8}$$

is released in the process. The difference in mass, ΔM, is called the *mass defect;* it is the amount of mass which would be converted to energy if a particular atom were to be assembled from the requisite numbers of protons, neutrons, and electrons. The same amount of energy would be

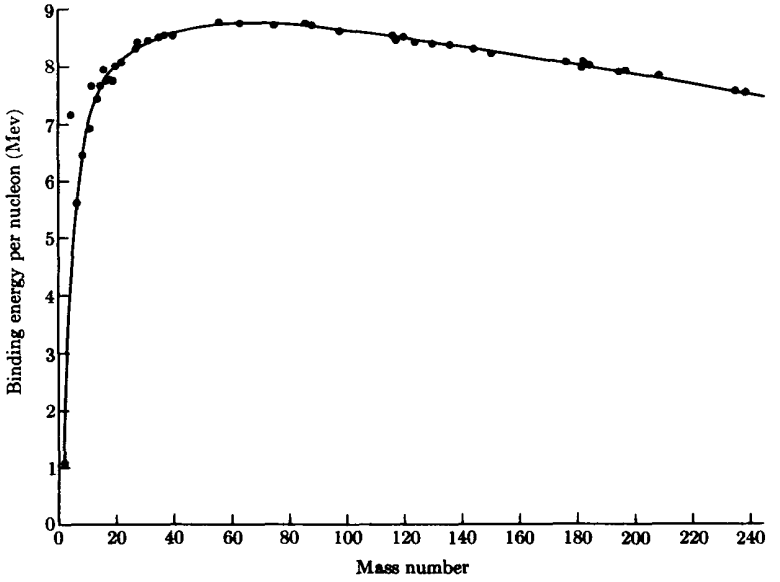

FIG. 9–11. Binding energy per nucleon as a function of mass number.

needed to break the atom into its constituent particles, and the energy equivalent of the mass defect is therefore a measure of the binding energy of the nucleus. The mass of the constituent particles is the sum of Z proton masses, Z electrons, and $A - Z$ neutrons. The proton and electron masses can be combined into the mass of Z hydrogen atoms because the minute change in mass which may accompany the formation of a hydrogen atom from a proton and electron is negligible. The mass defect can then be written

$$\Delta M = Zm_{\mathrm{H}} + (A - Z)m_n - M_{Z,A}, \tag{9–9}$$

where m_{H}, the mass of the hydrogen atom is 1.0081437 mass units and m_n, the mass of the neutron, is 1.0089830 mass units. Then

$$\Delta M = 1.0081437Z + 1.0089830(A - Z) - M_{Z,A}. \tag{9–10}$$

Since one atomic mass unit is equivalent to 931.145 Mev, the binding energy of the nucleus is given by

$$\Delta E(\mathrm{Mev}) = 931.145[1.0081437Z + 1.0089830(A - Z) - M_{Z,A}]. \tag{9–11}$$

The average binding energy per nucleon is obtained by dividing the total binding energy of the nucleus by the mass number A. Some values of

the binding energy obtained by the method just outlined are listed in the last two columns of Table 9–3, and a graph of the binding energy per nucleon as a function of the mass number is shown in Fig. 9–11. With the exception of He^4, C^{12}, and O^{16}, the values of the binding energy per particle lie on or close to a single curve. The binding energies of some of the very light nuclides, such as H^2, are very small. The binding energies of He^4, C^{12}, and O^{16} are considerably greater than those of their neighbors, as is shown clearly by the values in the last column of Table 9–3. The binding energy per particle rises sharply, and reaches a maximum value of about 8.8 Mev in the neighborhood of $A = 50$. The maximum is quite flat, and the binding energy is still 8.4 Mev at about $A = 140$. For higher mass numbers, the value decreases to about 7.6 Mev at uranium.

The magnitude of the binding energy is enormous, as can be shown by converting from Mev per nucleon to more familiar units such as Btu per pound. One Mev is equivalent to 1.519×10^{-16} Btu. One pound of an atomic species contains $453.6/M$ gram atomic weights (M is the atomic weight), or

$$453.6 \times 6.023 \times 10^{23} \times A/M \text{ nucleons.}$$

The mass number A and the atomic weight M are practically the same, so that one pound contains 2.73×10^{26} nucleons. The unit "1 Mev/nucleon" is then practically the same as 4.15×10^{10} Btu/pound. In the neighborhood of the maximum of the binding energy curve, the binding energy is about 8.8 Mev/nucleon or 350 billion Btu/pound. This enormous value of the energy that would be needed to dissociate a nucleus into its constituent protons and neutrons is another indication of the magnitude of the nuclear forces.

The application of the principle of the equivalence of mass and energy and the introduction of the concept of binding energy have, thus far in our treatment, only a theoretical basis. In recent years, however, many nuclear transmutations have been accurately studied and careful measurements have been made of the changes of mass and energy in these reactions. The validity of the relativistic mass-energy relationship has been proven, as well as that of its application to the problems of nuclear physics. The binding energy of a nucleus is, therefore, a quantity with real physical meaning, and the masses and binding energies of nuclei yield useful information about the constitution and stability of nuclei. In addition, the analysis of nuclear transformations has provided an independent means of determining atomic masses which is at present even more powerful than the mass spectrographic method. These matters will be discussed in detail in later chapters.

The subject of atomic masses should not be left without a brief discussion of a proposal[34] to replace the mass standard, O^{16}, by C^{12}, i.e.,

to assign to C^{12} the atomic mass 12.0000000 units. The use of C^{12} as the standard would have several advantages in mass spectrometry. Carbon forms many more chemical compounds which can provide molecular ions for use in a spectrometer than does oxygen. Doubly, triply, and quadruply charged ions of C^{12} occur at integral mass numbers and can be paired in doublets with ions of mass number 6, 4, and 3, respectively, so that C^{12} would be a convenient standard for atoms of low mass number. No other element besides carbon forms molecular ions containing as many atoms of one kind, up to 10 or more; this property would permit many more doublet comparisons to be made directly with the reference nuclide than are now possible, and would yield masses with increased precision at intermediate and large values of A. Thus, carbon forms many compounds with hydrogen, providing easy reference lines for doublets with masses up to 120 units; for values of A between 120 and 240, doubly charged ions of heavier elements could be compared directly with singly charged ions of the type $(C^{12})_n$ or $(C^{12})_n\,(H^1)_m$.

A table of atomic masses has been prepared[35] based on C^{12} as the standard and the following results have been obtained.

Nuclide	O^{16} Standard	C^{12} Standard
n	1.0089861	1.0086654
H^1	1.0081456	1.0078252
H^2	2.0147425	2.0141022
C^{12}	12.0038150	12.0000000
O^{16}	16.0000000	15.9941949

The relation between the atomic mass units on the two scales is

$$1 \text{ amu } (C^{12}) = 1.00031792 \text{ amu } (O^{16}).$$

The conversion factor from mass to energy is

$$1 \text{ amu } (C^{12}) = 931.441 \text{ Mev},$$

as compared with 1 amu (O^{16}) = 931.145 Mev. The values of binding energies are unchanged; thus, the binding energy of the deuteron is 2.2247 Mev when either mass standard is used.

Throughout this book, we shall use O^{16} as the mass standard and the atomic masses given in Table 9–3, but the reader should be aware of the possibility that the standard may be changed within the next few years.

Chapter (4) : Natural radioactivity & the laws of radioactive transformation .

Many of the ideas and techniques of atomic and nuclear physics are based on the properties of the radioactive elements and their radiations, and the study and use of radioactivity are essential to nuclear physics. It has been seen that the emission of α- and β-particles by certain atoms gave rise to the idea that atoms are built up of smaller units, and to the concept of atomic structure. The investigation of the scattering of α-particles by atoms led to the idea of the nuclear atom, which is fundamental to all of atomic theory. The analysis of the chemical relationships between the various radioactive elements resulted in the discovery of isotopes. The bombardment of atoms with swift α-particles from radioactive substances was found to cause the disintegration of atomic nuclei, and this led in turn to the discovery of the neutron and to the current theory of the composition of the nucleus. It will be shown in a later chapter that the transmuted atoms resulting from this kind of bombardment are often radioactive. This discovery of artificial, or induced, radioactivity by Joliot and Curie, in 1934, started a new line of research, and hundreds of radioactive nuclides have now been made by various methods. The investigation of the radiations from the natural and artificial radionuclides has shown that the nucleus has energy levels analogous to the atomic energy levels discussed in Chapter 7. *Nuclear spectroscopy*, which deals with the identification and classification of these levels, is an important source of information about the structure of the nucleus. Thus, radioactivity has been intimately connected with the development of nuclear physics, and it is impossible to conceive of nuclear physics as something separate from radioactivity.

The importance of radioactivity depends to a large extent on the ability to measure radioactive changes with high precision, and to describe them quantitatively by means of a straightforward theory. The laws of radioactive change were developed from information about the natural radioelements, but they are also valid for the artificial radionuclides. They can be applied, therefore, to any radioactive transformation, and are fundamental to a large part of the work to be discussed in the remaining chapters of this book.

10–1 The basis of the theory of radioactive disintegration. The first problem which will be considered is that of the quantitative description of radioactive growth and decay. A clue to the way in which one radio-

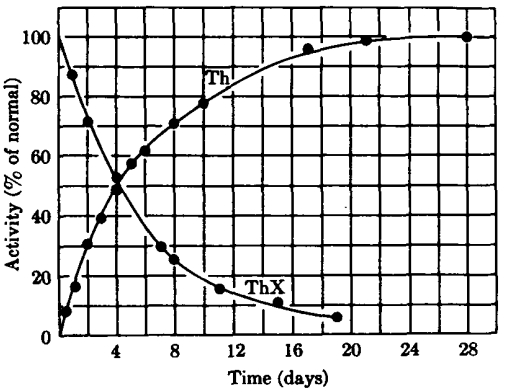

FIG. 10–1. The decay of thorium X activity and the recovery of thorium activity.

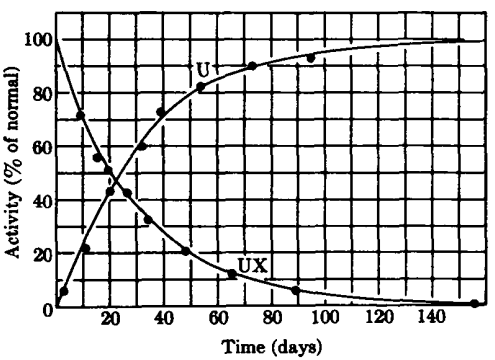

FIG. 10–2. The decay of uranium X activity and the recovery of uranium activity.

active substance is produced from another was provided by early experiments of Crookes, Becquerel, and Rutherford and Soddy.[1] Crookes (1900) found that if a uranium salt was precipitated from solution by the addition of ammonium carbonate, and then redissolved in excess of the reagent, a small residue was left. This residue, when removed from the solution, was found to be highly radioactive. The product obtained by evaporating the solution, which contained practically all the uranium, had very little activity. It appeared, therefore, that most of the observed activity of compounds of uranium was not caused by that element, but by another substance which could be separated from the uranium. The active substance was contained in the residue and was given the name

uranium X (UX) to distinguish it from uranium. Becquerel then found that if the uranium X and uranium fractions were allowed to stand separately for some time, the activity of the UX decreased, while that of the uranium fraction increased. Rutherford and Soddy (1902) [2] obtained similar results with thorium salts; an active material which was called thorium X was separated, and the main body of the thorium was practically inactive. After a few days, it was noticed that the thorium X was losing its activity, while the thorium, which had been freed from thorium X, was recovering its activity.

Rutherford and Soddy studied quantitatively the rate of decay of the ThX activity and the rate of recovery of the thorium activity, and obtained the curves shown in Fig. 10–1. The experimental decay curve for the ThX was exponential in nature, i.e., the activity could be expressed as a function of time by the equation

$$A_x(t) = A_{x0}e^{-\lambda t}, \tag{10–1}$$

where A_{x0} is the initial activity of the ThX, $A_x(t)$ is the activity after a time t, and λ is a constant, called the *disintegration constant*. The recovery curve for the thorium was found to fit the formula

$$A(t) = A_0(1 - e^{-\lambda t}), \tag{10–2}$$

in which the constant λ has the same value as in Eq. (10–1); the decay and recovery curves are therefore symmetrical. The results for UX and U are shown in Fig. 10–2. The curves are similar to those for the thorium bodies except that the time scale is different. Thorium X loses half of its activity in about 3.5 days, while UX loses half of its activity in 24 days, so that the value of λ is greater for ThX than for UX.

These experimental observations enabled Rutherford and Soddy to formulate a theory of radioactive change. They suggested that the atoms of radioactive elements undergo spontaneous disintegration with the emission of α- or β-particles and the formation of atoms of a new element. Then the intensity of the radioactivity, which has been called the *activity*, is proportional to the number of atoms which disintegrate per unit time. The activity, A, measured by one of the methods discussed in Chapter 2, may then be replaced by the number of atoms N, and Eq. (10–1) may be written

$$N_x(t) = N_{x0}e^{-\lambda t}. \tag{10–3}$$

The notation may be simplified by dropping the subscript x, which was used only to distinguish between the X body and its parent substance. Then

$$N(t) = N_0e^{-\lambda t} \tag{10–4}$$

is the equation which represents the change with time of the number of atoms of a single decaying radioactive substance. Differentiation of both sides of Eq. (10–4) gives

$$-\frac{dN}{dt} = \lambda N, \tag{10–5}$$

where $N(t)$ has been abbreviated as N. According to Eq. (10–5), the decrease per unit time in the number of atoms of a radioactive element because of disintegration is proportional to the number of atoms which have not yet disintegrated. The proportionality factor is the disintegration constant, which is characteristic of a particular radioactive species.

Equation (10–5) is the fundamental equation of radioactive decay. With this equation, and with two assumptions, it was possible to account for the growth of activity in the thorium or uranium fractions from which the ThX or UX had been removed. The assumptions are (1) that there is a constant production of a new radioactive substance (say UX) by the radioactive element (uranium), and (2) that the new substance (UX) itself disintegrates according to the law of Eq. (10–5). Suppose that Q atoms of UX are produced per second by a given mass of uranium, and let N be the number of atoms of UX present at time t after the complete removal of the initial amount of UX. Then the net rate of increase of UX atoms in the uranium fraction is

$$\frac{dN}{dt} = Q - \lambda N. \tag{10–6}$$

The first term on the right side of Eq. (10–6) gives the rate of formation of UX atoms from U atoms; the second term gives the rate of disappearance of UX atoms because of their radioactive disintegration. To integrate Eq. (10–6), write it in the form

$$\frac{dN}{dt} + \lambda N = Q,$$

and multiply through by $e^{\lambda t}$. Then

$$e^{\lambda t}\frac{dN}{dt} + \lambda N e^{\lambda t} = Q e^{\lambda t}, \qquad \text{or} \qquad \frac{d}{dt}(N e^{\lambda t}) = Q e^{\lambda t}.$$

The last equation can be integrated directly to give

$$N e^{\lambda t} = \frac{Q}{\lambda} e^{\lambda t} + C, \qquad \text{or} \qquad N = \frac{Q}{\lambda} + C e^{-\lambda t};$$

C is an integration constant determined by the condition that $N = 0$

when $t = 0$. This condition gives $C = -Q/\lambda$, and

$$N = \frac{Q}{\lambda}(1 - e^{-\lambda t}) = N_0(1 - e^{-\lambda t}), \tag{10–7}$$

with $N_0 = Q/\lambda$.

Equation (10–7) is the same as the recovery equation (10–2) so that the theory gives the correct result for the growth of activity in the uranium or thorium after the removal of the X body. Equation (10–7) also shows that the number of UX atoms in the mass of uranium approaches an equilibrium value for large values of t given by the ratio

$$\frac{Q}{\lambda} = \frac{\text{Number of atoms of UX produced from U per second}}{\text{Fractions of atoms of UX which decay per second}}.$$

The exponential law of decay was deduced by E. von Schweidler (1905) without any special hypothesis about the structure of the radioactive atoms or about the mechanism of disintegration. He assumed only that the disintegration of an atom of a radioactive element is subject to the laws of chance, and that the probability p for an atom to disintegrate in a time interval Δt is independent of the past history of the atom and is the same for all atoms of the same type. The probability of disintegration then depends only on the length of the time interval and, for sufficiently short intervals, is proportional to Δt. Then $p = \lambda \Delta t$, where λ is the disintegration constant characteristic of the particular radioactive substance. The probability that the given atom will not disintegrate during the short interval Δt is $1 - p = 1 - \lambda \Delta t$. If the atom has survived this interval, then the probability that it will not disintegrate in a second time interval Δt is again $1 - \lambda \Delta t$. The probability that the given atom will survive both the first and the second intervals is $(1 - \lambda \Delta t)^2$; for n such intervals, the probability of survival is $(1 - \lambda \Delta t)^n$. If the total time $n\Delta t$ is set equal to t, the probability of survival is $[1 - \lambda(t/n)]^n$. The probability that the atom will remain unchanged after time t is the limit of this quantity as Δt becomes vanishingly small, or as n becomes very large. Now, one of the definitions of the exponential functions is

$$e^{-x} = \lim_{n \to \infty} \left(1 - \frac{x}{n}\right)^n,$$

from which it follows that

$$\lim_{n \to \infty} \left(1 - \lambda \frac{t}{n}\right)^n = e^{-\lambda t}.$$

The statistical interpretation of this result is that if there are initially a large number N_0 of radioactive atoms, then the fraction remaining unchanged after a time t is $N/N_0 = e^{-\lambda t}$, where N is the number of unchanged atoms at time t.

The law of radioactive decay is thus a statistical law and is the result of a very large number of events subject to the laws of probability. The number of atoms which disintegrate in one second is, on the average, λN, but the number which break up in any second shows fluctuations around this value. The magnitude of these fluctuations can be calculated with the aid of the theory of probability, and the statistical considerations involved are important in the design and interpretation of experiments having to do with the measurement of radioactivity.[3]

The number of radioactive atoms N and the activity A have been used interchangeably so far on the grounds that the latter is proportional to the former. For a given radioactive substance, the two quantities are actually connected by the relationship

$$A = c\lambda N. \tag{10-8a}$$

The proportionality factor c, which is sometimes called the *detection coefficient*, depends on the nature and efficiency of the detection instrument and may vary considerably from one radioactive substance to another. For any one substance, the quantity in which we are usually interested is the ratio of the number of atoms at two values of the time. But, from Eq. (10-8a), it follows that

$$\frac{N(t_1)}{N(t_2)} = \frac{A(t_1)}{A(t_2)}, \tag{10-8b}$$

and the detection coefficient cancels out. Hence, the use of N and A as equivalent quantities usually leads to no confusion in the case of a single substance. When two different substances are considered, the measured activities are $A_1 = c_1\lambda_1 N_1$ and $A_2 = c_2\lambda_2 N_2$, respectively. If the number of atoms which disintegrate per unit time is the same for both substances, $\lambda_1 N_1 = \lambda_2 N_2$, but the measured activities, say in counts per minute, are not necessarily equal. They are equal only if the detection coefficients are equal. It will be assumed, with occasional exceptions, that the detection coefficients are all equal to unity, i.e., that each disintegration is detected. This condition usually cannot be achieved in practice, but it is adopted here to simplify the discussion. The activity will then be equal to the number of atoms disintegrating per unit time, $A = \lambda N$, unless otherwise noted.

10-2 The disintegration constant, the half-life, and the mean life. A radioactive nuclide may be characterized by the rate at which it disintegrates, and any one of three quantities, the disintegration constant, the half-life, or the mean life, may be used for this purpose. The disintegra-

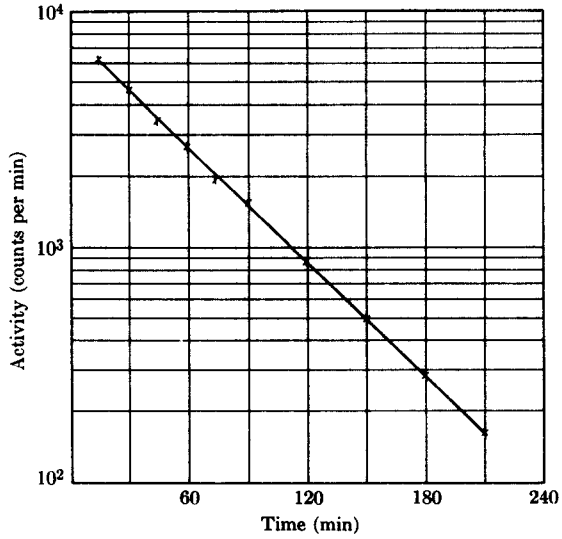

FIG. 10–3. Graphical method for determining the value of the disintegration constant.

tion constant λ can be determined experimentally, in many cases, with the help of Eq. (10–4), which may be written

$$\ln \frac{N(t)}{N_0} = -\lambda t, \tag{10–9}$$

where the symbol "ln" represents the natural logarithm. The latter can be transformed to the ordinary logarithm, denoted by "log," and Eq. (10–9) becomes

$$\log \frac{N(t)}{N_0} = -0.4343\lambda t, \tag{10–10}$$

since the logarithm to the base e is equal to 2.3026 times the logarithm to the base 10. The number of atoms $N(t)$ is proportional to the measured activity $A(t)$, so that $N(t)/N_0 = A(t)/A_0$, and Eq. (10–10) may be written

$$\log A(t) = \log A_0 - 0.4343\lambda t. \tag{10–11}$$

Hence, if the logarithm of the measured activity is plotted against the time, a straight line should result whose slope is equal to -0.4343λ. An example of this method of determining λ is shown in Fig. 10–3; for convenience, the plot is made on semilog paper. In the example shown, the slope is -0.00808, with the time expressed in minutes; λ is then 0.0186 min^{-1}, or 3.10×10^{-4} sec^{-1}.

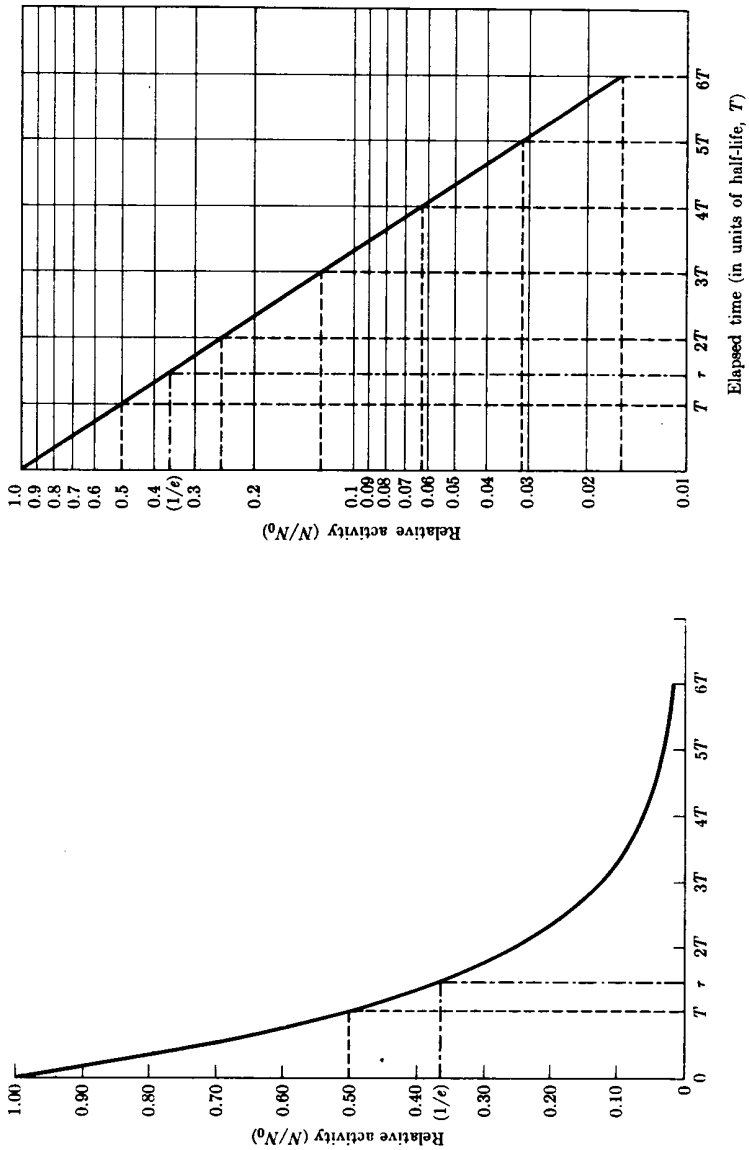

FIG. 10–4. Radioactive decay: the half-life. The curve on the left is plotted on linear graph paper, while the curve on the right is plotted on semilog paper.

Another quantity which is used to characterize a radionuclide is the *half-life*, T, the time needed for half of the radioactive atoms to disintegrate. After one half-life, $N(T)/N_0 = 0.5$, and it follows from Eq. (10–11) that $\log 0.5 = -0.4343\lambda T$ or $\log 2 = 0.4343\lambda T$. Since $\log 2 = 0.3010$,

$$\text{half-life} = T = 0.693/\lambda. \tag{10–12}$$

The relationship between the activity and the half-life is illustrated in Fig. 10–4. After n half-lives ($t = nT$), the fraction of the activity remaining is $(\frac{1}{2})^n$. This fraction never reaches zero, but it becomes very small; after seven half-lives the activity is 1/128, or less than one percent of the initial activity. After ten half-lives, the activity has fallen to 1/1024 or about 0.1% of the original amount, and is usually negligible in comparison with the initial value.

It is also possible to determine the *mean life*, or average life expectancy, of the atoms of a radioactive species. The mean life, usually denoted by τ, is given by the sum of the times of existence of all the atoms, divided by the initial number. Mathematically, it is found in the following way. The number of atoms which decay between t and $t + dt$ is

$$dN = \lambda N dt;$$

but the number of atoms still existing at time t is

$$N = N_0 e^{-\lambda t},$$

so that

$$dN = \lambda N_0 e^{-\lambda t}\, dt.$$

Since the decay process is a statistical one, any single atom may have a life from 0 to ∞. Hence, the mean life is given by

$$\tau = \frac{1}{N_0}\int_0^\infty N_0 \lambda t e^{-\lambda t}\, dt = \lambda \int_0^\infty t e^{-\lambda t}\, dt = \frac{1}{\lambda}, \tag{10–13}$$

and is simply the reciprocal of the disintegration constant. From Eqs. (10–12) and (10–13), it follows that the half-life and the mean life are proportional quantities:

$$T = 0.693\tau. \tag{10–14}$$

If the half-life of a single radioactive species has a value in the range from several seconds to several years, it can be determined experimentally by measuring the activity as a function of the time, as in the case of the disintegration constant. When the activity is plotted against the time on semilog paper, a straight line is obtained, and the half-life can be read off directly.

It often happens that two or more radioactive species are mixed together, in which case the observed activity is the sum of the separate activities. If the activities are independent, i.e., one component of the mixture does not give rise to another, the various activities can sometimes be distinguished, and the separate half-lives determined. When the total activity is plotted against the time on semilog paper, a curve like the solid one in Fig. 10–5 is obtained. The curve is concave upward because the shorter-lived components decay relatively rapidly, eventually leaving the long-lived components. After a sufficiently long time, only the longest-lived activity will remain, and the value of its half-life can be read from the late portion of the decay curve, which will be a straight line. If this straight-line portion is extrapolated back to $t = 0$, and if the values of the activity given by the line are subtracted from the total activity, the curve that remains will represent the decay of all the components of the mixture except the longest-lived. The example in Fig. 10–5 is a mixture of two activities, one with a half-life of 0.8 hour, the other with a half-life of 8 hours. The curve for the total activity is the sum of the two straight lines which represent the individual activities. Although, in principle, any complex decay curve can be analyzed into its components, practical difficulties may limit the usefulness of the method to three com-

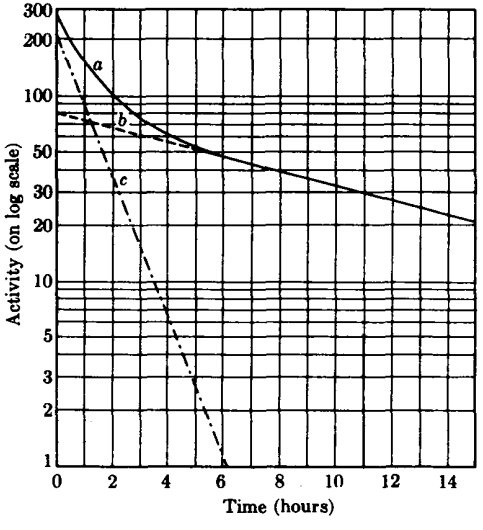

FIG. 10–5. Analysis of a composite decay curve. (a) Composite curve. (b) Longer-lived component ($T_{\frac{1}{2}}$ = 8.0 hr). (c) Shorter-lived component ($T_{\frac{1}{2}}$ = 0.8 hr). (Reprinted by permission from G. Friedlander and J. W. Kennedy, *Introduction to Radiochemistry*. New York: Wiley, 1949.)

ponents, and even a two-component mixture may be hard to resolve if the half-lives differ by less than a factor of about two.

If the half-life of a radionuclide is either very long or very short, methods different from those discussed so far must be used. When the half-life is very long, i.e., λ is very small, it may not be possible to detect a change in activity during the course of the measurement. The experimental activity, A, is equal to $c\lambda N$, where c gives the fraction of the disintegrating atoms detected by the measuring device. Then λ can be found from the relation

$$\lambda N = -\frac{dN}{dt} = \frac{A}{c},$$

provided that N, the number of atoms of the nuclide in the sample, is known, and that c is known as a result of an appropriate calibration. This method has been used successfully for long-lived α-emitters, and values of half-lives up to the order of 10^{10} years have been determined. For very short half-lives, other methods [4] must be used, the discussion of which is beyond the scope of this book; half-lives as short as 10^{-9} sec have been determined.

10–3 Successive radioactive transformations. It was found experimentally that the naturally occurring radioactive nuclides form three series. In each series, the parent nuclide decays into a daughter nuclide, which decays in turn, and so on, until finally a stable end product is reached. In the study of radioactive series, it is important to know the number of atoms of each member of the series as a function of time. The answer to a problem of this kind can be obtained by solving a system of differential equations. The procedure may be illustrated by treating the case of a radioactive nuclide, denoted by the subscript 1, which decays into another radioactive nuclide (subscript 2); the latter, in turn, decays into a stable end product (subscript 3). The numbers of atoms of the three kinds at any time t are denoted by N_1, N_2, and N_3, respectively, and the disintegration constants are λ_1, λ_2, and λ_3. The system is described by the three equations

$$\frac{dN_1}{dt} = -\lambda_1 N_1, \tag{10–15a}$$

$$\frac{dN_2}{dt} = \lambda_1 N_1 - \lambda_2 N_2, \tag{10–15b}$$

$$\frac{dN_3}{dt} = \lambda_2 N_2. \tag{10–15c}$$

These equations express the following facts: the parent nuclide decays according to the basic law Eq. (10–5); atoms of the second kind are formed

at the rate $\lambda_1 N_1$ because of the decay of parent atoms, and disappear at the rate $\lambda_2 N_2$; atoms of the stable end product appear at the rate $\lambda_2 N_2$ as a result of the decay of atoms of the second kind.

It is instructive to solve this system of equations in detail because the procedure is one which is often used. The number of atoms N_1 can be written down immediately,

$$N_1(t) = N_1^0 e^{-\lambda_1 t}, \tag{10–16}$$

where N_1^0 is the number of atoms of the first kind present at the time $t = 0$. This expression for N_1 is inserted into Eq. (10–15b), and gives

$$\frac{dN_2}{dt} = \lambda_1 N_1^0 e^{-\lambda_1 t} - \lambda_2 N_2,$$

or

$$\frac{dN_2}{dt} + \lambda_2 N_2 = \lambda_1 N_1^0 e^{-\lambda_1 t}. \tag{10–17}$$

Multiply Eq. (10–17) through by $e^{\lambda_2 t}$; this gives

$$e^{\lambda_2 t} \frac{dN_2}{dt} + \lambda_2 N_2 e^{\lambda_2 t} = \lambda_1 N_1^0 e^{(\lambda_2 - \lambda_1)t},$$

or

$$\frac{d}{dt}(N_2 e^{\lambda_2 t}) = \lambda_1 N_1^0 e^{(\lambda_2 - \lambda_1)t}.$$

The last equation can be integrated directly to give

$$N_2 e^{\lambda_2 t} = \frac{\lambda_1}{\lambda_2 - \lambda_1} N_1^0 e^{(\lambda_2 - \lambda_1)t} + C,$$

where C is a constant of integration. Multiplying through by $e^{-\lambda_2 t}$ gives

$$N_2(t) = \frac{\lambda_1}{\lambda_2 - \lambda_1} N_1^0 e^{-\lambda_1 t} + C e^{-\lambda_2 t}. \tag{10–18}$$

The value of the integration constant is determined by noting that when $t = 0$, the number of atoms of the second kind has some constant value, or $N_2 = N_2^0$, with N_2^0 equal to a constant. Then

$$C = N_2^0 - \frac{\lambda_1}{\lambda_2 - \lambda_1} N_1^0.$$

Inserting this value into Eq. (10–18) and rearranging, we obtain the solution for N_2 as a function of time:

$$N_2 = \frac{\lambda_1}{\lambda_2 - \lambda_1} N_1^0 (e^{-\lambda_1 t} - e^{-\lambda_2 t}) + N_2^0 e^{-\lambda_2 t}. \tag{10–19}$$

The number of atoms of the third kind is found by inserting this expression for N_2 into Eq. (10–15c) and integrating, which gives

$$N_3 = \left(\frac{\lambda_1}{\lambda_2 - \lambda_1} N_1^0 - N_2^0\right) e^{-\lambda_2 t} - \frac{\lambda_2}{\lambda_2 - \lambda_1} N_1^0 e^{-\lambda_1 t} + D, \quad (10\text{–}20)$$

where D is an integration constant, determined by the condition $N_3 = N_3^0$ at $t = 0$. This condition gives

$$D = N_3^0 + N_2^0 + N_1^0.$$

When this expression for D is inserted into Eq. (10–20), the result is

$$N_3 = N_3^0 + N_2^0(1 - e^{-\lambda_2 t}) + N_1^0\left(1 + \frac{\lambda_1}{\lambda_2 - \lambda_1} e^{-\lambda_2 t} - \frac{\lambda_2}{\lambda_2 - \lambda_1} e^{-\lambda_1 t}\right). \quad (10\text{–}21)$$

Equations (10–16), (10–19), and (10–21) represent the solution of the problem.

One of the cases met most often in practice is that in which only radioactive atoms of the first kind are present initially. In this case, the constants N_2^0 and N_3^0 are both equal to zero, and the solutions for N_2 and N_3 reduce to

$$N_2 = \frac{\lambda_1}{\lambda_2 - \lambda_1} N_1^0(e^{-\lambda_1 t} - e^{-\lambda_2 t}), \quad (10\text{–}22)$$

$$N_3 = N_1^0\left(1 + \frac{\lambda_1}{\lambda_2 - \lambda_1} e^{-\lambda_2 t} - \frac{\lambda_2}{\lambda_2 - \lambda_1} e^{-\lambda_1 t}\right). \quad (10\text{–}23)$$

The curves of Fig. 10–6 show what happens in this case if it is assumed that the half-lives of the active species are $T_1 = 1$ hour and $T_2 = 5$ hours, respectively; the corresponding values of the disintegration constants are $\lambda_1 = 0.693\ \text{hr}^{-1}$, and $\lambda_2 = 0.1386\ \text{hr}^{-1}$, respectively. The ordinates of the curves represent the relative numbers of the substances 1, 2, and 3 as functions of the time when the initial number of atoms of the substance 1 is taken as $N_1^0 = 100$. The number of atoms, N_1, of substance 1, decreases exponentially according to Eq. (10–16) with a half-life of 1 hour; N_2 is initially zero, increases, and passes through a maximum after about three hours, and then decreases gradually. The number of atoms N_3 of the stable end product increases steadily with time, although slowly at first; when t becomes very large, N_3 approaches 100, since eventually all the atoms of the substance 1 will be converted to atoms of the stable end product.

The treatment just discussed can be extended to a chain of any number of radioactive products, and the solution of this problem is often useful.

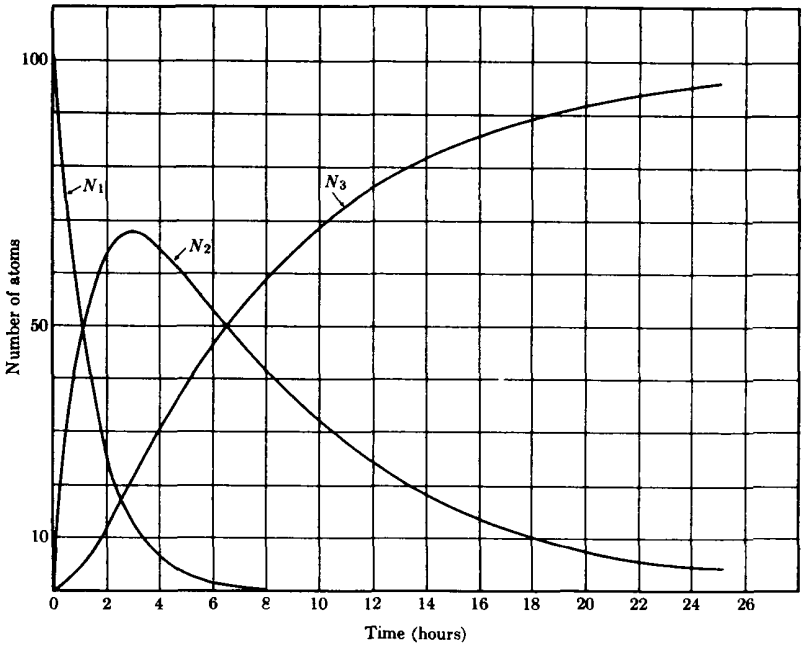

FIG. 10–6. A radioactive series with three members: only the parent ($T_{\frac{1}{2}}$ = 1 hr) is present initially; the daughter has a half-life of 5 hr, and the third member is stable.

The procedure is similar to that of the special case already considered except that the mathematics becomes more tedious and the expressions for the numbers of atoms become more complicated as the length of the chain increases. The differential equations of the system are

$$\begin{aligned}
\frac{dN_1}{dt} &= -\lambda_1 N_1, \\
\frac{dN_2}{dt} &= \lambda_1 N_1 - \lambda_2 N_2, \\
\frac{dN_3}{dt} &= \lambda_2 N_2 - \lambda_3 N_3, \\
&\vdots \\
\frac{dN_n}{dt} &= \lambda_{n-1} N_{n-1} - \lambda_n N_n.
\end{aligned} \tag{10–24}$$

The solution of this system of equations under the assumption that at

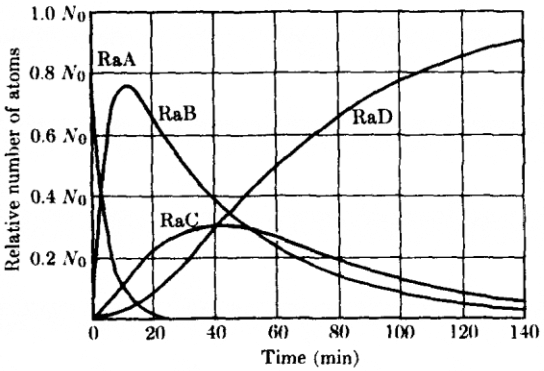

FIG. 10–7. The decay of Radium A. [Reprinted by permission from Rutherford, Chadwick, and Ellis, *Radiations from Radioactive Substances*, Cambridge University Press (Macmillan Co.), 1930.]

$t = 0$ only the parent substance is present was derived by Bateman.[5] The initial conditions are

$$t = 0; \qquad N_1 = N_1^0, \qquad N_2^0 = N_3^0 = \cdots = N_n^0 = 0. \tag{10–25}$$

The number of atoms of the nth member of the chain is given by

$$N_n(t) = C_1 e^{-\lambda_1 t} + C_2 e^{-\lambda_2 t} + C_3 e^{-\lambda_3 t} + \cdots + C_n e^{-\lambda_n t}, \tag{10–26}$$

with

$$\begin{aligned} C_1 &= \frac{\lambda_1 \lambda_2 \ldots \lambda_{n-1}}{(\lambda_2 - \lambda_1)(\lambda_3 - \lambda_1) \ldots (\lambda_n - \lambda_1)} N_1^0, \\ C_2 &= \frac{\lambda_1 \lambda_2 \ldots \lambda_{n-1}}{(\lambda_1 - \lambda_2)(\lambda_3 - \lambda_2) \ldots (\lambda_n - \lambda_2)} N_1^0, \\ &\vdots \\ C_n &= \frac{\lambda_1 \lambda_2 \ldots \lambda_{n-1}}{(\lambda_1 - \lambda_n)(\lambda_2 - \lambda_n) \ldots (\lambda_{n-1} - \lambda_n)} N_1^0. \end{aligned} \tag{10–27}$$

An example of the application of the Bateman equations, Eqs. (10–24) to (10–27), is shown in Fig. 10–7, taken from Rutherford, Chadwick, and Ellis' book *Radiations from Radioactive Substances*. The curves were obtained under the conditions which follow. A test body was exposed for a few seconds to radon (Em^{222}), and a certain number of atoms of the decay product of radon, RaA or Po^{218}, with a half-life of 3.05 min were deposited on the test body. The RaA decays into RaB (Pb^{214}) with a half-life of 26.8 min, which decays, in turn, into RaC (Bi^{214}) with a half-life of 19.7 min. Finally, the end product RaD or Pb^{210}, with a half-life of 22 years, is formed. The last half-life is sufficiently long so

that the number of radium D atoms which disintegrate may safely be neglected. The number of RaA atoms decreases exponentially. The number of RaB atoms is initially zero, passes through a maximum about 10 min later, and then decreases with time. The number of RaC atoms passes through a maximum after about 35 min. The number of RaD atoms increases, reaching a maximum when the RaA and RaB have disappeared. Eventually the RaD would decay exponentially with a half-life of 22 years. The sum of all the atoms present at any time is N_0, the initial number of atoms of RaA.

Solutions can be obtained for other problems with different initial conditions, and the reader is referred to the book by Rutherford, Chadwick, and Ellis for additional examples of the application of the theory.

10–4 Radioactive equilibrium. The term *equilibrium* is usually used to express the condition that the derivative of a function with respect to the time is equal to zero. When this condition is applied to the members of a radioactive chain described by Eqs. (10–24), it means that the derivatives $dN_1/dt, dN_2/dt, \ldots, dN_n/dt$ are all equal to zero, or that the number of atoms of any member of the chain is not changing. The conditions for equilibrium are then

$$\begin{aligned} \frac{dN_1}{dt} &= -\lambda_1 N_1 = 0, \\ \lambda_1 N_1 &= \lambda_2 N_2, \\ \lambda_2 N_2 &= \lambda_3 N_3, \\ &\vdots \\ \lambda_{n-1} N_{n-1} &= \lambda_n N_n, \end{aligned} \tag{10–28}$$

These conditions cannot be satisfied rigorously if the parent substance is a radioactive substance because the first of Eqs. (10–28) implies that $\lambda_1 = 0$, which is a contradiction. It is possible to achieve a state very close to equilibrium, however, if the parent substance decays much more slowly than any of the other members of the chain; in other words, if the parent has a half-life very long compared with that of any of its decay products. This condition is satisfied by the naturally occurring radioactive chains. Uranium I has a half-life of 4.5×10^9 years and the fraction of UI atoms transformed during the life of an experimenter is indeed negligible. In such a case, the number of atoms N_1 can be taken to be constant, and the value of λ_1 is very much smaller than that of any of the other λ's in the chain. The first of Eqs. (10–28) is then a very good approximation, and the rest of the conditions are rigorously valid. This

type of equilibrium is called *secular equilibrium*, and satisfies the condition

$$\lambda_1 N_1 = \lambda_2 N_2 = \lambda_3 N_3 = \cdots = \lambda_{n-1} N_{n-1} = \lambda_n N_n, \tag{10-29}$$

or, in terms of half-lives,

$$\frac{N_1}{T_1} = \frac{N_2}{T_2} = \frac{N_3}{T_3} = \cdots = \frac{N_{n-1}}{T_{n-1}} = \frac{N_n}{T_n}. \tag{10-30}$$

The relationships (10–29) and (10–30) may be applied whenever several short-lived products arise from successive decays beginning with a relatively long-lived parent. It is only necessary to be sure that the material has been undisturbed, that is, that no decay products have been removed or allowed to escape for a long enough time for secular equilibrium to be established. Secular equilibrium can also be attained when a radioactive substance is produced at a steady rate by some artificial method, such as a nuclear reaction in a cyclotron or chain-reacting pile. The term $\lambda_1 N_1$ in the second of Eqs. (10–24) is then constant, as in the case of a very long-lived parent, and the condition (10–29) is satisfied.

The relationships (10–30) can be used to find the half-life of a radionuclide whose half-life is very long. For example, uranium minerals in which secular equilibrium has been established have been shown to contain one atom of radium for every 2.8×10^6 atoms of uranium I. If uranium I is denoted by the subscript 1 and radium by the subscript 2, then at equilibrium $N_1/N_2 = 2.8 \times 10^6$. The half-life of radium is known from direct measurements to be 1620 years. Consequently, the half-life of uranium I is

$$T_1 = \frac{N_1}{N_2} T_2 = 2.8 \times 10^6 \times 1620 = 4.5 \times 10^9 \text{ years}.$$

We consider next an example of the approach to secular equilibrium. The case is that of a long-lived parent ($T \approx \infty$) and a short-lived daughter. It is assumed that the daughter has been separated from the parent, so that the latter is initially pure. The mathematical expressions for the number of atoms of parent and daughter may be obtained from Eqs. (10–16) and (10–22) if it is noted that $\lambda_1 \approx 0$, and $\lambda_1 \ll \lambda_2$. Then $e^{-\lambda_1 t} \approx 1$, and

$$N_1 \approx N_1^0, \tag{10-31}$$

$$N_2 \approx \frac{\lambda_1}{\lambda_2} N_1^0 (1 - e^{-\lambda_2 t}). \tag{10-32}$$

Equation (10–32) may be rewritten

$$\lambda_2 N_2 \approx \lambda_1 N_1^0 (1 - e^{-\lambda_2 t}). \tag{10-33}$$

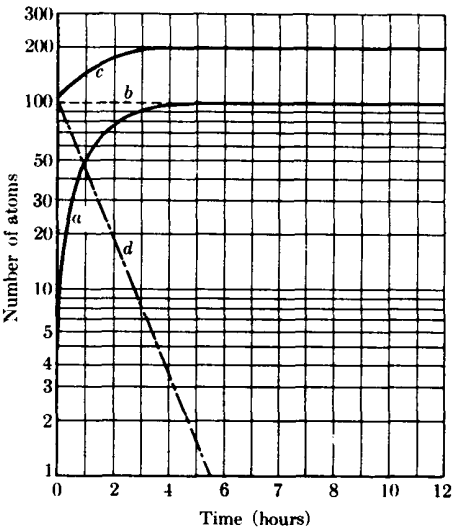

FIG. 10–8. Secular equilibrium. (a) Daughter activity growing in freshly purified parent fraction. (b) Activity of parent ($T_{\frac{1}{2}} = \infty$). (c) Total activity of an initially pure parent fraction. (d) Decay of freshly isolated daughter fraction ($T_{\frac{1}{2}} = 0.80$ hr). (Reprinted by permission from G. Friedlander and J. W. Kennedy, *Introduction to Radiochemistry*. New York: Wiley, 1949.)

The last equation gives the activity of the daughter as a function of the time, in terms of the (constant) activity of the parent. The total activity is given by

$$A_{\text{total}} = \lambda_1 N_1^0 + \lambda_2 N_2 \approx 2\lambda_1 N_1^0 - \lambda_1 N_1^0 e^{-\lambda_2 t}. \qquad (10\text{–}34)$$

Equation (10–33) shows that as t increases the activity of the daughter increases, and after several half-lives, $\lambda_2 N_2$ approaches $\lambda_1 N_1^0$, satisfying the condition for secular equilibrium. These relationships are shown graphically in curves *a* and *b* of Fig. 10–8; curve *c* gives the total activity. For comparison, curve *d* shows how a freshly isolated daughter fraction would decay.

A somewhat different state of affairs, called *transient equilibrium*, results if the parent is longer-lived than the daughter ($\lambda_1 < \lambda_2$), but the half-life of the parent is not very long. In this case, the approximation $\lambda_1 = 0$ may not be made. If the parent and daughter are separated so that the parent can be assumed to be initially pure, the numbers of atoms are again given by Eqs. (10–16) and (10–22). After t becomes sufficiently large, $e^{-\lambda_2 t}$ becomes negligible compared with $e^{-\lambda_1 t}$, and the number of

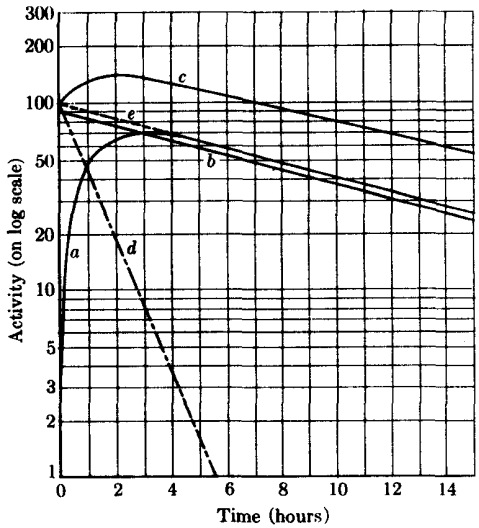

FIG. 10–9. Transient equilibrium. (a) Daughter activity growing in freshly purified parent fraction. (b) Activity of parent ($T_{\frac{1}{2}}$ = 8.0 hr). (c) Total activity of an initially pure parent fraction. (d) Decay of freshly isolated daughter fraction ($T_{\frac{1}{2}}$ = 0.80 hr). (e) Total daughter activity in parent-plus-daughter fractions. (Reprinted by permission from G. Friedlander and J. W. Kennedy, *Introduction to Radiochemistry*. New York: Wiley, 1949.)

atoms of the daughter becomes

$$N_2 \approx \frac{\lambda_1}{\lambda_2 - \lambda_1} N_1^0 e^{-\lambda_1 t}. \tag{10–35}$$

Thus, the daughter eventually decays with the same half-life as the parent. Since $N_1^0 e^{-\lambda_1 t} = N_1$, it follows from Eq. (10–35) that

$$\frac{N_1}{N_2} = \frac{\lambda_2 - \lambda_1}{\lambda_1}. \tag{10–36}$$

The ratio of the measured activities at equilibrium is

$$\frac{A_1}{A_2} = \frac{\lambda_1 N_1}{\lambda_2 N_2} = \frac{\lambda_2 - \lambda_1}{\lambda_2}, \tag{10–37}$$

and the daughter activity is greater than that of the parent by the factor $\lambda_2/(\lambda_2 - \lambda_1)$. The above results, which are characteristic of transient equilibrium between parent and daughter atoms, are shown graphically in Fig. 10–9.

When the parent has a shorter half-life than the daughter ($\lambda_1 > \lambda_2$), no state of equilibrium is attained. If the parent and daughter are separated initally, then as the parent decays, the number of daughter atoms will increase, pass through a maximum, and eventually decay with the half-life of the daughter.

10–5 The natural radioactive series. As a result of physical and chemical research on the naturally occurring radioactive elements, it was proved that each radioactive nuclide is a member of one of three long chains, or radioactive series, stretching through the last part of the periodic system. These series are named the uranium, actinium, and thorium series, respectively, after elements at, or near, the head of the series. In the uranium series, the mass number of each member can be expressed in the form $(4n + 2)$, where n is an integer, and the uranium series is sometimes called the "$4n + 2$" series. In the actinium and thorium series, the mass numbers are given by the expressions $4n + 3$ and $4n$, respectively. There

TABLE 10–1

THE URANIUM SERIES

Radioactive species	Nuclide	Type of disintegration	Half-life	Disintegration constant, sec^{-1}	Particle energy, Mev
Uranium I (UI)	$_{92}U^{238}$	α	4.50×10^9 y	4.88×10^{-18}	4.20
Uranium X_1 (UX_1)	$_{90}Th^{234}$	β	24.1 d	3.33×10^{-7}	0.19
Uranium X_2 (UX_2)	$_{91}Pa^{234}$	β	1.18 m	9.77×10^{-3}	2.32
Uranium Z (UZ)	$_{91}Pa^{234}$	β	6.7 h	2.88×10^{-5}	1.13
Uranium II (UII)	$_{92}U^{234}$	α	2.50×10^5 y	8.80×10^{-14}	4.768
Ionium (Io)	$_{90}Th^{230}$	α	8.0×10^4 y	2.75×10^{-13}	4.68 m
Radium (Ra)	$_{88}Ra^{226}$	α	1620 y	1.36×10^{-11}	4.777 m
Ra Emanation (Rn)	$_{86}Em^{222}$	α	3.82 d	2.10×10^{-6}	5.486
Radium A (RaA)	$_{84}Po^{218}$	α, β	3.05 m	3.78×10^{-3}	α:5.998 β:?
Radium B (RaB)	$_{82}Pb^{214}$	β	26.8 m	4.31×10^{-4}	0.7
Astatine-218 (At^{218})	$_{85}At^{218}$	α	1.5–2.0 s	0.4	6.63
Radium C (RaC)	$_{83}Bi^{214}$	α, β	19.7 m	5.86×10^{-4}	α:5.51 m β:3.17
Radium C′ (RaC′)	$_{84}Po^{214}$	α	1.64×10^{-4} s	4.23×10^3	7.683
Radium C″ (RaC″)	$_{81}Tl^{210}$	β	1.32 m	8.75×10^{-4}	1.9
Radium D (RaD)	$_{82}Pb^{210}$	β	19.4 y	1.13×10^{-9}	0.017
Radium E (RaE)	$_{83}Bi^{210}$	β	5.0 d	1.60×10^{-6}	1.155
Radium F (RaF)	$_{84}Po^{210}$	α	138.3 d	5.80×10^{-8}	5.300
Thallium-206 (Tl^{206})	$_{81}Tl^{206}$	β	4.2 m	2.75×10^{-3}	1.51
Radium G (RaG)	$_{82}Pb^{206}$	Stable			

is no natural radioactive series of nuclides whose mass numbers are represented by $4n + 1$.

The members of the uranium series are listed in Table 10–1 together with the mode of disintegration, the half-life,[6] the disintegration constant, and the maximum energy of the emitted particles.[6] The changes in atomic number and mass number are shown in Fig. 10–10. Table 10–2 and Fig. 10–11 give the corresponding information about the actinium series, while Table 10–3 and Fig. 10–12 are for the thorium series. The first column of each table gives the old-fashioned, historical names of the radionuclides, while the second column gives the modern symbol. Both are included because both are found in the literature of physics, and it is helpful to have a code for translation readily available. The older name usually indicates the series to which a radioactive substance belongs and gives some idea of the relative position in the series; the modern symbol gives the atomic and mass numbers. The mode of decay, the value of the half-life (or disintegration constant), and the energy of the emitted particle characterize the radioactivity. The half-life may be in years, days, hours, minutes, or seconds, abbreviated as y, d, h, m, s, respectively.

TABLE 10–2

THE ACTINIUM SERIES

Radioactive species	Nuclide	Type of disintegration	Half-life	Disintegration constant, sec^{-1}	Particle energy, Mev
Actinouranium (AcU)	$_{92}U^{235}$	α	7.10×10^8 y	3.09×10^{-17}	4.559 m
Uranium Y (UY)	$_{90}Th^{231}$	β	25.6 h	7.51×10^{-6}	0.30
Protoactinium (Pa)	$_{91}Pa^{231}$	α	3.43×10^4 y	6.40×10^{-13}	5.046 m
Actinium (Ac)	$_{89}Ac^{227}$	α, β	21.6 y	1.02×10^{-9}	α:4.94 β:0.046
Radioactinium(RdAc)	$_{90}Th^{227}$	α	18.17 d	4.41×10^{-7}	6.03 m
Actinium K (AcK)	$_{87}Fr^{223}$	α, β	22 m	5.25×10^{-4}	β:1.2 α:5.34
Actinium X (AcX)	$_{88}Ra^{223}$	α	11.68 d	6.87×10^{-7}	5.864
Astatine-219	$_{85}At^{219}$	α, β	0.9 m	1.26×10^{-2}	α:6.27
Ac Emanation (An)	$_{86}Em^{219}$	α	3.92 s	0.177	6.810 m
Bismuth-215	$_{83}Bi^{215}$	α, β	8 m	1.44×10^{-3}	?
Actinium A (AcA)	$_{84}Po^{215}$	α, β	1.83×10^{-3} s	3.79×10^2	α:7.37
Actinium B (AcB)	$_{82}Pb^{211}$	β	36.1 m	3.20×10^{-4}	1.39
Astatine-215	$_{85}At^{215}$	α	10^{-4} s	7×10^3	8.00
Actinium C (AcC)	$_{83}Bi^{211}$	α, β	2.15 m	5.28×10^{-3}	α:6.617 m
Actinium C′ (AcC′)	$_{84}Po^{211}$	α	0.52 s	1.33	7.442 m
Actinium C″ (AcC″)	$_{81}Tl^{207}$	β	4.79 m	2.41×10^{-3}	1.44
Actinium D (AcD)	$_{82}Pb^{207}$	Stable			

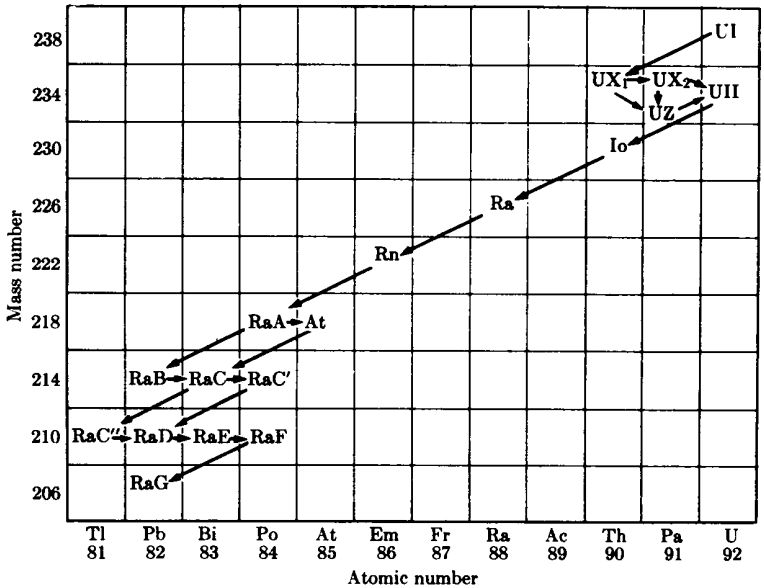

FIG. 10–10. The uranium (4n + 2) series.

TABLE 10–3

THE THORIUM SERIES

Radioactive species	Nuclide	Type of disintegration	Half-life	Disintegration constant, sec^{-1}	Particle energy, Mev
Thorium (Th)	$_{90}Th^{232}$	α	1.39×10^{10} y	1.58×10^{-18}	4.007
Mesothorium1(MsTh1)	$_{88}Ra^{228}$	β	6.7 y	3.28×10^{-9}	0.04
Mesothorium2(MsTh2)	$_{89}Ac^{228}$	β	6.13 h	3.14×10^{-5}	2.18
Radiothorium (RdTh)	$_{90}Th^{228}$	α	1.910 y	1.15×10^{-8}	5.423 m
Thorium X (ThX)	$_{88}Ra^{224}$	α	3.64 d	2.20×10^{-6}	5.681 m
Th Emanation (Tn)	$_{86}Em^{220}$	α	51.5 s	1.34×10^{-2}	6.280
Thorium A (ThA)	$_{84}Po^{216}$	α, β	0.16 s	4.33	6.774
Thorium B (ThB)	$_{82}Pb^{212}$	β	10.6 h	1.82×10^{-5}	0.58
Astatine-216 (At^{216})	$_{85}At^{216}$	α	3×10^{-4} s	2.3×10^{3}	7.79
Thorium C (ThC)	$_{83}Bi^{212}$	α, β	60.5 m	1.91×10^{-4}	α:6.086 m β:2.25
Thorium C' (ThC')	$_{84}Po^{212}$	α	3.0×10^{-7} s	2.31×10^{6}	8.780
Thorium C'' (ThC'')	$_{81}Tl^{208}$	β	3.10 m	3.73×10^{-3}	1.79
Thorium D (ThD)	$_{82}Pb^{208}$	Stable			

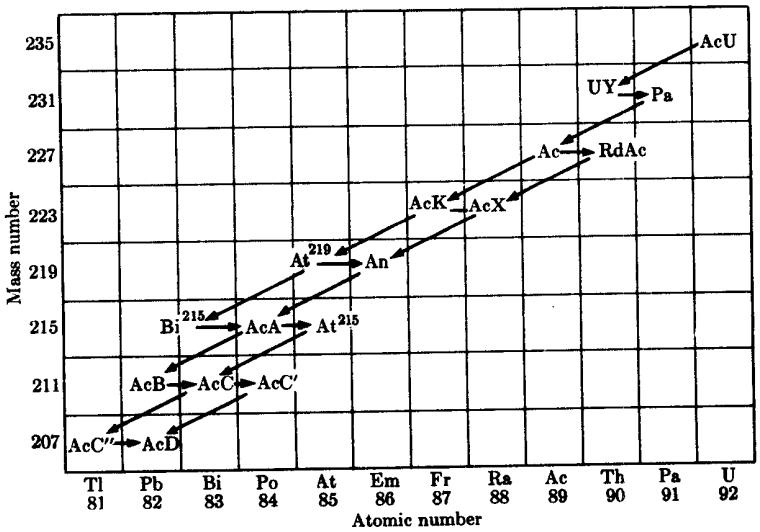

FIG. 10–11. The actinium (4n + 3) series.

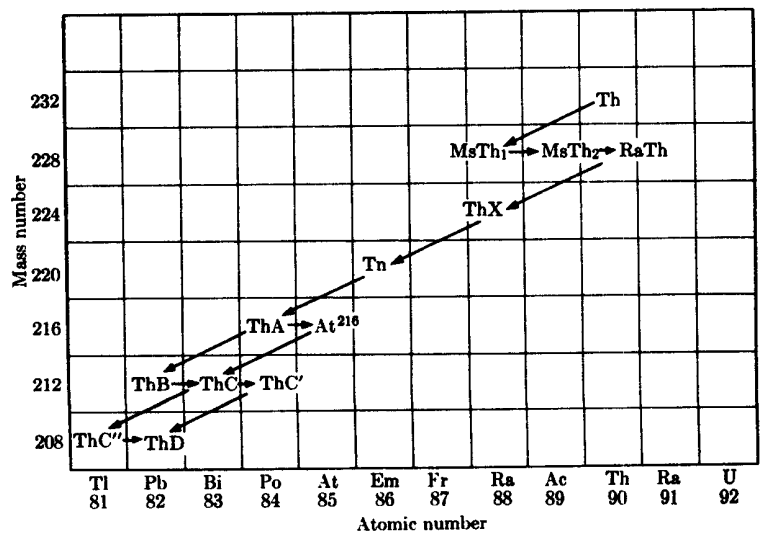

FIG. 10–12. The thorium (4n) series.

In the case of β-particles, the energy value listed is that of the most energetic particles. For some radionuclides, the α-particles are monoenergetic; for others, an α-particle may have one of several energy values, in which case the greatest value is listed and denoted by "m." Figures 10–10 through 10–12 illustrate Soddy's displacement law discussed in Section 9–1. It will be remembered that the emission of an α-particle decreases the charge of a nucleus by two units and the mass number by 4 units, while the emission of a β-particle increases the charge of the nucleus by one unit and leaves the mass number unchanged. In the figures, therefore, an α-disintegration is represented by an arrow sloping downward and to the left, and a β-transition by a horizontal arrow pointing to the right. All of the elements in any one column have the same atomic number and must occupy the same place in the periodic table. For example, RaA, RaC′, RaF, AcA, AcC′, ThA, and ThC′ all have the atomic number 84 and are isotopes of polonium. Similarly, RaB, RaD, RaG, AcB, AcD, ThB, and ThD all have the atomic number 82 and are isotopes of lead. Series schemes like those of Figs. 10–10 through 10–12 led Soddy (1913) to the discovery of the existence of isotopes.

In most of the disintegration processes that make up a radioactive series, each of the radionuclides breaks up in a definite way, giving one α- or β-particle and one atom of the product nuclide. In some cases, however, the atoms break up in two different ways, giving rise to two products with different properties. This kind of disintegration is called *branching decay* and is illustrated by the decay of Po^{218} (RaA), Bi^{214}(RaC), and Bi^{210} (RaE) in the uranium series; by Ac^{227}, Po^{215} (AcA), Bi^{211} (AcC), $_{87}Fr^{223}$ (AcK), and $_{85}At^{219}$ in the actinium series; and by Po^{216} (ThA) and Bi^{212} (ThC) in the thorium series. Each of these nuclides can decay either by α-emission or by β-emission. The probability of disintegration is the sum of the separate probabilities and $\lambda = \lambda_\alpha + \lambda_\beta$; the half-life is $T = 0.693/\lambda = 0.693/(\lambda_\alpha + \lambda_\beta)$. In most cases, one mode of decay is much more probable than the other. Radium A and AcA decay almost entirely by α-emission, with only a small fraction of one percent of the atoms disintegrating by β-emission. On the other hand, RaC, RaE, Ac, and AcC decay almost entirely by β-decay, with one percent or less of the atoms decaying by α-emission. The case of ThC (Bi^{212}) is especially interesting because 66.3% of the disintegrations are by β-emission, and 33.7% by α-emission, in contrast to the other cases mentioned. In each branched decay, the product atoms decay in turn to give the same nuclide. For example, ThC emits a β-particle to form ThC′ (Po^{212}) or an α-particle to form ThC″ (Tl^{208}); ThC′ then emits an α-particle to give stable Pb^{208} (ThD), while ThC″ emits a β-particle and also forms stable Pb^{208}.

10–6 Units of radioactivity. The intensity of radioactivity has so far been considered in terms of the number of atoms which disintegrate per unit time, or in terms of the number of emitted particles counted per unit time by a detector. As in other branches of physics, it is useful to have a standard quantitative unit with an appropriate name. In radioactivity, the standard unit is the *curie*, at present defined as that quantity of any radioactive material giving 3.70×10^{10} disintegrations/sec. The *millicurie*, which is one-thousandth of a curie, and the *microcurie*, equal to one-millionth of a curie, are also useful units; these would correspond to amounts of active materials giving 3.7×10^{7} and 3.7×10^{4} disintegrations/sec, respectively.

For various reasons, mainly historical, there has been some confusion about the use of the curie as the standard unit. Consequently, a new absolute unit of radioactive disintegration rate has been recommended, namely, the *rutherford* (rd), defined as that amount of a radioactive substance which gives 10^{6} disintegrations/sec. The millirutherford (mrd) and microrutherford (μrd) correspond to 10^{3} disintegrations/sec and 1 disintegration/sec, respectively.

To get an idea of some orders of magnitude, consider the problem of calculating the weight in grams of 1 curie and 1 rd of RaB (Pb^{214}), from its half-life of 26.8 min. The disintegration constant is

$$\lambda = 4.31 \times 10^{-4}\ \text{sec}^{-1}.$$

If W is the unknown weight, then

$$-dn/dt = \lambda N = 4.31 \times 10^{-4} \times W/214 \times 6.02 \times 10^{23}$$
$$= 1.21W \times 10^{18}\ \text{disintegrations/sec.}$$

If $-dN/dt = 3.70 \times 10^{10}$ disintegrations/sec (1 curie), then

$$W = \frac{3.70 \times 10^{10}}{1.21 \times 10^{18}} = 3.1 \times 10^{-8}\ \text{gm.}$$

For 1 rd,

$$W = \frac{10^{6}}{1.21 \times 10^{18}} = 8.3 \times 10^{-13}\ \text{gm.}$$

Thus, for a substance with a short, but not very short, half-life very little material is needed to provide a curie of activity. When the half-life is a small fraction of a second (Po^{214}, Po^{215}, At^{215}, At^{216}, or Po^{212}), the amount of material which gives a curie of activity is almost unimaginably

small. In the case of a nuclide with a very long half-life, such as U^{238} ($T = 4.50 \times 10^9$ y), $\lambda = 4.9 \times 10^{-18}$ sec^{-1}. Then

$$-\frac{dN}{dt} = \lambda N = 4.9 \times 10^{-18} \times \frac{W}{238} \times 6.02 \times 10^{23}$$

$$= 1.24 \times 10^4 W \text{ disintegrations/sec.}$$

For 1 curie of activity,

$$W = \frac{3.70 \times 10^{10}}{1.14 \times 10^4} = 3.2 \times 10^6 \text{ gm,}$$

and more than three metric tons are needed.

Chapter (5) : Properties of uses of natural radioactivity .

15.2 α-Particles and the Geiger–Nuttall Rule

The most important property of α-particles is their ability to ionize any material through which they pass. This property is connected with their range and absorption, and it is found that although they do not penetrate very far into normal materials they cause intense ionization. Thus the range in air for α-particles from $^{210}_{84}Po$ (earlier known as radium F) is about 38 mm, and the ionization along the path of the particles increases to a maximum before suddenly decreasing to zero. This was first shown by W. H. Bragg and a typical example of one of his ionization curves for $^{210}_{84}Po$ is shown in Fig. 15.1.

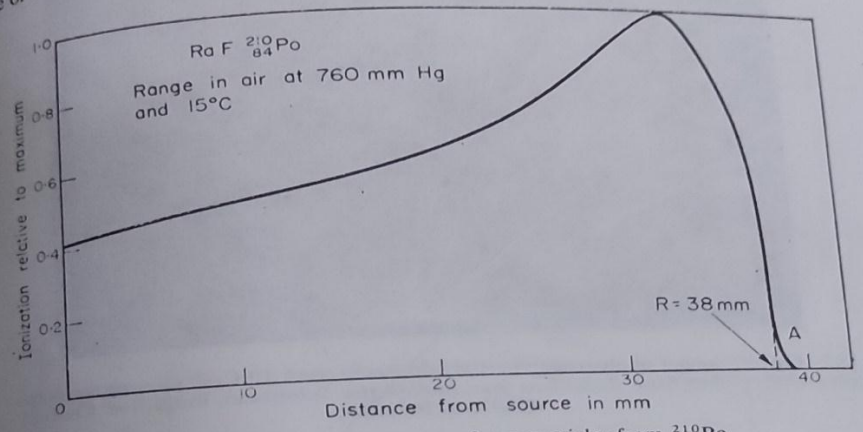

Fig. 15.1 Bragg curve for α-particles from $^{210}_{84}Po$.

As the velocity of the ions is reduced by multiple collisions with the electrons of the gas molecules the ionization efficiency increases until an optimum velocity for ionization is reached. The ionization thereafter decreases rapidly due to ion–electron neutralization, giving a characteristic 'range', i.e. a sharply defined ionization path length. This is best shown in the Wilson cloud chamber pictures given by Blackett (Fig. 15.2). Monoenergetic α-rays have therefore a range R depending on their energy and velocity v, given by the empirical relationship $R = av^3$, where a is a constant. This relationship was originally given by Geiger.

The range as shown in Fig. 15.2 is not always exactly the same for all particles from a given source, due to straggling, or statistical fluctuation in the energy loss process, shown as a slight curvature at the point A on the Bragg curve, Fig. 15.1. The 'range' is found by extrapolating the straight part of the curve to zero ionization, as shown.

Alpha particles are very easily absorbed. A sheet of newspaper will cut off most of them and a postcard will often absorb them completely. Thus from the safety point of view, clothing is sufficient to absorb α-particles and it is the internal hazard which is dangerous (as explained in Appendix B).

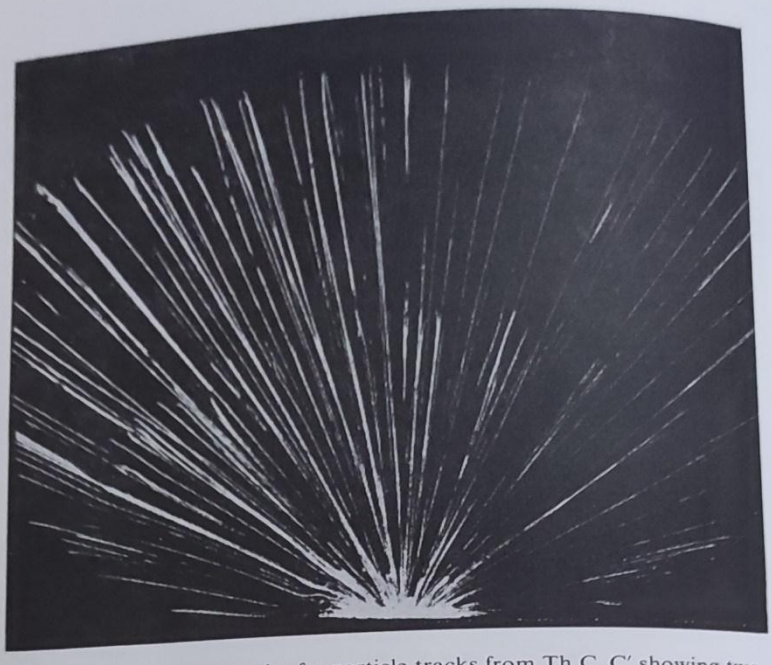

Fig. 15.2 Cloud chamber photograph of α-particle tracks from Th C, C′ showing two ranges and straggling effect. (Taken from *Radiations from Radioactive Substances*, Rutherford, Chadwick and Ellis. C.U.P., 1930.)

If we examine the ranges of the common natural α-emitters, together with their respective half-lives, it is apparent that there is a rough reciprocal relation between them. Table 15.2 shows these quantities in detail and it is important to notice the tremendous range of half-life $T_{1/2}$, ranging from $1{\cdot}4 \times 10^{10}$ a for $^{232}_{90}$Th which is therefore almost a stable isotope, to 300 ns for $^{212}_{84}$Po which is almost a non-existent isotope. Since these nuclides have the shortest and longest α-particle ranges respectively these figures suggest a reciprocal relation of the form:

$$T_{1/2} \cdot R^m = \text{constant}$$

i.e. $\lambda = AR^m$, where $\lambda = 0{\cdot}693/T_{1/2}$ (p. 49) and A is a constant. This gives $\log \lambda = m \log R + B$, putting $B = \log A$.

This is the Geiger–Nuttall rule, first discovered in 1911 as the result of a careful survey of the available data. The rule can be verified experimentally but is difficult to explain theoretically.

Plotting the results of Table 15.2 in Fig. 15.3 we find the slope $m = 60$ approximately, and the intercept $B = -44{\cdot}2$ giving $A = 10^{-84}$, so that

$$\lambda = 10^{-84}\ R^{60}$$

TABLE 15.2
Systematics of the Thorium Series α-Emitters

Radioactive species name	*Nuclide symbol*	*Range in air 760 nm and 15 °C mm*	*Energy (MeV)*	*Half-life* $T_{1/2}$	*Disintegration constant* (s^{-1}) λ
Th	$^{232}_{90}Th$	29·0	3·98	$1·39 \times 10^{10}$ a	$1·58 \times 10^{-18}$
RaTh	$^{228}_{90}Th$	40·2	5·42	1·9 a	$1·16 \times 10^{-8}$
Th X	$^{224}_{88}Ra$	43·5	5·68	3·64 d	$2·20 \times 10^{-6}$
Thoron	$^{220}_{86}Rn$	50·6	6·28	54·5 s	$1·27 \times 10^{-2}$
Th A	$^{216}_{84}Po$	56·8	6·77	0·16 s	4·33
Th C	$^{212}_{83}Bi$	47·9	6·05	60·5 min	$1·92 \times 10^{-4}$
Th C'	$^{212}_{84}Po$	86·2	8·77	3×10^{-7} s	$2·31 \times 10^{6}$

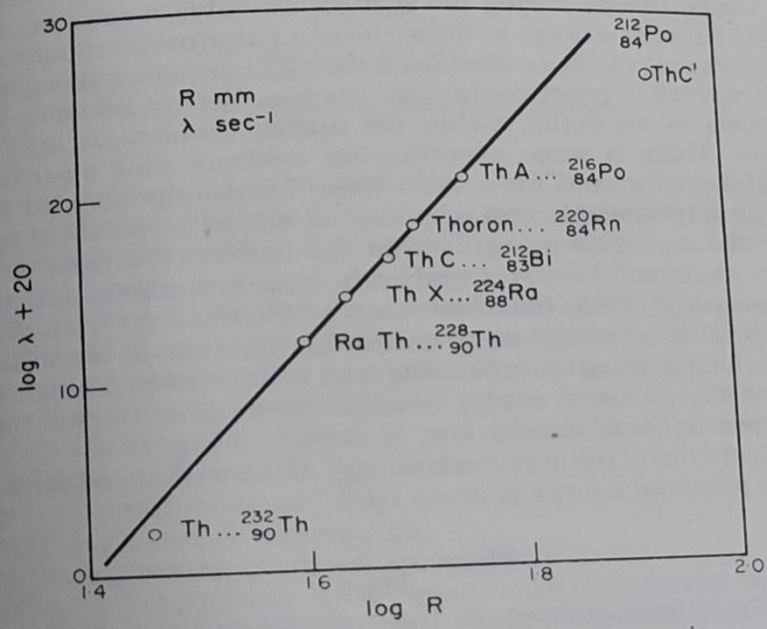

Fig. 15.3 Geiger–Nuttall rule for the thorium series.

or

$$T_{1/2}R^{60} = \frac{0·693}{10^{-84}} = 6·93 \times 10^{83} \text{ s mm.}$$

Different constants would be obtained for the other radioactive series.

Since the range R is connected with the energy of disintegration E by the equations $E = \frac{1}{2}mv^2$ and $R = av^3$, there must be a similar systematic reciprocal connection between half-life and disintegration energy (see Problem 15.1) which has to be explained by any satisfactory theory of the structure of the nucleus.

Furthermore, the α-particle must be a particularly stable combination of protons and neutrons to be ejected as an entity by a radioactive nucleus.

15.3 The Theory of α-decay

Apart from the empirical law of Gieger and Nuttall there are some other puzzling facts about α-particle emission which must be explained. The early α-particle bombarding experiments of Rutherford (see p. 41) showed that the Coulomb law held down to distances of 10^{-14} m with all α-energies of the order of 5 MeV. We are discussing here the naturally radioactive elements of $Z > 80$ and $A > 200$, which means that the range of particle energies is not large. As an example, $^{238}_{92}U$ is an α-emitter by

$$^{238}_{92}U \rightarrow ^{4}_{2}He\ (\alpha) + ^{234}_{90}Th + Q_\alpha$$

where Q_α is the energy of the emitted α-particle, about 4·18 MeV. These α-particles are emitted continuously, although infrequently since $T_{1/2} = 4{\cdot}5 \times 10^9$ a. On the other hand the $^{235}_{92}U$ nucleus withstood all attempts to disintegrate it by α-particle bombardment. Firing the swiftest available α-particles of energy 8·3 MeV at $^{238}_{92}U$ failed to disrupt it. So we have a paradoxical situation where 4·18 MeV α-particles are readily emitted from the $^{238}_{92}U$ nucleus whereas α-particles of twice this energy fail to penetrate into the nucleus. We are assuming here that the α-particle exists as an entity within the nuclear volume at least just before disintegration. There is some experimental evidence that α-particles exist as 'clusters' within the nucleus for a short time. The energy paradox suggests the existence of an impenetrable wall or potential barrier of potential energy much greater than the α-particle energy within the barrier. This idea of a potential barrier can be understood if we remember the quantum-mechanical discussion of the model atom on p. 139. In that discussion we put the atom in an infinitely deep potential well with infinitely thick walls. In the case of α-emission we are discussing, we have a situation where the wall is finite in both height and width. Inside the well the potential energy is negative, outside the well the potential barrier is subject to the Coulomb law, as shown in Fig. 15.4.

A rough calculation of the maximum energy of the well can be made as follows. The repulsion potential energy is given by

$$V(r) = \frac{2 \times Ze^2}{4\pi\varepsilon_0 r},$$

where Z is the atomic number of the residual nucleus. Now independent experiments show that the effective radius of the uranium nucleus is about 8·6 $\times 10^{-15}$ m (see p. 000), so that the maximum potential energy of the barrier is

$$\begin{aligned} V(r) &= \frac{2 \times 90 \times 1{\cdot}6^2 \times 10^{-38}}{\frac{1}{9} \times 10^{-9} \times 8{\cdot}6 \times 10^{-15}}\ \text{J} \\ &= 4{\cdot}82 \times 10^{-12}\ \text{J} \\ &= \frac{4{\cdot}82 \times 10^{-12}}{1{\cdot}6 \times 10^{-13}}\ \text{MeV} \\ &= 30\ \text{MeV} \end{aligned}$$

This is the peak barrier height, although the actual shape of the distribution is more like the dotted portion of Fig. 15.4. In order to get out of the well, the α-

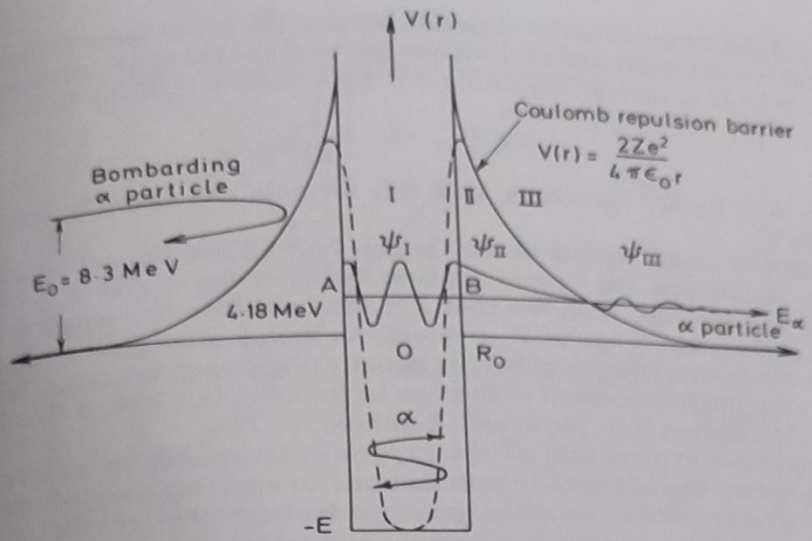

Fig. 15.4 'Tunelling' effect for α-particles.

particle has to surmount this 30 MeV barrier. Classically this is impossible because the α-particle 'rattles' about inside the well and fails to rise above the 4·18 MeV energy level shown as AB in Fig. 15.4. Thus classical physics fails to solve the paradox just as it failed to predict the Geiger–Nuttall law.

At once we see here a case for a quantum-mechanical approach. We saw in Chapter 10 that the atom (although here we are discussing a charged α-particle) behaved as a wave represented by a wave function ψ. Early quantum-mechanical calculations showed that the α-particle had a finite probability of penetrating the barrier from inside the well, and could be represented by three different wave functions as follows, referring to Fig. 15.4:

in region I, ψ_{I}, which is sinusoidal,
in region II, ψ_{II}, which is exponential,
in region III, ψ_{III}, which decreases sinusoidally.

After solving the Schrödinger wave equation for each region and inserting the boundary and continuity conditions, the transmission coefficient from inside can be calculated from the amplitudes of the wave functions. The probability of an α-particle escaping can be calculated and the decay constant is of the form

$$\lambda = A\mathrm{e}^{-B},$$

where A depends on the nuclear radius R and B depends both on Z and on the velocity of emission. Thus we get

$$\log \lambda = a_0 - \frac{b_0}{v_\alpha}$$

(where v_α is the velocity of emission of the α-particle) or

$$\log \lambda = a - \frac{b}{E_\alpha^{1/2}},$$

where a depends on R and b depends on Z. This is not quite the same as the empirical law of Geiger and Nuttall but can be regarded as a theoretical 'Geiger–Nuttall' rule. It is completely borne out by experiment. It can be written as

$$\log T_{1/2} = k_1 + \frac{k_2}{E_\alpha^{1/2}},$$

where k_1 and k_2 are constants, and this formula can easily be verified from Appendix C.

Although an exact replica of the Geiger–Nuttall law has not been found by quantum mechanics, the linear relation between $\log \lambda$ and $E_\alpha^{-1/2}$ has been predicted and verified. It shows that λ is very sensitive to changes in E_α or v_α, as found in the great range of $T_{1/2}$ values. As such it gives great credence to the quantum-mechanical theory of barrier penetration sometimes called the 'tunnelling effect'. A complete account of this can be found in H. Clark, *A First Course in Quantum Mechanics*, Van Nostrand Reinhold, p. 79.

The successful explanation of the experimental results for α-particle systematics represents one of the early justifications for applying quantum-mechanical methods to the problems of nuclear structure. It also enabled the nuclear radius R to be calculated from α-particle emission, and tables of α-particle nuclear radii show that most of the natural α-emitters have nuclear radii of about $(9{\cdot}2-9{\cdot}5) \times 10^{-15}$ m. This agrees well with radii measured by other probes (see p. 000).

15.4 β-Rays and the Neutrino

The identification of β^--rays with fast electrons (see Chapter 3) means that all the β^--emitters change their chemical nature and atomic numbers but do not appreciably change their atomic mass numbers, i.e. isobars are different chemical elements. It is possible to measure the energies of nuclear β^--rays by means of the magnetic spectrograph and it is found that the velocities of ejected electrons are not constant, but are spread out in a spectrum as shown in Fig. 15.5.

This continuous velocity spectrum refers to nuclear electrons only and shows that the energy of disintegration of a nucleus is not always given completely to the ejected β^--particle. The most probable value of the energy of an ejected electron is given by E_1 (Fig. 15.5) but the most energetic electrons are actually comparatively few in number. At first sight this suggests that the law of conservation of energy fails with β^--emitters, but Pauli in 1931 suggested informally that there is no violation of the conservation laws if *another* particle as well as the electron is simultaneously emitted by each nucleus. This particle is known as the antineutrino ($\bar{\nu}$), and the energy balance now becomes

$$E_{\beta_{\text{Total}}} = E_\nu + E_\beta$$

where both E_ν and E_β are variable, as shown in Fig. 15.5.

This equation was verified in cloud-chamber experiments with β-rays and careful measurements showed that the conservation of linear momentum was also violated unless another particle was emitted with the β^- particle.

We shall see later that a positron may be emitted from proton-rich nuclides. Positrons are positive electrons, β^+, and are accompanied by neutrinos ν. They are antiparticles to negative electrons (see p. 000) and their neutrinos are antiparticles to antineutrinos. Experiments on nuclear spins show that all odd-A

$$E_{\beta\text{-Total}} = E_{\tilde{\nu}} + E_{\beta^-}$$

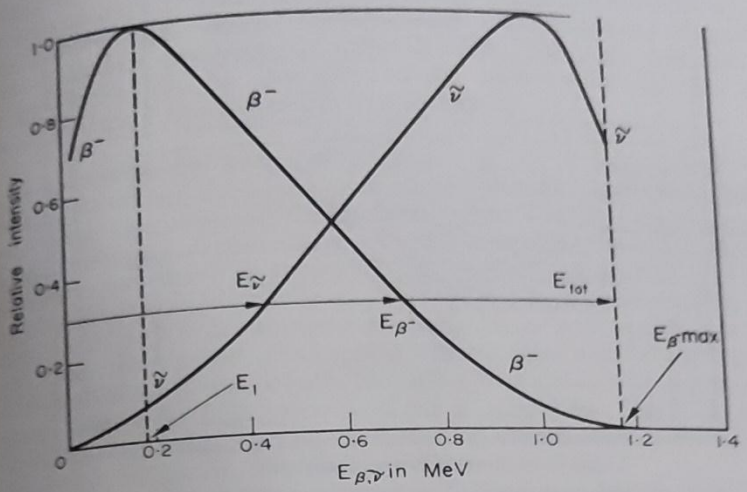

Fig. 15.5 Typical β^-, $\tilde{\nu}$ energy spectrum.

nuclides have half-integral spins, and many have $s=\frac{1}{2}$, so that a decay equation such as

$$^{A}_{Z}\mathrm{X} \rightarrow {}_{Z+1}{}^{A}\mathrm{Y} + {}^{0}_{-1}\mathrm{e}\ (\beta^-)$$

may have spins

$$\tfrac{1}{2} \rightarrow \tfrac{1}{2} + \tfrac{1}{2}$$

when A is odd. Conservation of angular momentum thus requires another particle to be ejected simultaneously with the β^--particle and with the same spin $\frac{1}{2}\hbar$ but opposite in sense. All $\beta^{\pm}$ decays are isobaric, so that the nucleon number remains unchanged. The angular momentum of the nucleus must therefore remain the same or change by an integral number of $\hbar$ units (all nucleons have spin $\frac{1}{2}\hbar$). To conserve angular momentum the spins of the $\tilde{\nu}$ and β^- particles must each be $\frac{1}{2}\hbar$ and oriented to give a total change of 0 or 1 units. Thus considerations of energy, linear momentum and angular momentum all point to the existence of a neutrino. The basic equation for all β^--decays is

$$\mathrm{n}^0 \rightarrow \mathrm{p}^+ + \mathrm{e}^- + \tilde{\nu}$$

and it is from this equation that we infer that the spin of the neutrino is $s=\frac{1}{2}$.

It was 25 years (after Pauli's original suggestion) before the elusive neutrino and antineutrino became 'respectable', i.e. were accepted as real particles interacting with matter. Reines and Cowan in the mid-1950s tested the inverse equation

$$\tilde{\nu} + \mathrm{p}^+ \rightarrow \mathrm{n}^0 + \beta^+$$

in a classic experiment using the high flux of antineutrinos from the β^- decays in a nuclear reactor. The neutrinos were fired into a large liquid collision chamber containing an organic liquid or water of high proton density and surrounded by liquid scintillation counters (see Fig. 15.6). By detecting the presence of n^0 and β^+

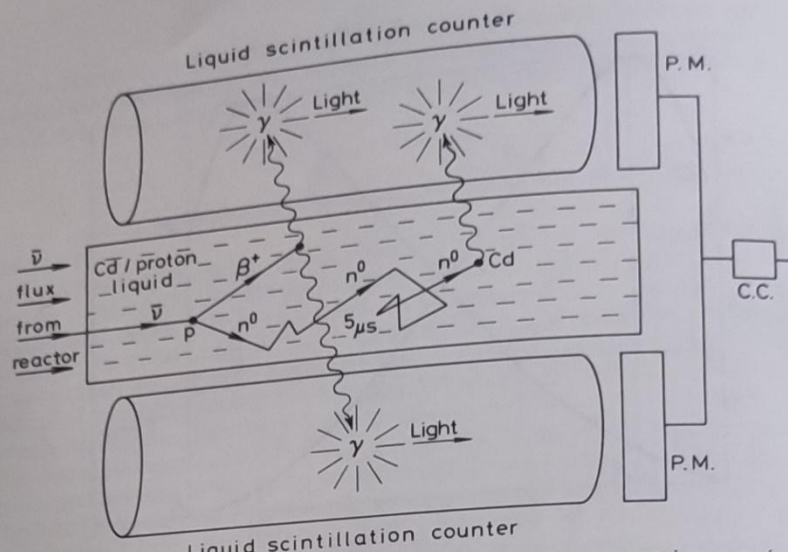

Fig. 15.6 Diagrammatic representation of the Reines and Cowan neutrino experiment.

simultaneously the neutrino equation was confirmed. For detecting the neutrons, the liquid was doped with a cadmium salt. Cadmium has a high neutron capture cross-section through the n, γ reaction. The neutrons travel in a random direction for about 5 μs before producing simultaneous γ-rays from the cadmium collisions. The positrons from the neutrino collisions also produced γ-rays from their decay in flight by the annihilation process. On entering the scintillator tube the γ-rays ionize and excite the liquid molecules. The light radiation from the de-excitation of these molecules causes the 'scintillations' which are then detected by the photomultiplier tubes (P.M. in Fig. 15.6). The calculated time difference between the two γ-pulses was such that the neutron γ's were expected to be recorded about 5 μs after the annihilation γ's. A delayed coincidence counter (C.C. in Fig. 15.6) was therefore set at this figure to detect the existence of neutron- and positron-produced γ's simultaneously. The count rate for these coincidences was $0{\cdot}41 \pm 20$ counts per minute or about 2·88 counts per hour. This very low figure agreed well with the anticipated cross-section of only 10^{-48} m^2.

Reines and Cowan proved conclusively that the $\tilde{\nu}p^+ \rightarrow n^0\beta^+$ reaction was real. Checking the energy of the β^+ γ-pulse against that from a known β^+ emitter such as ^{64}Cu identified it unambiguously and removing the Cd from the scintillation liquid removed the second pulse completely, as expected.

The two neutrinos are now well established as free particles in collision experiments. They are fermions with spin $\frac{1}{2}\hbar$, with no charge, no magnetic moment, no rest mass and they do not cause ionization on passing through matter. Like the photon, which is a boson of spin 1, the neutrino has a finite energy and momentum in flight. It travels with the speed of light c and is subject to the laws of relativity. Unlike the photon, the neutrino does not interact with the

electromagnetic field, but it does interact with particle matter although with a cross-section of only 10^{-48} m^2. Matter is almost totally transparent to neutrinos.

The shapes of both β^- and β^+ curves such as in Fig. 15.5 can be explained by quantum mechanics, assuming that the neutrino has zero rest mass. Direct experiment shows that the rest mass of the neutrino is certainly less than $0{\cdot}0005m_e$. The theory was originally due to Fermi.

15.5 The Absorption and Range of β^- rays

The maximum energy of the β^--rays is almost the energy of disintegration and for experimental purposes can be taken as such. The β^-- and $\bar{\nu}$-particles are ejected simultaneously, so that along with the recoil of the product nucleus they conserve linear momentum and together they conserve spin angular momentum.

Beta particles are comparatively easily absorbed by thin sheets of metal, e.g. a sheet of Al 5 mm thick will cut down the intensity of a β^--beam by about 90%. They are thus rather more penetrating than α-rays and in consequence the ionization caused by β^--particles is less than that caused by α-particles of the same energy, due to the high velocity of the β^--particles. The hazard from β^--particles is therefore mainly an internal one by ingestion of contaminated food and drink or by inhalation of airborne radioactive dust.

The absorption of β^--particles by matter follows roughly the exponential law

$$I = I_0 e^{-\mu x}$$

where I_0 is the initial intensity of beam, I is the final intensity of beam after passing through thickness x, μ is the absorption coefficient as measured by this equation.

This equation is rather fortuitous as the β^--rays are not monoenergetic. It is therefore to be treated as an experimental relation. On testing this equation experimentally for pure β^--emitters it is found that the graph of $\log I$ against thickness x is not a straight line as the above equation suggests. Furthermore, the intensity persists even for very thick absorbers and remains constant up to large values of x, as shown in Fig. 15.7. This constant intensity arises from the formation of '*Bremsstrahlung*', or 'braking radiation', by the sudden arrest of the β^--particles within the absorber. This radiation is equivalent to the formation of penetrating X-rays of short wavelength at high values of x, so giving the effect of a beam of β^--particles of constant intensity.

As a single β^--particle passes through an absorbing material it loses energy by multiple collisions until it is no longer able to ionize the atoms of the absorber. It therefore has a fairly well-defined range beyond which it has no ionizing effect. The exponential equation mentioned above which is used to describe this attenuation is purely fortuitous and the range R as shown in Fig. 15.7 then corresponds to those β^--particles in the spectrum with maximum energy $E_{\beta^- \max}$, i.e. the end point of Fig. 15.5. This is also the value of the decay energy. The range of β^--particles can be determined by a simple absorption experiment. Instead of plotting the logarithm of the activity to the thickness x, it is customary to plot it to the area density, in mg cm^{-2} units. The reason for this is twofold. It is much easier to weight a foil and measure its area than to measure its thickness. Also it appears that to a good approximation absorber thicknesses expressed as mg cm^{-2} are nearly independent of the material of the absorber for a given β^- energy. This is

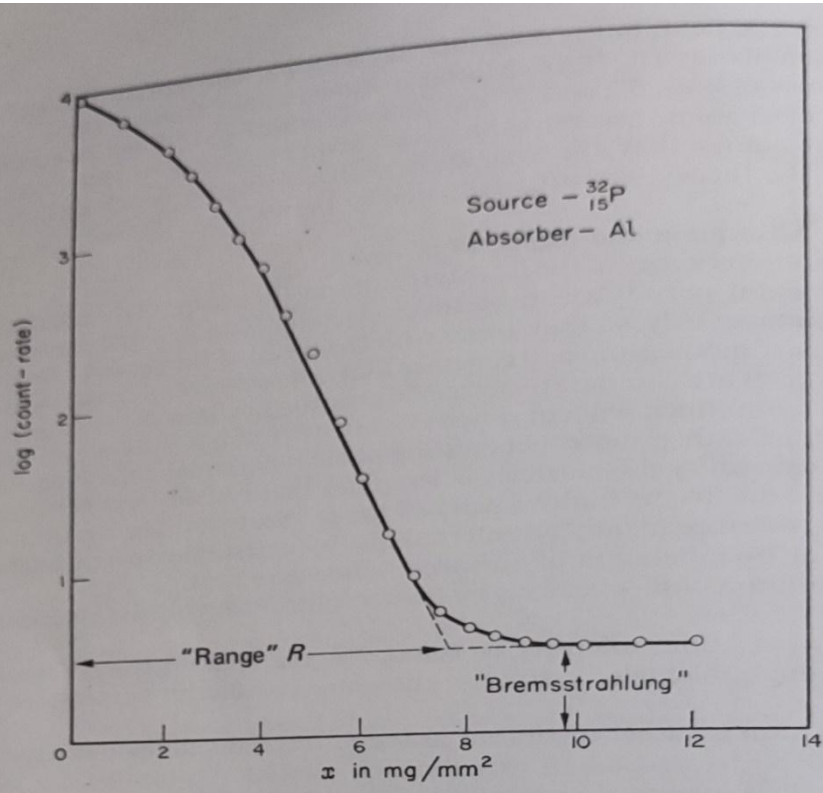

Fig. 15.7 Logarithmic β^--absorption curve.

because the measured intensity of the beam depends on the number of atoms struck, i.e. on the material density, as well as on the initial β^- energy. The ranges of β^--articles in many metal foils are therefore roughly the same, being of the order of 500 mg cm^{-2}. Experimental range–energy curves are therefore much the same for many metals.

A convenient metal absorber is aluminium and Feather has given a formula for the extrapolated range of β^--particles in aluminium in terms of the maximum energy of the β^--particles. This is

$$R = 543E_{\beta^-\max} - 160$$

with R in mg cm^{-2} and $E_{\beta\max}$ in MeV. From Fig. 15.7 we see that R is 7·7 mg mm^{-2} for $^{32}_{15}P$ β^--particles, i.e. 770 mg cm^{-2} in aluminium. From the Feather formula, the value of $E_{\beta^-\max}$ for $^{32}_{15}P$ is given by

$$E_{\beta^-\max} = \frac{770 + 160}{543}$$

$$= 1{\cdot}71 \text{ MeV}$$

This corresponds with the true value as found in Appendix C.

The absorption method outlined above is very convenient for measuring the

unknown β^--decay energy of radioactive elements, and many empirical formulae have been used to cover a wide range of energies. It is not as accurate as the magnetic spectrograph method, but is good enough for most purposes.

Chapter (6) : Photon interactions.

5.5. INTERACTIONS OF PHOTONS WITH MATTER

Attenuation of a photon beam by an absorbing material is caused by five major types of interactions. One of these, photodisintegration, was considered in Section 2.8F. This reaction between photon and nucleus is only important at very high photon energies (>10 MeV). The other four processes are coherent scattering, the photoelectric effect, the Compton effect, and the pair production. Each of these processes can be represented by its own attenuation coefficient, which varies in its particular way with the energy of the photon and with the atomic number of the absorbing material. The total attenuation coefficient is the sum of individual coefficients for these processes:

$$\mu/\rho = \sigma_{coh}/\rho + \tau/\rho + \sigma_c/\rho + \pi/\rho \qquad (5.15)$$

where σ_{coh}, τ, σ_c, and π are attenuation coefficients for coherent scattering, photoelectric effect, Compton effect, and pair production, respectively.

5.6. COHERENT SCATTERING

The coherent scattering, also known as classical scattering or Rayleigh scattering, is illustrated in Figure 5.4. The process can be visualized by considering the wave nature of electromagnetic radiation. This interaction consists of an electromagnetic wave passing near the electron and setting it into oscillation. The oscillating electron reradiates the energy at the same frequency as the incident electromagnetic wave. These scattered x-rays have the same wavelength as the incident beam. Thus, no energy is changed into electronic motion and no energy is absorbed in the medium. The only effect is the scattering of the photon at small angles. The coherent scattering is

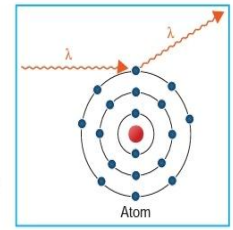

Figure 5.4. Diagram illustrating the process of coherent scattering. The scattered photon has the same wavelength as the incident photon. No energy is transferred.

probable in high-atomic-number materials and with photons of low energy. The process is only of academic interest in radiation therapy.

5.7. PHOTOELECTRIC EFFECT

The photoelectric effect is a phenomenon in which a photon is absorbed by an atom, and as a result one of its orbital electrons is ejected (Fig. 5.5). In this process, the entire energy ($h\nu$) of the photon is first absorbed by the atom and then essentially all of it is transferred to the atomic electron. The kinetic energy of the ejected electron (called the photoelectron) is equal to $h\nu - E_B$, where E_B is the binding energy of the electron. Interactions of this type can take place with electrons in the K, L, M, or N shells.

After the electron has been ejected from the atom, a vacancy is created in the shell, thus leaving the atom in an excited state. The vacancy can be filled by an outer orbital electron with the emission of a characteristic x-ray (Section 3.4B). There is also the possibility of emission of Auger electrons (Section 2.7C), which occurs when the energy released as a result of the outer electron filling the vacancy is given to another electron in a higher shell, which is subsequently ejected. Because the K-shell binding energy of soft tissues is only about 0.5 keV, the energy of the characteristic photons produced in biologic absorbers is very low and can be considered to be locally absorbed. For higher-atomic-number materials, the characteristic photons are of higher energy and may deposit energy at large distances compared with the range of the photoelectron. In such cases, the local energy absorption is reduced by the energy emitted as characteristic radiation (also called fluorescent radiation), which is considered to be remotely absorbed.

The probability of photoelectric absorption depends on the photon energy as illustrated in Figure 5.6, where the mass photoelectric attenuation coefficient (τ/ρ) is plotted as a function of photon energy. Data are shown for water, representing a low-atomic-number material similar to tissue, and for lead, representing a high-atomic-number material. On logarithmic paper, the graph is almost a straight line with a slope of approximately –3; therefore, we get the following relationship between τ/ρ and photon energy:

$$\tau/\rho \propto 1/E^3 \tag{5.16}$$

The graph for lead has discontinuities at about 15 and 88 keV. These are called *absorption edges*, and correspond to the binding energies of L and K shells. A photon with energy less than 15 keV does not have enough energy to eject an L electron. Thus, below 15 keV, the interaction is limited to the M- or higher-shell electrons. When the photon has an energy that just equals the

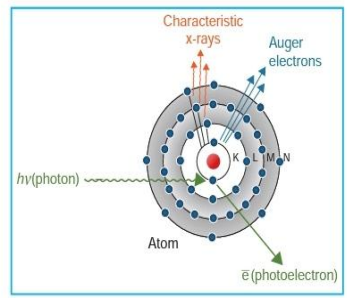

Figure 5.5. Illustration of the photoelectric effect.

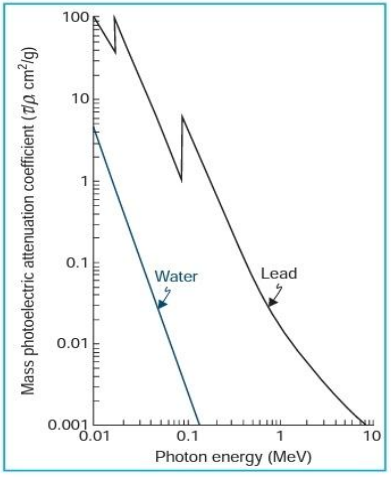

Figure 5.6. Mass photoelectric attenuation coefficient (τ/ρ) plotted against photon energy. Curves for water (Z_{eff} = 7.42) and lead (Z = 82). (Data from Grodstein GW. *X-ray Attenuation Coefficients from 10 keV to 100 MeV.* Pub. No. 583. Washington, DC: U.S. Bureau of Standards; 1957.)

binding energy of the L shell, resonance occurs and the probability of photoelectric absorption involving the L shell becomes very high. Beyond this point, if the photon energy is increased, the probability of photoelectric attenuation decreases approximately as $1/E^3$ until the next discontinuity, the K absorption edge. At this point on the graph, the photon has 88 keV energy, which is just enough to eject the K electron. As seen in Figure 5.6, the absorption probability in lead at this critical energy increases dramatically, by a factor of about 10.

The discontinuities or absorption edges for water are not shown in the graph because the K absorption edge for water occurs at very low photon energies (~0.5 keV).

The data for various materials indicate that photoelectric attenuation depends strongly on the atomic number of the absorbing material. The following approximate relationship holds:

$$\tau/\rho \propto Z^3 \tag{5.17}$$

This relationship forms the basis of many applications in diagnostic radiology. The difference in Z of various tissues such as bone, muscle, and fat amplifies differences in x-ray absorption, provided the primary mode of interaction is photoelectric. This Z^3 dependence is also exploited when using contrast materials such as $BaSO_4$ mix and Hypaque. In therapeutic radiology, the low-energy beams produced by superficial and orthovoltage machines cause unnecessary high absorption of x-ray energy in bone as a result of this Z^3 dependence; this problem will be discussed later in Section 5.10. By combining Equations 5.16 and 5.17, we have

$$\tau/\rho \propto Z^3/E^3 \tag{5.18}$$

The angular distribution of electrons emitted in a photoelectric process depends on the photon energy. For a low-energy photon, the photoelectron is emitted most likely at 90 degrees relative to the direction of the incident photon. As the photon energy increases, the photoelectrons are emitted in a more forward direction.

5.8. COMPTON EFFECT

In the Compton process, the photon interacts with an atomic electron as though it were a "free" electron, that is, the binding energy of the electron is much less than the energy of the bombarding photon. In this interaction, the electron receives some energy from the photon and is emitted at an angle θ (Fig. 5.7). The photon, with reduced energy, is scattered at an angle ϕ.

The Compton process can be analyzed in terms of a collision between two particles, a photon and an electron. By applying the laws of conservation of energy and momentum, one can derive the following relationships:

$$E = h\nu_0 \frac{\alpha(1 - \cos\phi)}{1 + \alpha(1 - \cos\phi)} \tag{5.19}$$

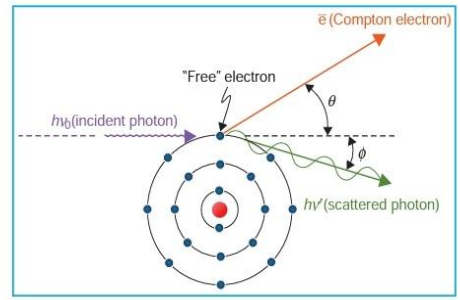

Figure 5.7. Diagram illustrating the Compton effect.

$$h\nu' = h\nu_0 = \frac{1}{1 + \alpha(1 - \cos\phi)} \tag{5.20}$$

$$\cot\theta = (1 + \alpha)\tan\phi/2 \tag{5.21}$$

where $h\nu_0$, $h\nu'$, and E are the energies of the incident photon, scattered photon, and electron, respectively, and $\alpha = h\nu_0/m_0c^2$, where m_0c^2 is the rest energy of the electron (0.511 MeV). If $h\nu_0$ is expressed in MeV, then $\alpha = h\nu_0/0.511$.

A. SPECIAL CASES OF COMPTON EFFECT

Direct Hit

If a photon makes a direct hit with the electron, the electron will travel forward ($\theta = 0$ degrees) and the scattered photon will travel backward ($\phi = 180$ degrees) after the collision. In such a collision, the electron will receive maximum energy E_{max} and the scattered photon will be left with minimum energy $h\nu'_{min}$. One can calculate E_{max} and $h\nu'_{min}$ by substituting $\cos\phi = \cos 180$ degrees $= -1$ in Equations 5.19 and 5.20:

$$E_{max} = h\nu_0\frac{2\alpha}{1 + 2\alpha} \tag{5.22}$$

$$h\nu'_{min} = h\nu_0\frac{1}{1 + 2\alpha} \tag{5.23}$$

Grazing Hit

If a photon makes a grazing hit with the electron, the electron will be emitted at right angles ($\theta = 90$ degrees) and the scattered photon will go in the forward direction ($\phi = 0$ degrees). By substituting $\cos\phi = \cos 0$ degrees $= 1$ in Equations 5.19 and 5.20, one can show that for this collision $E = 0$ and $h\nu' = h\nu_0$.

90-Degree Photon Scatter

If a photon is scattered at right angles to its original direction ($\phi = 90$ degrees), one can calculate E and $h\nu'$ from Equations 5.19 and 5.20 by substituting $\cos\phi = \cos 90$ degrees $= 0$. The angle of the electron emission in this case will depend on α, according to Equation 5.21.

EXAMPLES. Some useful examples will now be given to illustrate application of the Compton effect to practical problems.

a. *Interaction of a low-energy photon.* If the incident photon energy is much less than the rest energy of the electron, only a small part of its energy is imparted to the electron, resulting in a scattered photon of almost the same energy as the incident photon. For example, suppose $h\nu_0 = 51.1$ keV; then $\alpha = h\nu_0/m_0c^2 = 0.0511$ MeV/0.511 MeV $= 0.1$. From Equations 5.22 and 5.23:

$$E_{max} = 51.1\,(\text{keV})\frac{2(0.1)}{1 + 2(0.1)} = 8.52\,\text{keV} \tag{5.24}$$

$$h\nu'_{min} = 51.1\,(\text{keV})\frac{1}{1 + 2(0.1)} = 42.58\,\text{keV} \tag{5.25}$$

Thus, for a low-energy photon beam, the Compton scattered photons have approximately the same energy as the original photons. Indeed, as the incident photon energy approaches zero, the Compton effect becomes the classical scattering process described in Section 5.6.

b. *Interaction of a high-energy photon.* If the incident photon has a very high energy (much greater than the rest energy of the electron), the photon loses most of its energy to the Compton electron and the scattered photon has much less energy. Suppose $h\nu_0 = 5.11$ MeV; then $\alpha = 10.0$. From Equations 5.22 and 5.23,

$$E_{max} = 5.11\,(\text{MeV})\,\frac{2(10)}{1+2(10)} = 4.87\,\text{MeV} \tag{5.26}$$

$$h\nu'_{min} = 5.11\,(\text{keV})\,\frac{1}{1+2(10)} = 0.24\,\text{MeV} \tag{5.27}$$

In contrast to example (a) above, the scattered photons produced by high-energy photons carry away only a small fraction of the initial energy. Thus, at high photon energy, the Compton effect causes a large amount of energy absorption compared with the Compton interactions involving low-energy photons.

c. *Compton scatter at $\phi = 90$ degrees and 180 degrees.* In designing radiation protection barriers (walls) to attenuate scattered radiation, one needs to know the energy of the photons scattered at different angles. The energy of the photons scattered by a patient under treatment at 90 degrees with respect to the incident beam is of particular interest in calculating barrier or wall thicknesses against scattered radiation.

By substituting $\phi = 90$ degrees in Equation 5.20, we obtain

$$h\nu' = \frac{h\nu_0}{1+\alpha} \tag{5.28}$$

For high-energy photons with $\alpha >> 1$, the previous equation reduces to

$$h\nu' \approx \frac{h\nu_0}{\alpha} \tag{5.29}$$

or

$$h\nu' = m_0c^2 = 0.511\ \text{MeV}$$

Similar calculations for scatter at $\phi = 180$ degrees will indicate $h\nu' = 0.255$ MeV. Thus, if the energy of the incident photon is high ($\alpha >> 1$), we have the following important generalizations:

a. the radiation scattered at right angles is independent of incident energy and has a maximum value of 0.511 MeV;
b. the radiation scattered backward is independent of incident energy and has a maximum value of 0.255 MeV.

The maximum energy of radiation scattered at angles between 90 and 180 degrees will lie between the above energy limits. However, the energy of the photons scattered at angles less than 90 degrees will be greater than 0.511 MeV and will approach the incident photon energy for the condition of forward scatter. Because the energy of the scattered photon plus that of the electron must equal the incident energy, the electron may acquire any energy between zero and E_{max} (given by Equation 5.22).

B. DEPENDENCE OF COMPTON EFFECT ON ENERGY AND ATOMIC NUMBER

It was mentioned previously that the Compton effect is an interaction between a photon and a free electron. Practically, this means that the energy of the incident photon must be large compared with the electron-binding energy. This is in contrast to the photoelectric effect, which becomes most probable when the energy of the incident photon is equal to or slightly greater than the binding energy of the electron. Thus, as the photon energy increases beyond the binding energy of the K electron, the photoelectric effect decreases rapidly with energy (Equation 5.16) (Fig. 5.6) and the Compton effect becomes more and more important. However, as shown in Figure 5.8, the Compton effect also *decreases with increasing photon energy*.

Because the Compton interaction involves essentially free electrons in the absorbing material, *it is independent of atomic number Z*. It follows that the Compton mass attenuation coefficient (σ_c/ρ) is independent of Z and depends only on the number of electrons per gram. Although the number of electrons per gram of elements decreases slowly but systemically with atomic number, most materials except hydrogen can be considered as having approximately the same number of electrons per gram (Table 5.1). Thus, *σ_c/ρ is nearly the same for all materials*.

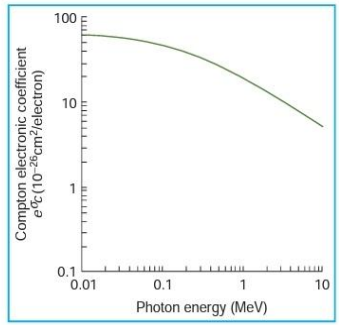

Figure 5.8. A plot of Compton electronic coefficient ${}_e\sigma_c$ against photon energy. The mass coefficient (σ_c/ρ) is obtained by multiplying the electronic coefficient with the number of electrons per gram for a given material. (Data from Hubbell JH. *Proton Cross Sections Attenuation Coefficients and Energy Absorption Coefficients from 10 keV to 100 GeV*. Pub. No. 29. Washington, DC: U.S. National Bureau of Standards; 1969.)

TABLE 5.1 Number of Electrons per Gram of Various Materials

Material	Density (g/cm^3)	Atomic Number	Number of Electrons per Gram
Hydrogen	0.0000899	1	6.00×10^{23}
Carbon	2.25	6	3.01×10^{23}
Oxygen	0.001429	8	3.01×10^{23}
Aluminum	2.7	13	2.90×10^{23}
Copper	8.9	29	2.75×10^{23}
Lead	11.3	82	2.38×10^{23}
		Effective Atomic Number	
Fat	0.916	6.46	3.34×10^{23}
Muscle	1.04	7.64	3.31×10^{23}
Water	1.00	7.51	3.34×10^{23}
Air	0.001293	7.78	3.01×10^{23}
Bone	1.65	12.31	3.19×10^{23}

(Data from Johns HE, Cunningham JR. *The Physics of Radiology*. 4th ed. Springfield, IL: Charles C Thomas; 1983.)

From the previous discussion, it follows that if the energy of the beam is in the region where the Compton effect is the only possible mode of interaction, approximately the same attenuation of the beam will occur in any material of equal density thickness,[2] expressed as g/cm^2. For example, in the case of a ^{60}Co γ-ray beam that interacts by Compton effect, the attenuation per g/cm^2 for bone is nearly the same as that for soft tissue. However, 1 cm of bone will attenuate more than 1 cm of soft tissue, because bone has a higher electron density,[3] ρ_e (number of electrons per cubic centimeter), which is given by density times the number of electrons per gram. If the density of bone is assumed to be 1.65 g/cm^3 and that of soft tissue 1.04 g/cm^3, then the attenuation produced by 1 cm of bone will be equivalent to that produced by 1.53 cm of soft tissue:

$$(1\text{ cm})\frac{(\rho_e)_{\text{bone}}}{(\rho_e)_{\text{muscle}}} = (1\text{ cm}) \times \frac{1.65\text{ (g/cm}^3) \times 3.19 \times 10^{23}\text{ (electrons/g)}}{1.04\text{ (g/cm}^3) \times 3.31 \times 10^{23}\text{ (electrons/g)}} = 1.53\text{ cm}$$

5.9. PAIR PRODUCTION

If the energy of the photon is greater than 1.02 MeV, the photon may interact with matter through the mechanism of pair production. In this process (Fig. 5.9), the photon interacts strongly with the electromagnetic field of an atomic nucleus and gives up all its energy in the process of

[2]Density thickness is equal to the linear thickness multiplied by density (i.e., cm × g/cm^3 = g/cm^2).

[3]In the literature, the term *electron density* has been defined both as the number of electrons per gram and as the number of electrons per cubic centimeter. The reader should be aware of this possible source of confusion.

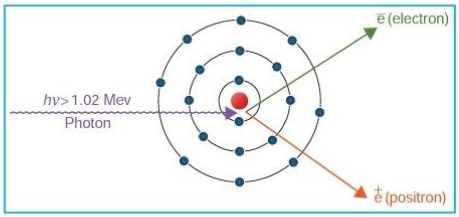

Figure 5.9. Diagram illustrating the pair production process.

creating a pair consisting of a negative electron (e^-) and a positive electron (e^+). Because the rest mass energy of the electron is equivalent to 0.51 MeV, a minimum energy of 1.02 MeV is required to create the pair of electrons. Thus, the *threshold energy* for the pair production process is 1.02 MeV. The photon energy in excess of this threshold is shared between the particles as kinetic energy. The total kinetic energy available for the electron–positron pair is given by ($h\nu$ – 1.02) MeV. The particles tend to be emitted in the forward direction relative to the incident photon.

The most probable distribution of energy is for each particle to acquire half the available kinetic energy, although any energy distribution is possible. For example, in an extreme case, it is possible that one particle may receive all the energy, while the other receives no energy.

The pair production process is an example of an event in which energy is converted into mass, as predicted by Einstein's equation $E = mc^2$. The reverse process, namely the conversion of mass into energy, takes place when a positron combines with an electron to produce two photons, called the annihilation radiation.

A. ANNIHILATION RADIATION

The positron created as a result of pair production process loses its energy as it traverses the matter by the same type of interactions as an electron does, namely by ionization, excitation, and bremsstrahlung. Near the end of its range, the slowly moving positron combines with one of the free electrons in its vicinity to give rise to two annihilation photons, each having 0.51 MeV energy. Because momentum is conserved in the process, the two photons are ejected in opposite directions (Fig. 5.10).

B. VARIATION OF PAIR PRODUCTION WITH ENERGY AND ATOMIC NUMBER

Because the pair production results from an interaction with the electromagnetic field of the nucleus, the probability of this process increases rapidly with atomic number. The attenuation coefficient for pair production (Π) varies with Z^2 per atom, Z per electron, and approximately Z per gram. In addition, for a given material, the likelihood of this interaction increases as the logarithm of the incident photon energy above the threshold energy; these relationships are shown in Figure 5.11. To remove the major dependence of the pair production process on atomic number, the coefficients per atom have been divided by Z^2 before plotting. For energies up to about 20 MeV, the curves are almost coincident for all materials, indicating that ${}_a\Pi \propto Z^2$. At higher energies, the curves for high-Z materials fall below the low-Z materials because of the screening of the nuclear charge by the orbital electrons.

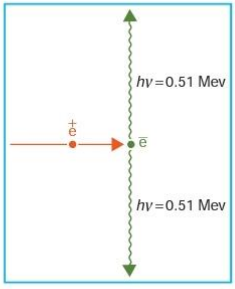

Figure 5.10. Diagram illustrating the production of annihilation radiation.

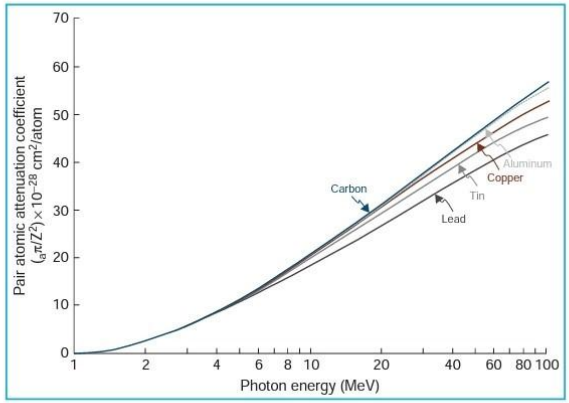

Figure 5.11. Plot of the pair atomic attenuation coefficient divided by the square of the atomic number as a function of photon energy for carbon ($Z = 6$) and lead ($Z = 82$). The mass attenuation coefficient can be obtained by multiplying ${}_a\pi / Z^2$ obtained from the graph, first by Z^2 and then by the number of atoms per gram of the absorber. (Data from Hubbell JH. *Proton Cross Sections Attenuation Coefficients and Energy Absorption Coefficients from 10 keV to 100 GeV.* Pub. No. 29. Washington, DC: U.S. National Bureau of Standards; 1969.)

5.10. RELATIVE IMPORTANCE OF VARIOUS TYPES OF INTERACTIONS

The total mass attenuation coefficient (μ/ρ) is the sum of the four individual coefficients:

$$\underset{\text{total}}{(\mu/\rho)} = \underset{\text{photoelectric}}{(\tau/\rho)} + \underset{\text{coherent}}{(\sigma_{coh}/\rho)} + \underset{\text{Compton}}{(\sigma_c/\rho)} + \underset{\text{pair}}{(\pi/\rho)} \qquad (5.30)$$

As noted previously, coherent scattering is only important for very low photon energies (<10 keV) and high-Z materials. At therapeutic energies, it is often omitted from the sum.

Figure 5.12 is the plot of total coefficient $(\mu/\rho)_{total}$ versus energy for two different materials, water and lead, representative of low- and high-atomic-number materials. The mass attenuation

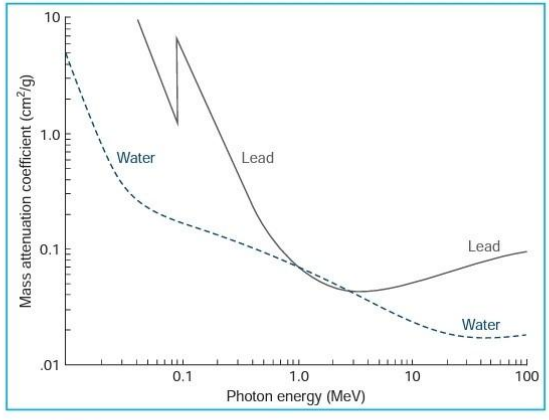

Figure 5.12. Plot of the total mass attenuation coefficient (μ/ρ) as a function of photon energy for lead and water. (Reprinted with permission from Johns HE, Cunningham JR. *The Physics of Radiology.* 3rd ed. Springfield, IL: Charles C Thomas; 1969.)

TABLE 5.2 Relative Importance of Photoelectric (τ), Compton (σ), and Pair Production (π) Processes in Water

	Relative Number of Interactions (%)		
Photon Energy (MeV)	τ	σ	π
0.01	95	5	0
0.026	50	50	0
0.060	7	93	0
0.150	0	100	0
4.00	0	94	6
10.00	0	77	23
24.00	0	50	50
100.00	0	16	84

(Data from Johns HE, Cunningham JR. *The Physics of Radiology.* 3rd ed. Springfield, IL: Charles C Thomas; 1969.)

Chapter (7) : Accelerating machines as used in nuclear physics .

18.1 Introduction

The first bombarding particles to be used in nuclear physics were the α-particles available from natural radioactive elements, and we have seen that the upper energy limit of these is a few MeV. It was realized by the Cambridge school in the 1920s that there was a limit to the transmutations that could be obtained with these and that if other particles could be used as missiles the whole range of information would increase, as different types of nuclear reaction became possible. The only other feasible bombarding particles then known were protons, since electrons do not produce nuclear effects. The first research was directed towards the acceleration of protons to energies of a few MeV. This culminated in the Cockcroft–Walton accelerator which appeared in 1932, and was the forerunner of the machines we have today giving energies up to 500 GeV.

The design of successful accelerating machines depends not only on classical physics, electrical engineering, electronics and vacuum techniques, but also on precise mechanical engineering before accurately collimated beams of charged particles can be made available for nuclear bombardment experiments. Moreover, one must remember that the maximum particle energies which can be produced artificially are far less than those energies found in cosmic ray particles. Although cosmic rays have energies of the order of many millions of GeV, the advantage of the particle accelerators lies in the fact that the intensity of the beam is far greater than the intensity of cosmic rays at sea-level.

18.2 The Cockcroft–Walton Proton Accelerator

The principle which Cockcroft and Walton adopted was that of the voltage doubler arrangement shown diagrammatically in Fig. 18.1. In this diagram two capacitor banks C_1C_3 and C_2C_4 are connected across the transformer giving a peak potential of V_0 volts with rectifiers $R_1R_2R_3$ and R_4 acting as switches.

In the following argument we shall assume there are no current losses across any of the components. We consider first the simple circuit formed by the transformer, R_1 and C_1, i.e. OPT in Fig. 18.1. For the first half-cycle assume O goes positive and T negative so that the rectifier R_1 conducts and C_1 is charged to

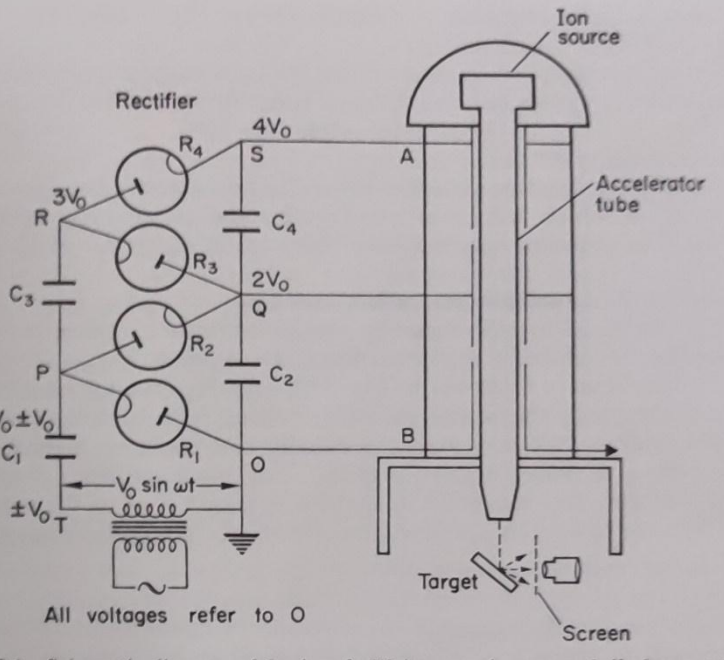

Fig. 18.1 Schematic diagram of Cockcroft–Walton accelerator and discharge tube.

V_0 and the potential of T is $-V_0$. During the second (reverse) half-cycle R_1 no longer conducts, leaving the point P isolated at a potential of V_0 while O drops to $-V_0$, producing a maximum potential difference between P and O of $2V_0$. If now we include R_2, which is conducting during the second half-cycle, the charge accumulated on C_1 is now shared with C_2 and on repeating the first half-cycle C_1 is recharged up to V_0. In this (third) half-cycle C_2 retains its charge, but this is increased by sharing with C_1 again during the fourth half-cycle. After repeating this procedure for a few cycles, C_2 becomes fully charged since it cannot lose charge by current leakage. Eventually an equilibrium is reached in which there is no current through either R_1 or R_2 at any time. The potential of Q is now equal to the *maximum* potential of P with respect to O, i.e. a steady potential difference of $2V_0$ appears across C_2, while the instantaneous potential of P with respect to O consists of a periodic component from the transformer superimposed on the steady V_0 when R_1 is not conducting. Thus an alternating potential difference of peak value V_0 appears across P and Q, with Q always at a steady potential of $2V_0$. Thus if we now add C_3 and C_4 through the rectifiers R_3 and R_4 we can repeat the whole of the above argument and the potential finally appearing at S is $2V_0$ with respect to Q and $4V_0$ with respect to O.

In principle the potential V_0 can be multiplied up to any multiple of V_0 by using the simple voltage doubler in cascade. Cockcroft and Walton reached a final potential of about 0·7 MeV in 1932. This is not very high by modern standards and it is the reason why the early Cockcroft–Walton proton reactions

were limited to light elements — lithium, boron, beryllium, etc., as already described (p. 235).

Usually the reaction is a (p, α) reaction. As in α-particle reactions, the direct collisions are rare events but are those of most interest. Thus the reaction

$$^{6}_{3}\mathrm{Li} + ^{1}_{1}\mathrm{H}\,(\mathrm{p}) \rightarrow ^{4}_{2}\mathrm{He}\,(\alpha) + ^{3}_{2}\mathrm{He}$$

is the (p, α) reaction on $^{6}_{3}$Li.

A survey of (p, α) reactions studied shows that many new isotopes were found by this method which were not possible by the (α, p) type of reaction of Rutherford. The reaction energies involved were of the order of 10 MeV.

18.3 The Van de Graaf Electrostatic Generator

This instrument, although originally conceived as an accelerator for research purposes, is now available in many teaching laboratories as a replacement for the Wimshurst machine. It is shown in Fig. 18.2 and depends for its action on the collection of charge by the hollow conductor which then discharges at the points shown. The endless belt *A* is driven vertically and picks up a charge at a few thousand volts at *B*, from a high voltage set. The point *C* induces a positive charge on to the belt and this is carried up until it is transferred to the sphere by the points *E* by a corona discharge, and hence to the terminal of the ion source. The

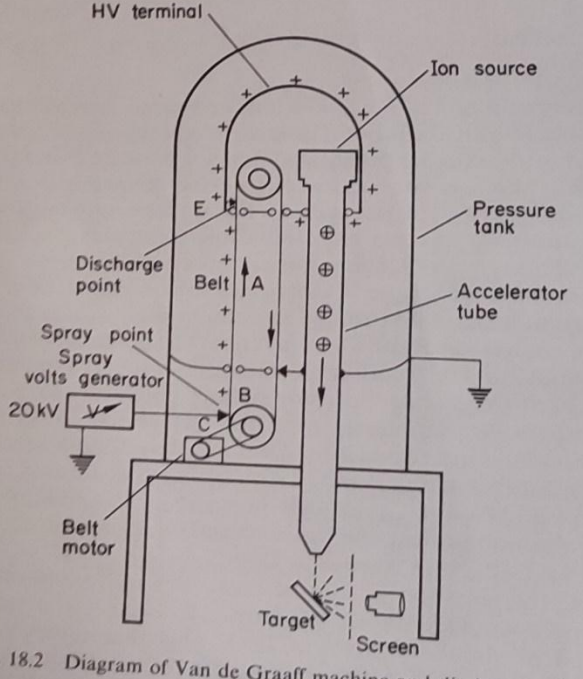

Fig. 18.2 Diagram of Van de Graaff machine and discharge tube.

usual potential is about 6 MeV but the most up-to-date generators can give about 12 MeV and there are now tandem Van de Graaff machines which give up to 20 MeV by electron stripping devices. This technique is to utilize the positive high potential twice, first by accelerating negatively charged particles and subsequently repelling them when they have been stripped of their electrons to become positive ions again. A typical arrangement would be to add electrons to the ions from the ion source, so that the emergent beam consists of a relatively high percentage of *negative* ions which are accelerated down the tube to the positively charged terminal. Here they travel along a stripping tube which removes most of the extra electrons and the resultant positive ion beam is accelerated to earth potential again. The final energy then corresponds to twice the terminal potential, although the ion current is only about 2 μA, compared with the single Van de Graaff current of about 200 μA. The tandem Van de Graaff at Aldermaston is shown in Fig. 18.3.

The Van de Graaff machine can be used to accelerate electrons by reversing the potential of the spray voltage and using a hot filament for thermionic electrons instead of the ion chamber.

18.4 The Linear Accelerator

It is to be noticed that in both the Cockcroft–Walton and the Van de Graaff machines, the high potential is generated by electrostatic devices and applied to the discharge tube containing the ions to be accelerated. In the linear accelerator the energies of the charged particles are increased by a series of linear pulses arranged to give the ions an extra push at the right moment of time, as shown in Fig. 18.4. The accelerator tubes, or drift tubes, are narrow cylinders connected alternately, as shown, to a source of a high-frequency potential. Thus, when cylinders 1, 3, 5 are positive, the cylinders 2, 4, 6, etc., are negative and reversal of potential takes place periodically according to the frequency. The positive ions are generated at S and pass through cylinder C_1 to the gap between C_1 and C_2, where the potential is such that the positive ion is accelerated in the gap into C_2, where it travels with constant velocity to the gap between C_2 and C_3. Here the acceleration process is repeated. The lengths of the cylinders have to be adjusted so that the time taken within the cylinder is just half the period, i.e. the ion always enters the potential field on leaving any one cylinder just as the potential is changing favourably. Since the ions are constantly increasing their velocities the successive cylinders have to be longer and longer. The frequencies required for protons are much higher than for heavy ions and it is now possible to accelerate protons up to about 50 MeV.

The separation between the gaps is governed by the applied high-frequency field and the gap velocity of the ions. It is the distance travelled during one half-cycle and is given by $l = v(T/2) = v/2f$, where v is the instantaneous velocity of the ions and f is the frequency of the applied field. Thus drift tubes of a few centimetres long require oscillating fields with frequencies of the order of hundreds of megahertz. The maximum gain of energy at each gap is Ve, where V is the potential difference across the gap.

The linear accelerator for electrons is different from the proton accelerator. It consists of a tube down which an electromagnetic wave progresses. The tube is

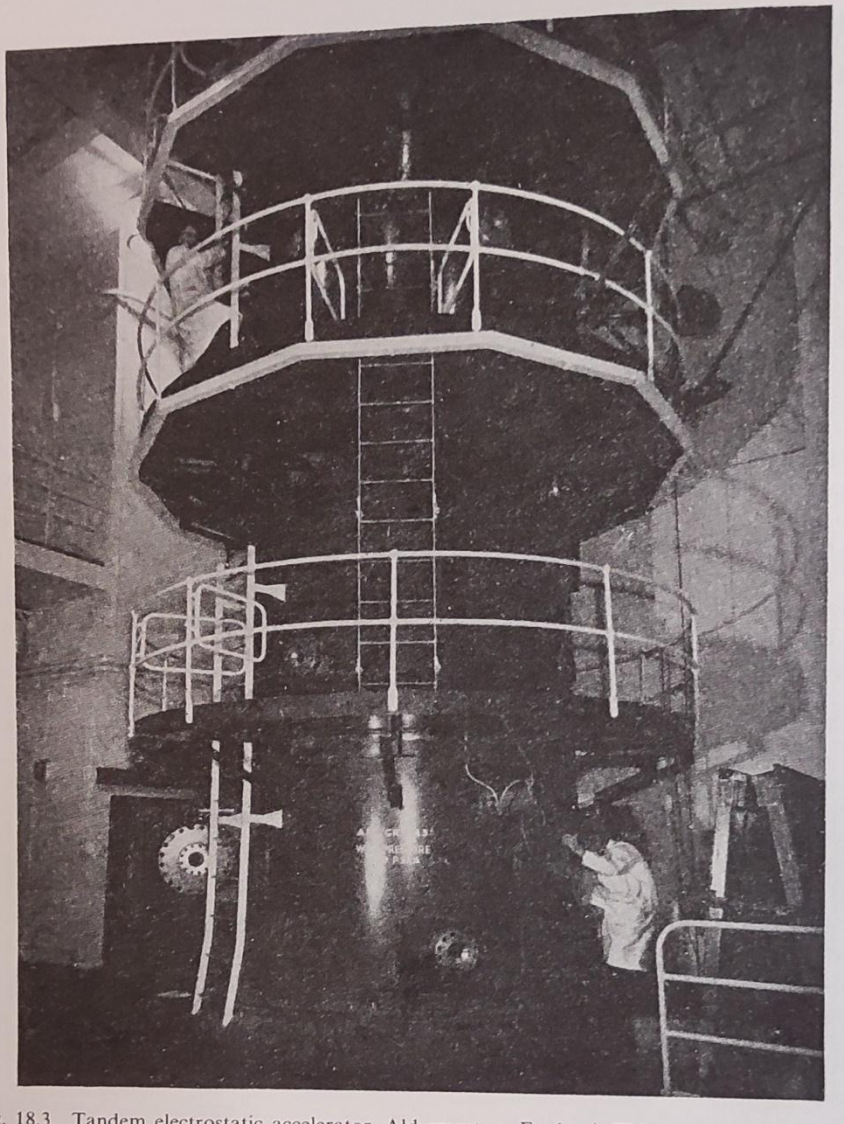

Fig. 18.3 Tandem electrostatic accelerator, Aldermaston, England. This machine and a similar accelerator at Harwell are designed to yield basic information on the behaviour of nuclei. (By courtesy of U.K.A.E.A.)

really a wave-guide since it contains apertures spaced according to the frequency of the travelling wave and the size of the tube. Electrons are injected at about 80 kV in the case of the Stanford University electron linear accelerator, which has an output of 1 GeV (10^9 eV) and is 91 m long.

The most powerful electron linear accelerator in the world is at the Stanford

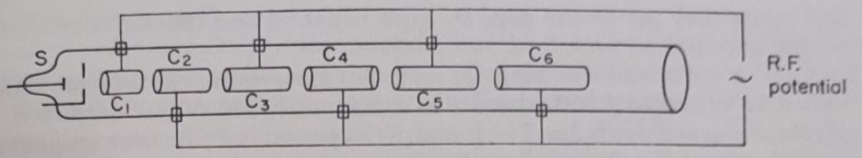

Fig. 18.4 Linear accelerator showing drift tubes of increasing length.

Linear Accelerator Center, U.S.A. It hurls electrons in a straight line over a distance of 3 km (2 miles). Obviously over this distance great precision is required of the engineering components. The maximum electron energy reached is 22 GeV. Such high-energy electrons have been used to investigate the weak electric forces within the nucleus and by firing them into liquid hydrogen and measuring the angular distribution of the scattered electrons the structure of the proton has been studied. We shall discuss the meaning of this work in Chapter 28.

18.5 The Lawrence Cyclotron

It is obvious that in the linear accelerator the length required for really high energies is enormous. Thus, it is possible to see the advantages of bending the charged particles in spirals before finally using them. This was the basis of the famous cyclotron developed in 1930 by E. O. Lawrence and his team in California. Figure 18.5 shows the cyclotron diagrammatically. The source S produces electrons which ionize the gas around S and these ions are then bent in a magnetic field within two hollow conductors, known as 'dees', inside a closed vessel containing hydrogen gas at low pressures. The magnetic field passes across the dees perpendicular to the path of ions. The potential between D_1 and D_2 must change over just as the ions are crossing the gap, as was necessary with the linear accelerator. The magnetic field causes the ions to move in a circular path through

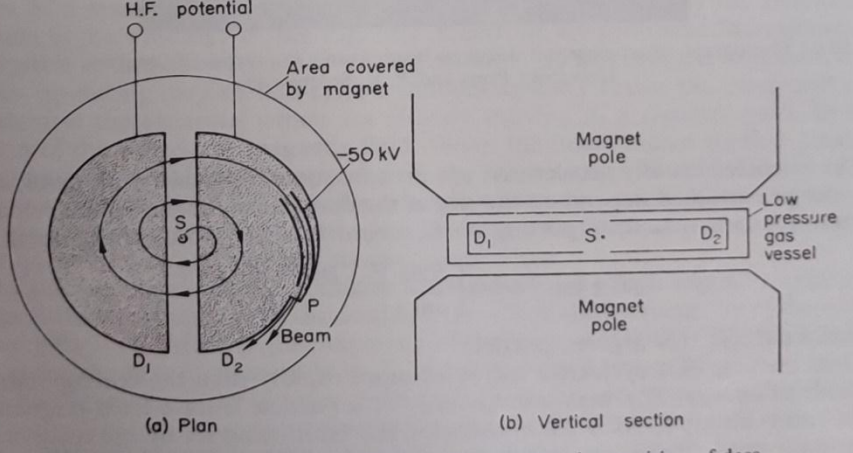

Fig. 18.5 Simplified diagram of cyclotron showing position of dees.

D_1 and when they get to the gap, D_2 goes negative and the ion is accelerated across the gap and so on.

Thus, $mv^2/r = Bev$ and $v = rBe/m$ for an ion of mass m and charge e moving in a circular path of radius r with speed v in a magnetic field of flux density B. The length of path in one dee is $2\pi r/2 = \pi r$ and, if the period is T, the time spent in each dee is $T/2$, where $T = 2\pi r/v = 2\pi m/Be$. The period is therefore independent of speed and radius, and is thus the same for all particles. The ion is always in phase once the potentials on the dees are correctly adjusted so that the energy is increased each time the ion passes a gap. When the ion has reached the maximum radius, it is led out by a channel some 60° long curved to follow the path of the ions with the outer plate at a negative potential to draw the ions away from the magnetic field. They emerge at P. Figure 18.6 shows a photograph of the emergent beam from a cyclotron.

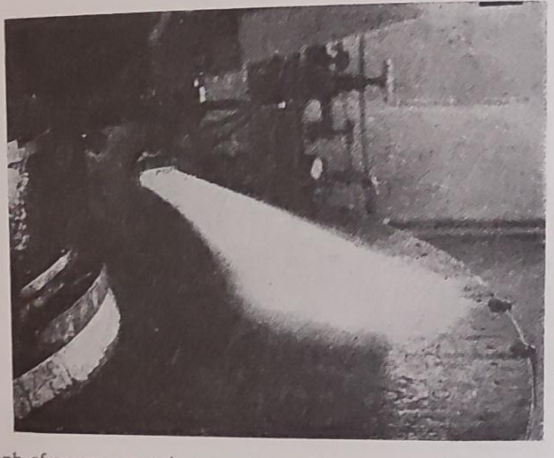

Fig. 18.6 Photograph of an emergent deuteron beam from a cyclotron. (By courtesy of Harvard University Press and A. K. Solomons.)

The particles usually accelerated are protons, deuterons and α-particles, and the energies attained depend on the size of the dees. Since the maximum velocity at circumference $= BeR/m$ (putting $r = R$, where R is the radius of the dees),

$$E = \tfrac{1}{2}mv^2 = \tfrac{1}{2}m\left[\frac{RBe}{m}\right]^2 = \frac{B^2R^2}{2}\frac{e^2}{m}.$$

Therefore $E \propto R^2$ for a given particle.

Thus the size of a cyclotron increases more rapidly than the corresponding increase of energy. The maximum energy of a particle from a fixed-frequency cyclotron is about 40 MeV for α-particles, the limit being set by the relativistic mass increase as well as mechanical engineering difficulties and expense.

18.6 The Synchrocyclotron

It will be noticed in the previous section that the expression used for the kinetic energy was the non-relativistic value $\frac{1}{2}mv^2$. For the early cyclotrons, working at low velocities, this was accurate enough but for higher speeds relativity changes become important. Thus, if $v=0{\cdot}8c$, $v^2/c^2=0{\cdot}64$ and $\sqrt{1-\beta^2}=\sqrt{0{\cdot}36}=0{\cdot}6$ and $m=1{\cdot}66\ m_0$, where m_0 is the rest mass of the particle and $\beta=v/c$.

Now from $T=2\pi m/Be$ we see that as m increases so does the period T, and the particle therefore gradually gets out of phase with the high-frequency potential on the dees. The frequency on the dees must therefore be decreased to compensate for the gain in mass. This is carried out by a rotating variable capacitor giving the imposed frequency modulation required. Ions can then be accelerated to very high velocities, and the cyclotron becomes a synchrocyclotron. The famous 4·67 m synchrocyclotron in the Lawrence Radiation Laboratory produced 380 MeV α-particles, and was later redesigned to give 720 MeV protons.

The difference between the cyclotron and the synchrocyclotron is that in the former the output is continuous but in the case of the latter the ions starting out from the centre are subject to a frequency modulation as they approach the periphery and so come out in bursts of a few hundred per second, each burst lasting about 100 μs.

18.7 Electron Accelerating Machines. The Betatron

The possible electron accelerators so far described are the Van de Graaff generator and the linear accelerator. The cyclotron cannot be used for electrons since m_e is so small that the change of mass occurs at low energies. Thus, a 1 MeV electron has a velocity $=0{\cdot}9c$, and its moving mass is about three times greater than its rest mass, whereas for a 1 MeV proton the increase of mass factor is only 1·001. An alternative method of accelerating electrons uses an alternating magnetic field rather than an electrostatic one. In the *betatron*, the electrons are contained in a circular tube, referred to as the 'doughnut', placed between the poles of a specially shaped magnet B which are energized by an alternating current in the windings W, see Fig. 18.7. Electrons are produced thermionically and given an initial electrostatic energy of about 50 keV. As the magnetic field builds up during the first half-cycle it induces an e.m.f. inside the doughnut and accelerates the electrons which are already moving in a circular path, by the action of the transverse magnetic field. When the field reaches its first positive maximum it is suddenly stopped and the high-energy electrons leave their circular paths tangentially to strike a target which then emits X-rays. Electrons are always ejected into the target when the magnetic field has just completed its first quarter-cycle and reached its maximum value.

As already explained, the velocities acquired are very high and may approach $0{\cdot}98c$. If the circumference of the doughnut is ~ 3 m, the frequency is $v/2\pi r=(0{\cdot}98\times 3\times 10^8)/3=98$ MHz. If the frequency of the magnetic field is 50 Hz, the time taken for the first quarter-cycle is $\frac{1}{200}$ s and the electrons make $(9{\cdot}8\times 10^7)/200=4{\cdot}9\times 10^5$ journeys per quarter-cycle. If the average energy acquired is 200 eV per cycle, the total energy on ejection is about 100 MeV, the mass now being about 200 m_0. Energies up to 300 MeV are currently available from betatrons

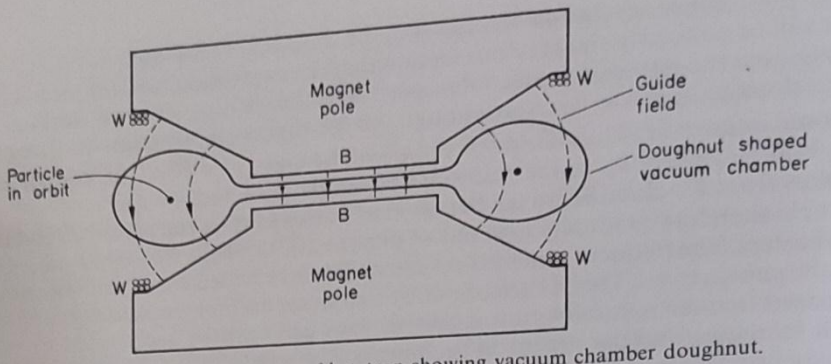

Fig. 18.7 Sectional diagram of betatron showing vacuum chamber doughnut.

which give bursts of X-rays at a repetition rate of one pulse every hundredth of a second.

18.8 Electron Synchrotron

In this machine modulation is provided, as explained for the synchrocyclotron, giving electron energies of the order of 1 GeV, although a 6 GeV electron synchrotron is now operating in the Soviet Union. This is achieved by varying the intensity of the magnetic field used for deflecting the electrons. The arrangement is not unlike the betatron except that the magnet pole pieces are annular and follow the outline of the doughnut (Fig. 18.8). In the central gap some soft iron flux bars serve as the central core of the magnet to start up the machine as a betatron. Part of the interior of the doughnut is coated with copper or silver to give a resonance cavity *G*, which is attached to a high-frequency oscillator of a few thousand volts. When the oscillator is on, the electron is accelerated each time it crosses through the resonator.

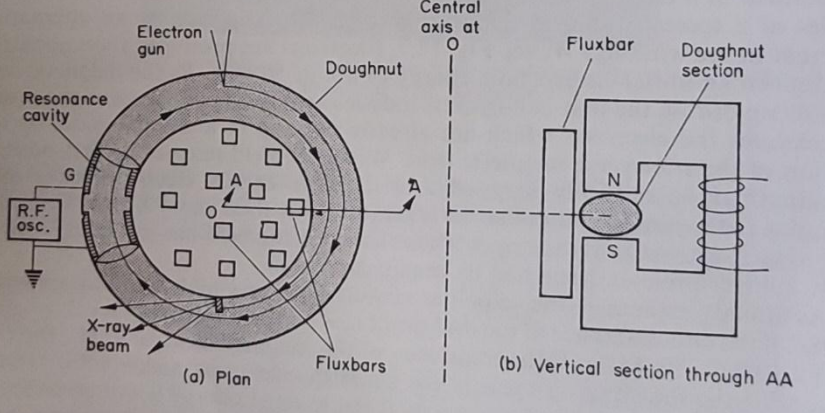

Fig. 18.8 Electron-sycnhrotron. (*a*) Plan with magnet removed; (*b*) vertical section through AA showing annular magnet.

Primary electrons are injected into the doughnut at about 100 keV and as the field changes the electrons travel in circular paths and increase their energy as in the betatron. At about 2 MeV the flux bars are magnetically saturated and cannot induce further effects. The betatron action then ceases and the resonant cavity comes into operation. If the potential applied to G operates at the proper frequency the electrons are all kept in phase and receive increments of energy at each revolution. The oscillating potential is switched off when the electrons reach their maximum velocity governed by the maximum intensity of the magnetic field. The electrons then strike the target which gives off short wavelength X-rays or '*Bremsstrahlung*'. The rays emerge in pulses as in the betatron.

18.9 Proton Synchrotron

In order to probe farther into the nucleus positive ions of many GeV are necessary and if this is to be done with synchrocyclotron the size and cost would be prodigious. To overcome this the proton synchrotron was devised, based on the electron synchrotron. A ring-shaped magnet is used — much less in mass than the equivalent synchrocyclotron — in which the particle travels with constant radius. There are four quadrants to the magnet covering the annular doughnut, as shown in Fig. 18.9. The protons are injected into the doughnut at low energy from a linear accelerator, or a Van de Graaff machine, and are recovered by magnetic deflection as a pulsed beam after many revolutions. A high-frequency resonator cavity accelerator is used in one of the straight parts with an increasing frequency corresponding to the increased speed of the protons. The field strength of the magnets is also increased to maintain the accelerated protons in a circular path of constant radius. The synchrotron action is applied at the beginning of

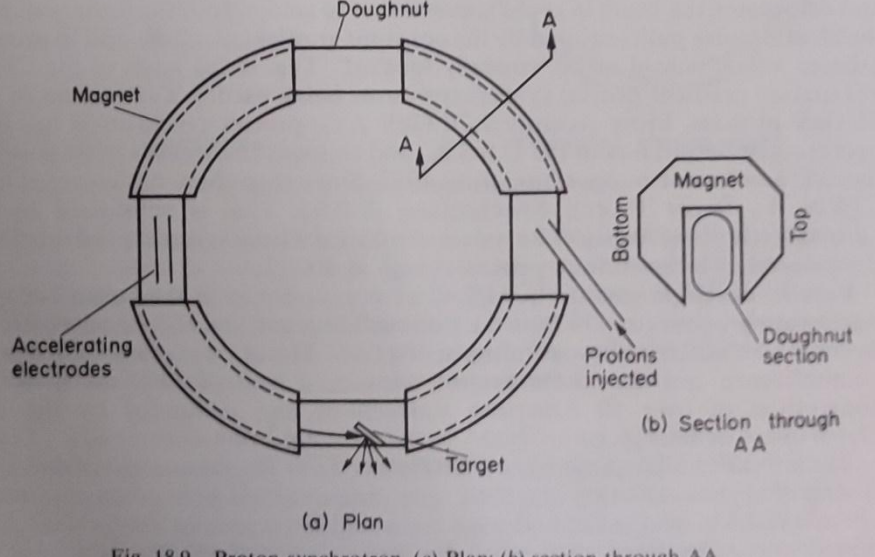

Fig. 18.9 Proton synchrotron. (*a*) Plan; (*b*) section through AA.

References

1 - Nuclear physics by Irving Kaplan (2nd edition) , 1962 .

2 - Atomic & nuclear physics …. An introduction 3rd edition by T.A.Littlfield & N.Thorly , 1979 .

3 - Physics and radiobiology of nuclear medicine by Gopal B , Saha , Third edition , 2006 .

4 – The physics of radiation therapy by Khan FM. 4th edition , 2009 .

5 – Basic physics of nuclear medicine by Keiran Maher and other wikibooks contributors .